University of Nairobi

Institute of Nuclear Science and Technology

Hybridization of Cooling System of Olkaria II Geothermal Power Plant: Utilization of Energy and Exergy Analysis Concepts

by

NAHSHON NYAMBANE

(S56/70445/2011)

A thesis submitted in partial fulfillment for the degree of Master of Science in Nuclear Science in the Institute of Nuclear Science and Technology in the University of Nairobi.

Declaration

This thesis is my original work and has not been presented for a degree in any other university.

Nahshon Nyambane (S56/70445/2011) Date: 3rd August, 2015

This thesis has been submitted for examination with our knowledge as university supervisors.

Supervisors

Dr. Michael J. Gatari
Institute of Nuclear Science and Technology,
College of Architecture and Engineering
University of Nairobi

Dr. John G. Githiri
Physics Department,
College of Pure and Applied Sciences
Jomo Kenyatta University of Agriculture and Technology

Dr. Nicholas O. Mariita
Geothermal Training and Research Institute
Dedan Kimathi University of Technology

Dedication

This research work is dedicated to my family for their immeasurable support during my study period.

Acknowledgements

With much gratitude I would like to dedicate this work to everyone who helped me directly and indirectly during my research work. I would like to thank with utmost gratitude Dr. Michael J. Gatari, Dr. John G. Githiri and Dr. Nicholas O. Mariita for spending their precious time to provide me with all the guidance and support I needed to complete my research on time. Your consistent supervision enabled me to attain the right level of focus and optimism that I needed to take this work right to the end.

Dr. Nicholas Mariita from Dedan Kimathi University of Technology went beyond his daily routine to provide me with the much needed friendly support during my data collection and analysis. Through his well-connected network of friends, I received technical help all that reinforced my focus to see light at the end of the tunnel.

I would not have been able to acquire MSc studies without scholarship support from Kenya Nuclear Electricity Board neither could I have managed the thesis without the support of National Commission of Science, Technology and Innovations, Kenya; International Science Programme, Uppsala University, Sweden and Olkaria Geothermal Project, Kenya.

Mr. Clety Kwambai of Olkaria Geothermal Project was kind enough to assist me through my data analysis and answer my email questions most of which related to work he has done on exergy analysis of geothermal power plant. He helped me understand programming in EES. I will forever be greatly indebted to his kindness.

I could also like to extend my appreciation to my lecturers Mr. David Maina (Director, Institute of Nuclear Science and Technology, University of Nairobi), Mr. Michael Mangala and my course mates who were a source of encouragement for me. I will never forget the time we spent together at the University of Nairobi.

To my parents and family who endured my fulltime absence while undertaking my MSc. deserves more than just words. They sacrificed a lot to make me what I am, and this GOD GUIDED achievement belongs to you.

Abstract

Improved energy supply is the main challenge facing most African countries because energy is fundamental for the sustainable development of all sectors of an economy. Currently, 65% of the Kenyan population do not have access to electricity. Therefore, there is need to reverse this situation by investing in energy generating projects and improving the efficiency of the current power plants by adopting or researching on new technologies to reduce energy and exergy losses. In this study, we have focused on geothermal energy with the aim of improving the power output by lowering the exergy losses in the condenser. Condensers of geothermal power plants need to operate at low pressures to ensure optimal use of energy resources. To optimize the condenser pressure, cooling water temperature is varied to determine the value that gives a higher condenser efficiency resulting in more power output. This study focused on modelling the cooling system towards lowering the temperature of cooling water in which an absorption chiller was integrated into the system. The relevant energy and exergy balance, and efficiency equations for the Olkaria II (Kenya) geothermal power plant subsystem were derived. Codes were then developed from the equations and solved using the Engineering Equation Solver software. The evaporator temperature was varied for a constant refrigerant load temperature and changes in condenser exergy efficiency and turbine output were recorded. Simulation results shows that by adoption of an absorption chiller as the secondary cooling system, cooling water temperature reduced to 16^{o}C from the current temperature of 25^{o}C. The exergy destroyed in the condenser and turbine decreased from 2.89 MW to 2.3 MW and 7.7 MW to 7.3 MW respectively. The power output increased by approximately 1.6 MWh which translates to an annual cash flow of US $ 981,120 having taken the electricity sale price at 0.07 US $/kWh. The economic analysis of investing in the absorption refrigeration system in terms of discounted payback period resulted in payback years being approximately 9.4 years. Therefore, investing in the absorption chiller system for Geothermal Power Plants is economically feasible.

Contents

Declaration i

Dedication ii

Acknowledgements iii

Abstract iv

Contents v

List of Figures vii

List of Tables viii

List of Symbols and Abbreviations ix

Chapter One: Introduction 1

1.1 Background 1

1.2 Statement of the problem 3

1.3 Justification 4

1.4 Scope of study 4

1.5 Objectives 5

1.5.1 General objective 5

1.5.2 Specific objectives 5

Chapter Two: Literature Review 6

2.1 Introduction 6

2.2 Modelling 11

2.2.1 Typical geothermal Power Plant 13

2.2.1.1 Principles of Flow process for Olkaria II plant 13

2.2.1.2 Geothermal power plant modelling 16

2.2.2 Absorption Chiller 23

2.2.2.1 Principle of operation of absorption chiller 23

2.2.2.2 Absorption chiller components modeling 26

2.2.2.3 Performance Evaluation of the system 33

Chapter Three: Methodology 34

3.1 Collection of model parameters 34

3.2 Absorption chiller model 34

3.3 Code development and Simulation 35

3.4 Economic analysis module 37

Chapter Four: Results and Discussions 39

4.1 Simulation 39

4.1.1 Exergy analysis results for the current system design 39

4.1.2 Exergy analysis for unit 3 system with hybrid system using absorption chiller. 41

4.2 Absorption chiller sizing 42

4.3 Comparison of efficiencies between the current system design and the hybridized cooling system 43

4.4 Operating graphs for the power plant with hybridized cooling system 43

4.5 Economic Analysis 54

Chapter Five 58

5.1 Conclusions 58

5.2 Recommendations 58

References 60

Appendices 64

Appendix A - Simulation results 64

Appendix B - Collected data 67

Appendix C - Analysed data 74

Appendix D - Models 77

Appendix E - Sample Exergy Analysis Codes for Olkaria II Power Plant 79

List of Figures

Figure 2.1: Condenser pressure vs exergy efficiency and thermal efficiency. 8
Figure 2.2: Effect of ambient temperature on energy and exergy efficiency at constant condenser pressure. 8
Figure 2.3: Effect of ambient temperature on energy and exergy efficiency at varying condenser pressure. 9
Figure 2.4: Illustration of exergy flow through a system. 12
Figure 2.5: Olkaria II plant. 15
Figure 2.6: Separator inflows and outflows 16
Figure 2.7: Turbine inflows and outflows for a steam expanding turbine 17
Figure 2.8: h-s diagram for turbine operation with inlet and exit pressures of 521.3 kPa and 7.5 kPa respectively 18
Figure 2.9: Condenser temperature distribution. 19
Figure 2.10: Condenser inlets and outlets 20
Figure 2.11: Gas extraction system 23
Figure 2.12: Absorption Refrigeration System 25
Figure 2.13: Absorber subsystem 27
Figure 2.14: Desorber subsystem 28
Figure 2.15: Condenser subsystem 29
Figure 2.16: Evaporator subsystem 30
Figure 2.17: Solution Heat Exchanger subsystem 31
Figure 2.18: Refrigerant Heat Exchanger subsystem 32
Figure 2.19: Expansion Valve 33
Figure 3.1: Exergy flow simulation process. 36
Figure 3.2: Flow diagram illustrating economical analysis module 38
Figure 4.1: A Graph of Condenser pressure (kPa) against refrigerant load temperature (^{o}C). 44
Figure 4.2: A Graph of condenser exergy efficiency against Condenser pressure. 45
Figure 4.3: A Graph of Condenser pressure against cooling water temperature. 46
Figure 4.4: Graph of turbine energy and exergy efficiency against condensing pressure. 47
Figure 4.5: A Graph of turbine power output against condenser pressure. 48

Figure 4.6: Graph of overall exergy efficiency against condenser pressure. 49
Figure 4.7: A Graph of condenser heat transfer rate against Condensing pressure for different cooling water flow rates. 50
Figure 4.8: Graph of condenser exergy efficiency against evaporator temperature changes. 51
Figure 4.9: Graph of Absorption chiller COP against refrigeration load inlet temperature. 52
Figure 4.10: Effect of ambient temperature on energy and exergy efficiency at variable condenser pressure for a geothermal power plant. 53
Figure 4.11: Condenser heat transfer rate due to cooling water temperature and flow rate changes at constant condenser pressure of 5 kPa. 54
Figure D.1. Flow chart diagram for Olkaria II power plant (unit 3) 77
Figure D.2. Flow chart diagram for the proposed plant design for Olkaria II with hybridized cooling system (unit 3) 78

List of Tables

Table 4.1: Exergy wasted, destroyed and efficiency for specific subsystem 39
Table 4.2: Other subsystems efficiencies 39
Table 4.3: Exergy wasted, destroyed and efficiency for unit 3 specific subsystems ...41
Table 4.4: Other subsystems efficiencies 41
Table 4.5: Required area of the absorption chiller components 42
Table 4.6: Specific subsystem 43
Table 4.7: Other subsystems efficiencies 43
Table 4.8: Estimation of total capital investment for single effect lithium bromide-water ARS 56
Table 4.9: Payback period analysis 57
Table A.1. Simulation results of the mass, energy and exergy balance of Olkaria II Geothermal Power Plant 64
Table A.2. Simulation results of the mass, energy and exergy balance of Olkaria II Geothermal Power Plant with HS of Cooling. 65
Table B.1: Average daily measured values for the month of June-2013 68
Table B.2: Daily steam status report as at 20.05.2013 73
Table C.1: Geothermal Field Parameters 74
Table C.2.Power plant parameters 74

List of Symbols and Abbreviations

Abbreviations

EV	Expansion valve
TV	Throttling Valve
PW	Production Well
IW	Injection Well
IC	Inter-condenser
AC	After condenser
HS	Hybrid System
EES	Engineering Equation Solver
COP	Coefficient of Performance
RHX	Refrigerant Heat Exchanger
SHX	Solution Heat Exchanger
NCG	Non-Condensable Gas
GES	Gas Extracting System
TTD	Total Temperature Difference
CT	Cooling Tower
CCW	Common Cooling Water
CCWP	Common Cooling Water Pump
LH	Left Hand
RH	Right Hand
GPP	Geothermal Power Plant
AHD	Adiabatic Heat Drop
T.S.R	Total Steam Rate
SJET	Steam Jet Ejectors
MDGs	Millennium Development Goals

Symbols

U	Coefficient of heat transfer
A	Area
ΔT_{lm}	Logarithmic mean temperature difference (LMTD)
LiBr	Lithium Bromide
H_2O	Water
kWe	Kilowatts electricity
w	Mass ratio of steam
E	Exergy
i	Interest rate
I	exergy loss
h	Enthalpy
$\dot{m}$	Mass flow rate
p	Pressure
T	Temperature
s	Entropy
x	Dryness fraction
η	Efficiency
W_{tur}	Turbine work
W_{pump}	Pump work
W_{fan}	electrical power consumed by fans
W_{aux}	Work output by auxiliary systems
Q_{cond}	Condenser energy
η_{plant}	Plant efficiency
W_{net}	Net power output
P_{cond}	Condenser pressure
W_a	Actual turbine work

Ws	Isentropic turbine work
W_{gen}	Generator power
T_o	Ambient temperature
P_o	Ambient pressure

Subscripts

abs	Absorber
d	Desorber
c	Condenser
e	Evaporator
gen	generator
sjet	steam jet ejectors

Chapter One

Introduction

1.1 Background

Geothermal Energy is an essential element for economic development of any country. Research has shown that world leading economies in America, Asia and Europe have banked on energy as their main ingredient in their economic superiority. According to Bertani (2015) total worldwide installed capacity of geothermal energy as at 2015 stands at 12,635 MWe. America, Asia, Europe, Oceania and Africa accounts for 5,089 MWe, 3,756 MWe, 2,133 MWe, 1,056 MWe and 601 MWe respectively. Kenya's geothermal installed capacity as at 2015 stands at 594 MWe out of the 601 MWe installed in all African countries.

Increased demand for energy, decline of energy resources and environmental impact due to energy utilization have resulted to calls for a sustainable approach to development and management of energy resources (Rosen and Dincer, 2001). According to Gong and Wall (1997) increased pressure on the finite energy resources as a result of rapid growth in population, urbanization, industrialization and technology development has triggered a wakeup call on research and development of systems that will efficiently utilize the energy resources.

Since energy demand is far much higher than the available resources, the energy conversion systems must be designed to ensure efficient resource utilization as well as minimal exergy losses (Gong and Wall, 1997). The performance of a geothermal power plant is evaluated through energy conversion performance that is based on the first law of thermodynamics. However, in the recent decades, a useful tool based on the second law of thermodynamics (exergy performance) has gained popularity among engineers dealing with energy systems. The tool is useful in determining the location, magnitude and causes of exergy losses besides providing meaningful information on the efficiency of each subsystem within the power plant (Dorj, 2005).

According to Rosen and Dincer (2001) exergy is an indication of how much work can be done by a resource within a given environment. It is useful to devise ways to minimize the exergy losses to attain optimum working conditions for power systems.

For example, the geothermal fluid mixtures exploited from the ground need to be separated to extract steam from the liquid. The extracted steam is then used to drive the turbines, which are coupled to an electric generator. The liquid separated from steam is considered a waste and in most cases is injected back to the ground. However, the waste liquid referred to as brine possesses a considerable amount of exergy, which can be utilized for other thermal applications. It is therefore clear that exergy efficiency of the geothermal power plant is lowered due to irreversibility during energy conversion process within the subsystems and exergy quality is lost.

In order to improve conversion efficiency of a geothermal power plant, cooling is essential for it increases the heat rejection, raises power output and increases heat to power conversion ratio. A study conducted on Mindanao II power plant, in Philippines, showed that the cooling water system and turbines were the major sources of overall exergy losses (Aligan, 2001). A similar study was conducted at geothermal fluid network in Larderello, Italy and the findings revealed that the turbines, condensers and cooling towers contributed a greater percentage of exergy losses (Bettaglin and Bidin, 1996). An exergy analysis conducted on Olkaria l geothermal power plant, in Kenya, showed the overall exergy efficiency of the plant to be 43% with reference to the total exergy from the connected wells. However, the energy efficiency was found to be 15%, which greatly differed with the exergy efficiency. The analysis revealed that the difference in the two efficiencies were due to exit of most energy from the plant while still containing substantial exergy. It was reported that most exergy losses occurred in the turbine(s) and condenser (s) where most exergy is rejected and destroyed (Kwambai, 2005).

In a turbine, exergy performance is influenced by the availability of an efficient and effective cooling system. The efficiency of a cooling system is solidly grounded on a number of factors which include; ambient temperature, surface area of cooling system and flow rate of the condensate. Cooling towers ensure prolonged life of the system by preventing turbines from overheating. It also lowers the fluid pressure, which contributes to increased vacuum pressure at the condenser thus lowering the turbine backpressure leading to increased turbine capacity. However, in tropical areas, high air temperature has emerged as an obstacle to the steam condensation process. Condensation process is completed in the condenser, and if it occurs at high

temperature the left over steam increases. This leads to increased condenser pressure that lowers the exergy performance hence decreasing the turbine capacity. There is, therefore, a need to ensure improved capacity for heat rejection by adopting systems that work towards increasing the coefficient of performance of the cooling cycle.

One of the systems that have been proved effective in increasing the performance of cooling cycle is an absorption chiller. This is an artificial cooling system that uses Lithium Bromide as the absorbent and water as the refrigerant. The system works on either a single effect, double effect or multiple effect refrigeration principle. The single effect refrigeration system works under two pressures, the high pressure region and the low pressure region. Pressure differences occur across solution pumps and flow restrictions. The system consists of two flow restrictors, one solution pump and four heat exchangers, absorber, desorber, condenser and evaporator. Solution heat exchanger and refrigerant heat exchanger are incorporated into the system to improve the performance of the system. The refrigerant which is the real working fluid is separated from the absorbent in the desorber then directed to condenser in vapour form. The essence of the absorbent is to treat the refrigerant to a specific condition for a complete cycle continuation.

The high pressure occurs in the refrigerant heat exchanger, condenser, desorber and solution heat exchanger while low pressure occurs in the absorber and evaporator. The low pressure in the evaporator probably far below the atmospheric pressure makes it easier for the refrigerant molecules to enter the vapour phase at a much lower temperature. This makes it easier for the refrigerant to extract more heat from the load into the evaporator thus lowering its temperature further.

1.2 Statement of the problem

Kenya lies in the tropical regions and experiences high ambient temperatures. The temperature ranges between 20 – 30^{o}C in daytime while in arid and semi-arid areas it can go to as high as 30 – 35^{o}C. Most of the geothermal prospects are located in the Rift Valley region. In this area, the temperature of the water used for cooling in the condenser and auxiliary systems does not have enough capacity to ensure exhaustive heat rejection from the steam. Heat rejection is influenced by the high ambient temperatures. Since cooling water temperature is dependent on the ambient

temperature, increase in this temperature lowers the steam condensation process. The lower the steam condensation process the lower the condenser exergy efficiency, thus, translating to a higher turbine exhaust temperature and lower power output.

1.3 Justification

Increasing the condenser exergy efficiency is an essential element in improving the performance of geothermal power plant turbine. The design of these power plants is such that condensation process is supposed to be completed in the condenser; however, the high temperatures inhibit the heat rejection capability leading to accumulation of left over steam. Subsequently, this leads to increased condenser pressure and exergy losses that ultimately lowers the condenser exergy efficiency and turbine capacity, increase water consumption and operational cost as well as steam consumption.

The adoption of an absorption refrigeration system as a secondary cooling system will significantly lower the temperature of the cooling water and therefore would boost the capacity of the condenser to reject heat. Increased heat rejection will increase turbine performance as well as energy and exergetic efficiencies of the geothermal power plant. Improved exergy efficiency in Olkaria II geothermal power plant would result in huge economic savings, increased plant power output, reduced steam consumption, reduced maintenance costs, reduced waste of water thus contributing to the interest of Kenya Vision 2030 and the Millennium Development Goals (MDGs) that aims at ensuring access to reliable energy.

The adoption of the absorption refrigeration system that is thermally powered would also serve as a direct user of the brine thermal energy, which is normally wasted for Olkaria II. The absorption refrigeration system would also work towards lowering the amount of the cooling water required by the cooling towers. Our study therefore targets the improvement of the cooling system.

1.4 Scope of study

Our study involved an exergy flow analysis of the Olkaria II geothermal power plant to ascertain the magnitude of exergy losses and exergetic efficiency. Effects of incorporating an absorption chiller as the secondary cooling system were analyzed.

The absorption refrigeration system is used to reduce further the cooling water temperature. It included understanding the effect of varying cooling water temperature on condenser exergy efficiency and turbine output power.

1.5 Objectives

1.5.1 General objective

Model and design a cooling system that would lower the temperature of cooling water to improve turbine capacity in geothermal electricity generation installations.

1.5.2 Specific objectives

1. Carry out an exergy analysis on the cooling system to determine the exergy destroyed and efficiencies of each subsystem as well as the overall exergetic efficiency of the plant.
2. Model and simulate a hybridized cooling system.
3. Assess the effect of the hybridized cooling system on the condenser pressure and overall power plant exergetic performance.
4. Carry out an economic evaluation on the payback period for new cooling system based on the current unit cost of power.

Chapter Two

Literature Review

2.1 Introduction

Vosough et al. (2011) did an energy and exergy analysis of an ideal Rankine cycle. A Rankine cycle is a thermodynamic cycle used in steam turbines using heat in order to produce electricity. Their study aimed at improving the power plant efficiency by changing the condenser pressure. Through modelling and simulation of the system, they found the exergy destruction in the condenser was 13.75% and there were significant energy losses in the condenser that accounted for 60.86% of the energy input to the plant. On analyzing the effect of condenser pressure on the plant efficiency it was evident the efficiency decreased with an increase in condenser pressure. They concluded that increase in turbine capacity, required reduction of condenser pressure. However, they realized the following limitations: (1) the steam quality decreased at turbine exhaust leading to formation of water droplets that created a drag force, which reduced the turbine output power and (2) the water droplets were responsible for wearing of the turbine blades. Based on the above limitations the condenser pressure was estimated to vary between 6.9 kPa to 13.5 kPa. Figure 2.1 shows the effect of condenser pressure on both the exergy and thermal efficiency of the power plant. The graph shows that as the condenser pressure increases, both the exergy and thermal efficiency of the plant decreases.

A study by Zhang and Lior (2007) revealed that to achieve a high turbine capacity; the backpressure in a turbine must be lowered significantly to reduce the exergy losses in the condensation process. Sharma et al. (2011) did an exergetic optimization of inlet cooling water temperature of cross flow steam condensers. In their study they focused on optimizing inlet temperature of cooling water during condensation of saturated water vapor within a shell and tube condenser, through minimization of exergy destruction. They calculated the optimum inlet cooling water temperature under various operating conditions of the steam condenser with the aim of determining the variation of exergy destruction and exergy efficiency at various condenser pressures, different mass flow rates of steam and cooling water with the effect of atmospheric temperature being considered. Their findings showed that optimum cooling water temperature decreased with decrease in condenser pressure.

Dutta et al. (2013) did a study on the effect of cooling water temperature rise on the efficiency of condenser for a 210 MW thermal power plant. The study was done at fixed condenser pressure and mass flow rate of steam into the condenser. Other parameters that were fixed included; mass flow rate of cooling water, total surface area of cooling tubes and material properties. Their findings show that the condenser efficiency increased with increase in temperature rise of cooling water.

Mehdis and Amir (2012) studied the effect of ambient temperature on the energy and exergy efficiencies of Ramin supercritical power plant in, Iran. This was done at constant and varying condenser pressure respectively an in Fig. 2.2 and 2.3. The study revealed that at constant condenser pressure, the energy efficiency of the power plant remained constant as the ambient temperature increased. When the condenser pressure was varied, the energy efficiency decreased with increase in ambient temperature. However, the exergy efficiency of the plant decreased as the ambient temperature increased at both constant and varying condenser pressure with the rate being higher at varying condenser pressure.

Acir et al. (2012) investigated the effect of varying dead state temperature on energy and exergy of Cayirhan thermal power plant. The findings showed that varying dead state temperature do not have an effect on energy efficiency (first law efficiency), whereas it has an effect on the exergy efficiency (second law efficiency). The study also revealed that most heat losses occurred in the condenser.

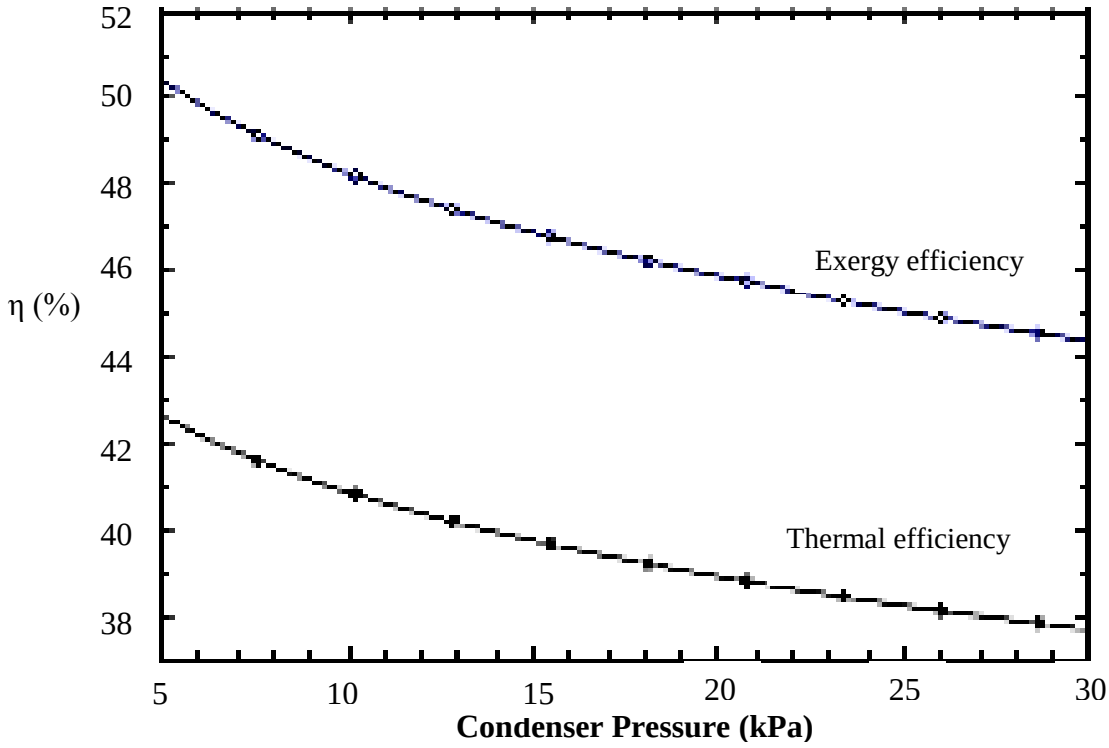

Figure 2.1: Condenser pressure vs exergy efficiency and thermal efficiency. (Adopted from Vosough et al., 2011)

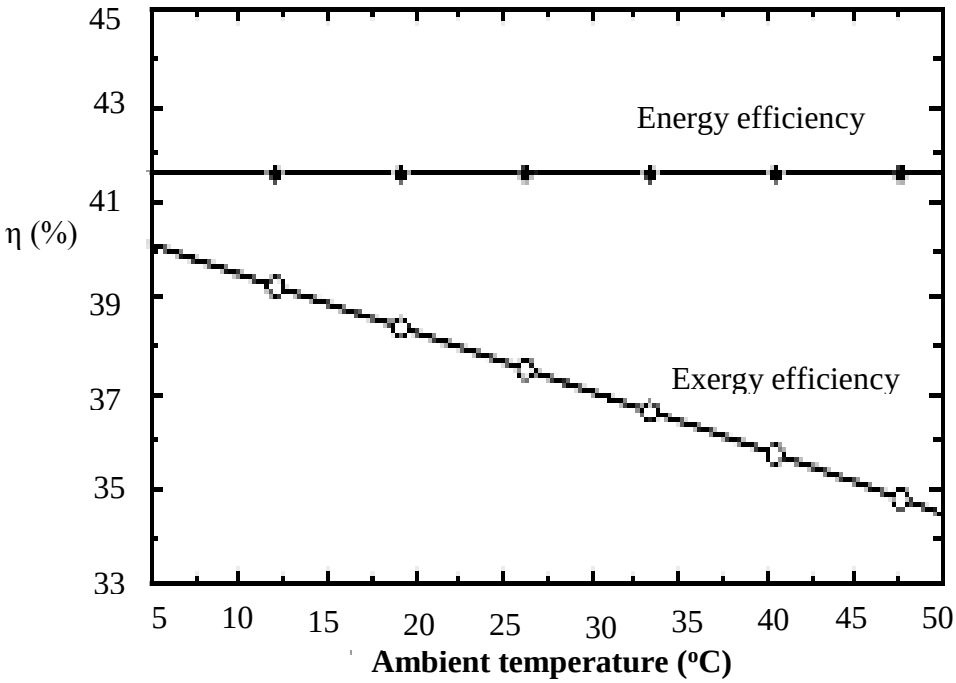

Figure 2.2: Effect of ambient temperature on energy and exergy efficiency at constant condenser pressure. (Adopted form Mehdis and Amir, 2012)

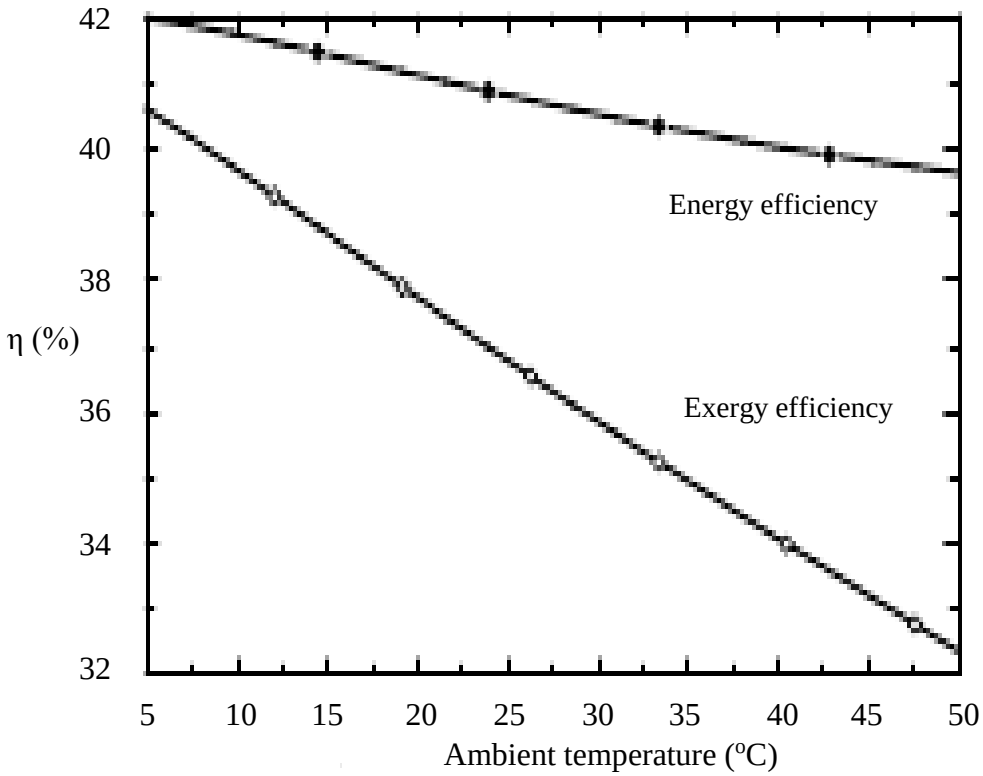

Figure 2.3: Effect of ambient temperature on energy and exergy efficiency at varying condenser pressure. (Adopted from Mehdis and Amir, 2012)

Despite the location of areas where exergy losses are dominant, fewer efforts have been made to address the issue on how to counter the effects. However, Bharathan and Nix (2001) studied the effect of incorporating ammonia absorption pump in air-cooled geothermal power plant. They recorded a 21% increase in the net power production by increasing the flow rate of the brine by 30%. A study by Kozubal and Kutscher (2003) showed that an increase in net power output from a geothermal power plant could be realized through a series arrangement of the air cooled and wet-cooled condensers. This was useful as it ensured increased net power output during the hot periods of the day.

For the last four decades, absorption refrigeration systems have gained popularity as preferred choice for industrial cooling. Holdmann and Erickson (2006) studied the impact of using absorption chillers in Chena Hot Springs for Aurora Ice Museum. They found adopting the absorption refrigeration system, as opposed to conventional mechanical compressor chillers could lower temperature to the system. This lowers

the operation and maintenance costs, and significantly improves the coefficient of performance of the system.

Kececiler et al. (2000) studied the effect of using low temperature geothermal resource to power a LiBr/H_2O system. His findings showed the system yielded chilled water at a temperature of between 4 – 10^oC and this would significantly improve the cooling system for geothermal power plant. A study on the effect of ambient temperature on the surface area of the desorber, condenser, evaporator, absorber and solution heat exchanger of an air-cooled absorption machine found ambient temperate did not affect the absorber and condenser surface area. However, it was reported that to maintain the same efficiency, the surface area of the desorber and solution heat exchanger required to be increased slightly with increase in the ambient temperature. In addition, the evaporator surface area required to be decreased as the ambient temperature increased (Mostafavi and Agnew, 1996).

Tesha (2009) studied the effect of change in condenser pressure on power output. The simulation results showed that by lowering the condenser pressure from 11. 178 kPa to 8.651 kPa an extra power of 45 kW was achieved for a single flash system. He also studied the effect of incorporating an absorption refrigeration system as an integrated condenser unit in a geothermal power plant. The analysis involved using energy concept to determine the effect on power output through use of an absorption system. The findings obtained showed that by adopting the system an extra 131 KWe was obtained.

Izquierdo (2008) conducted trials to determine the performance of a commercial (Rotarian 045v) 4.5 kW air-cooled, single effect LiBr/H_2O absorption chiller for residential use. One of their findings was that the cooling power tends to decline with raising outdoor dry bulb temperature, and at temperature from 35^oC to 41.3^oC the chilled water outlet temperature in the evaporator increased to over 15^oC.

According to Woodruff (1998) the turbine outlet enthalpy is a function of condenser pressure. Theoretically, a decrease in the turbine outlet enthalpy causes the turbine capacity to increase. An increase in the turbine steam rate (T.S.R) is noted with increased condenser pressure and is given by Eq.2.1,

$$T.S.R=\frac{3600}{\left[(AHD)\times 0.85\left(1-\frac{w}{2}\right)-17.43\right]0.95} \quad [2.1]$$

Where, T.S.R is the ratio of the required steam mass flow rate for delivering 1 KWh of electrical power, w is the mass ratio of water to steam and water mixture at the turbine outlet and A.H.D is the adiabatic heat drop between the inlet and outlet turbine pressure as expressed in Eq. 2.2. Adiabatic heat drop occurs as a result of temperature changes between the turbine inlet and outlet without any heat loss.

Therefore,

$$A.H.D=h_{in}-h_{out} \quad [2.2]$$

where h_{in} is the turbine inlet enthalpy and h_{out} is the turbine outlet enthalpy.

Turbine inlet and outlet enthalpies are functions of inlet and outlet pressures of the turbine respectively. Equations 2.3 show the relationship between turbine power and turbine steam rate.

$$W_{tur}=\frac{1}{T.S.R} \quad [2.3]$$

where W_{tur} is output turbine power in (MW).

By increasing the condenser pressure, T.S.R increases rapidly and decreases the turbine output power. Therefore, to increase the turbine power and efficiency, the condenser pressure must be lowered.

2.2 Modelling

In geothermal power plant modeling three main parameters are considered. These are mass, energy and exergy. For mass and energy balance two important assumptions hold, that total mass flow rate into the system is equal to the total mass flow rate out of the system as expressed in Eq. 2.4,

$$\sum \dot{m}_{in}=\sum \dot{m}_{out} \quad [2.4]$$

where $\dot{m}$ is the mass flow rate.

Whereas, the energy into the system is equal to the energy out of the system as expressed in Eq. 2.5,

$$\sum(\dot{m}\times h)_{in} = \sum(\dot{m}\times h)_{out} \quad [2.5]$$

where h is the enthalpy.

For the case of exergy balance we consider a control volume as shown in Fig.2.4.

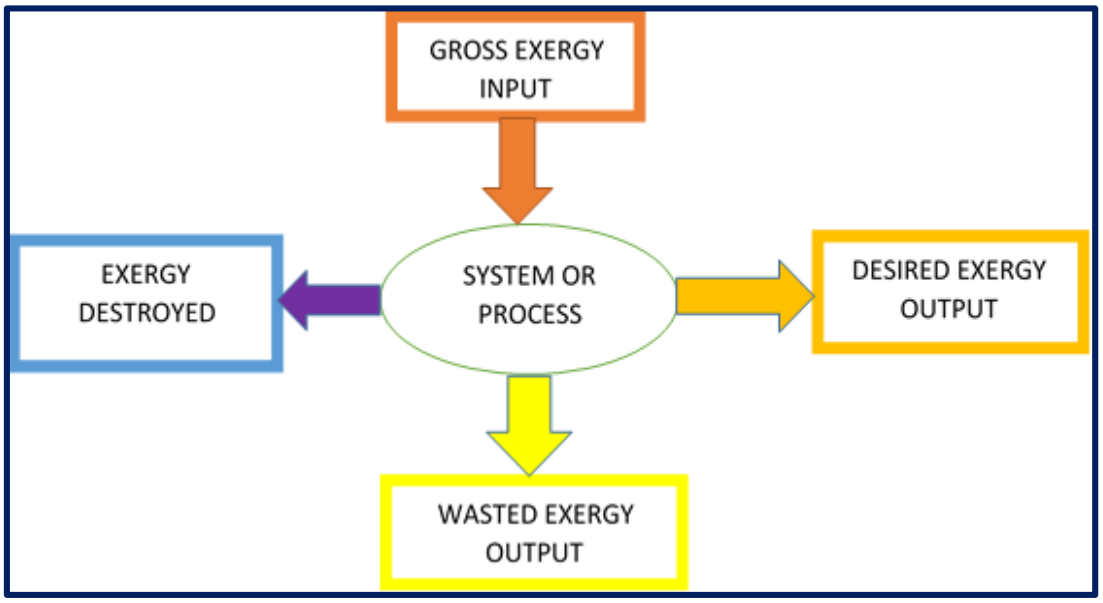

Figure 2.4: Illustration of exergy flow through a system. (Adopted from Kwambai, 2005)

For this study, only physical exergy will be considered since processes involve only fixed composition flow (Rosen, 1999). The exergy balance equation for the system in Fig.2.4 is given by Eq. 2.6,

$$E_{in} = E_{out} + E_{destroyed} \quad [2.6]$$

where,

$$E_{out} = E_{desired} + E_{waste} \quad [2.7]$$

E_{in} (MW) is the exergy into the system, E_{out} (MW) is the exergy out of the system and $E_{destroyed}$ (MW) is the exergy lost.

Exergy destroyed is expressed as the product of ambient temperature and entropy as shown in Eq. 2.8.

$$E_{destroyed} = T_o \cdot S \quad [2.8]$$

where T_o is ambient temperature and S is entropy.

Exergy is a function of environmental parameters that include temperature and pressure. The generalized equation for calculation of exergy is as shown in Eq. 2.9. The equation forms the basis of Engineering Equation Solver (EES) codes development.

$$E = \dot{m} \cdot \left[\left(h - h_o \right) - T_o \cdot \left(S - S_o \right) \right] \quad [2.9]$$

where S_o and h_o is the entropy and enthalpy at ambient temperature and pressure respectively.

Therefore,

$$\eta_E = \frac{E_{desired}}{E_{in}} \quad [2.10]$$

where η_E is the exergy efficiency of the system and $E_{desired}$ is the desired exergy.

Overall exergetic efficiency of the plant is expressed in Eq. 2.11,

$$\eta_{overall} = \frac{W_{net}}{E_{in}} \quad [2.11]$$

where W_{net} (MW) is the net power output.

2.2.1 Typical geothermal Power Plant

2.2.1.1 Principles of Flow process for Olkaria II plant

Figure 2.5 describes the flow process of the steam in Olkaria II power plant. State point, r describes the flow of two phase fluid from the reservoir into the separator through a throttling valve (TV). Once in the separator the two phase fluid is separated into steam and brine. Steam flows into the transmission line 3 while brine flows into reinjection line 1. From the transmission line the steam is passed through a steam scrubber, 4 and some is tapped to the ejector, 4a. The purpose of the steam scrubber is to collect any water vapour in the steam so as to ensure that only dry steam moves into the turbine, 5. The steam is used to drive an impulse-reactive turbine that is

coupled to a generator to produce electric power. Steam is then exhausted into the condenser, 6, where it is condensed before being directed into the hotwell pumps, 7, for pumping into the cooling towers, 10. A small mass flow is re-injected in as cold re-injection, 9. In the cooling tower hot condensate is cooled by evaporative process using cold air, 40. The cooled water, 11, is then directed back to the condenser, 13, as well as other auxiliary system, 19, and common cooling water (CCW). In the condenser non-condensable gases (ncg) are extracted by the ejector, 60, before being directed into the inter-condenser (IC), 61, and then sucked by the vacuum pump, 63, into the cooling tower (CT). The condensate from the inter-condenser, 20, is directed into the main condenser.

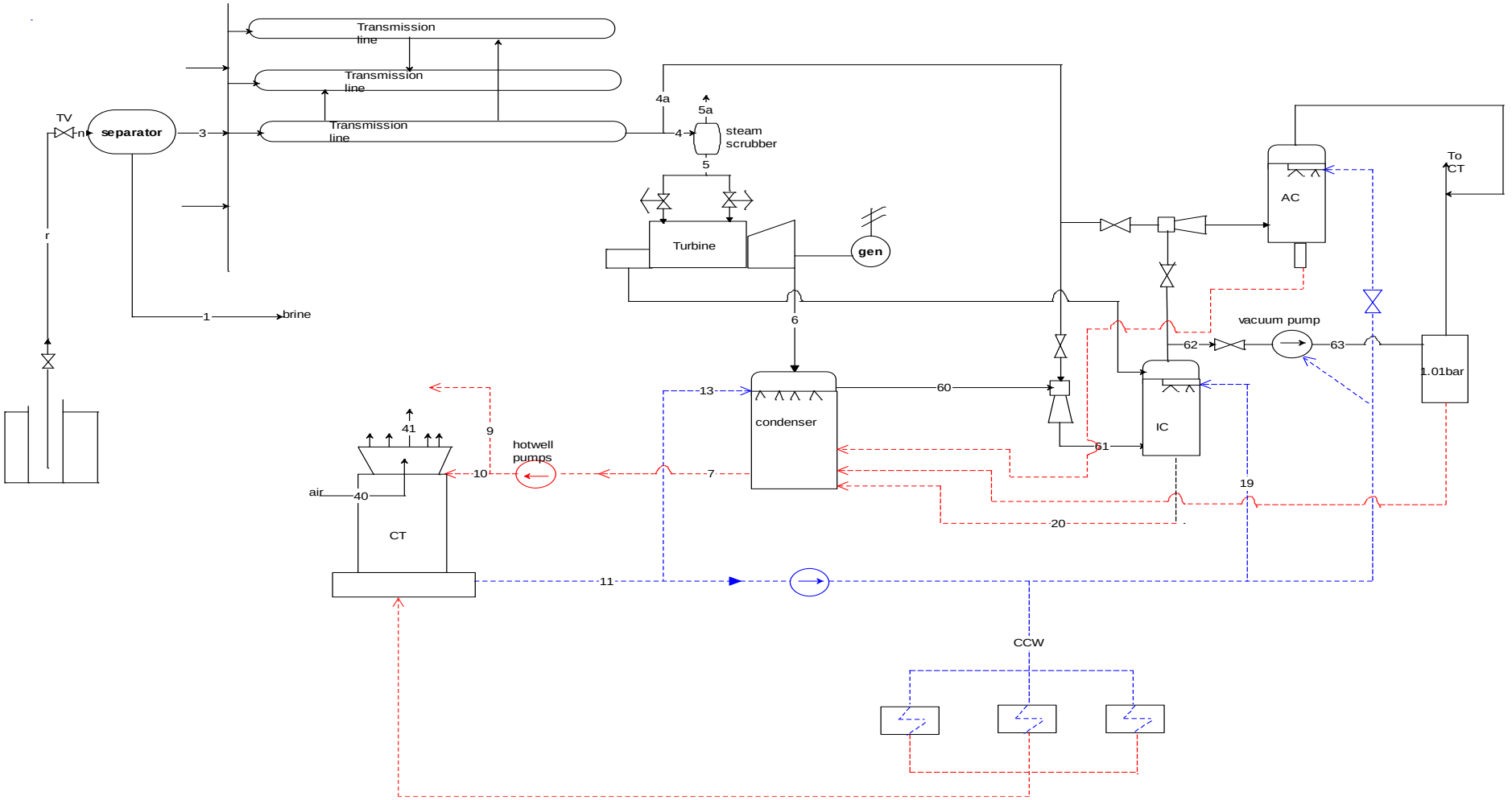

Figure 2.5: Olkaria II plant.

2.2.1.2 Geothermal power plant modelling

When modelling geothermal power plant using energy and exergy concepts one needs to first model each of the plant subsystem before coming up with a final expression for overall exergy efficiency. The subsections below for each plant subsystem show the exergy balance equations for determination of exergy losses and exergetic efficiency expressions. The subscript numbers in the equations refers to the state points in Fig. 2.5.

I. Separator

A separator is very essential in a geothermal power plant. It help in separating the liquid (brine) [1] from steam [3] as shown in Fig.2.6.

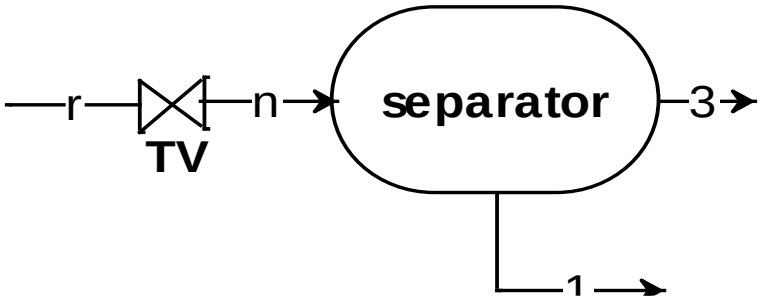

Figure 2.6: Separator inflows and outflows

According to Fig.2.6, Eq. 2.12 to 2.17 defines the conditions at each state point.

$$h_r = h_n \quad [2.12]$$

$$P_n = P_1 = P_3 = P_{sep} \quad [2.13]$$

Dryness fraction, x at state n is given by Eq. 2.14,

$$x_n = \frac{\dot{m}_3}{\dot{m}_n} \quad [2.14]$$

Flow rate of brine ($\dot{m}_1$) is expressed as,

$$\dot{m}_1 = (1\text{-}x_n) \times \dot{m}_n \quad [2.15]$$

Exergy loss is expressed by Eq. 2.16,

$$E_n = E_1 + E_3 + I_{sep} \quad [2.16]$$

where I_{sep} is the exergy loss during separation, and exergetic efficiency is given by Eq. 2.17,

$$\eta_{E,sep} = \frac{E_3}{E_n} \quad [2.17]$$

II. Steam Scrubber

A steam scrubber is used to remove any left over condensate from the steam to make sure dry steam is introduced to the turbine. According to Swandaru (2006) the pressure drop through the steam scrubber is taken to be 10 kPa and the flashed mass flow rate is considered as 1% of the steam flow rate as expressed in Eq.2.18.

$$m_{5a} = 0.01 \times \dot{m}_4 \quad [2.18]$$

Equation 2.19 shows the expression for exergy balance in the steam scrubber,

$$E_4 = E_{5a} + E_5 + I_{scrubber} \quad [2.19]$$

where $I_{scrubber}$ is the exergy loss in the steam scrubber, and the exergetic efficiency is given by Eq. 2.20,

$$\eta_{E,scrubber} = \frac{E_5}{E_4} \quad [2.20]$$

III. Turbine

The turbine is the most important component in a geothermal power plant. It receives dry steam from the steam scrubber, and then expands it before being exhausted into the condenser. Figure 2.7 shows the turbine inflow and outflow for a steam-expanding turbine.

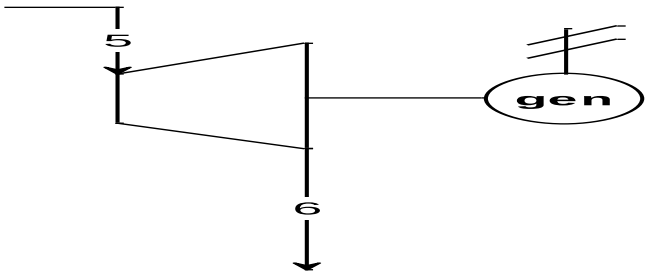

Figure 2.7: Turbine inflows and outflows for a steam expanding turbine

Based on Fig.2.8, actual turbine work is expressed as in Eq. 2.21

$$W_a = W_{tur} = x_5 \dot{m}_5 (h_5 - h_6) \quad [2.21]$$

Turbine efficiency is given by Eq. 2.22

$$\eta_t = \frac{W_a}{W_s} = \frac{h_5 - h_6}{h_5 - h_{6s}} \quad [2.22]$$

where W_a is actual turbine work and W_s is isentropic turbine work.

The work output of an adiabatic turbine simply becomes the change in enthalpy (Swandaru, 2006)

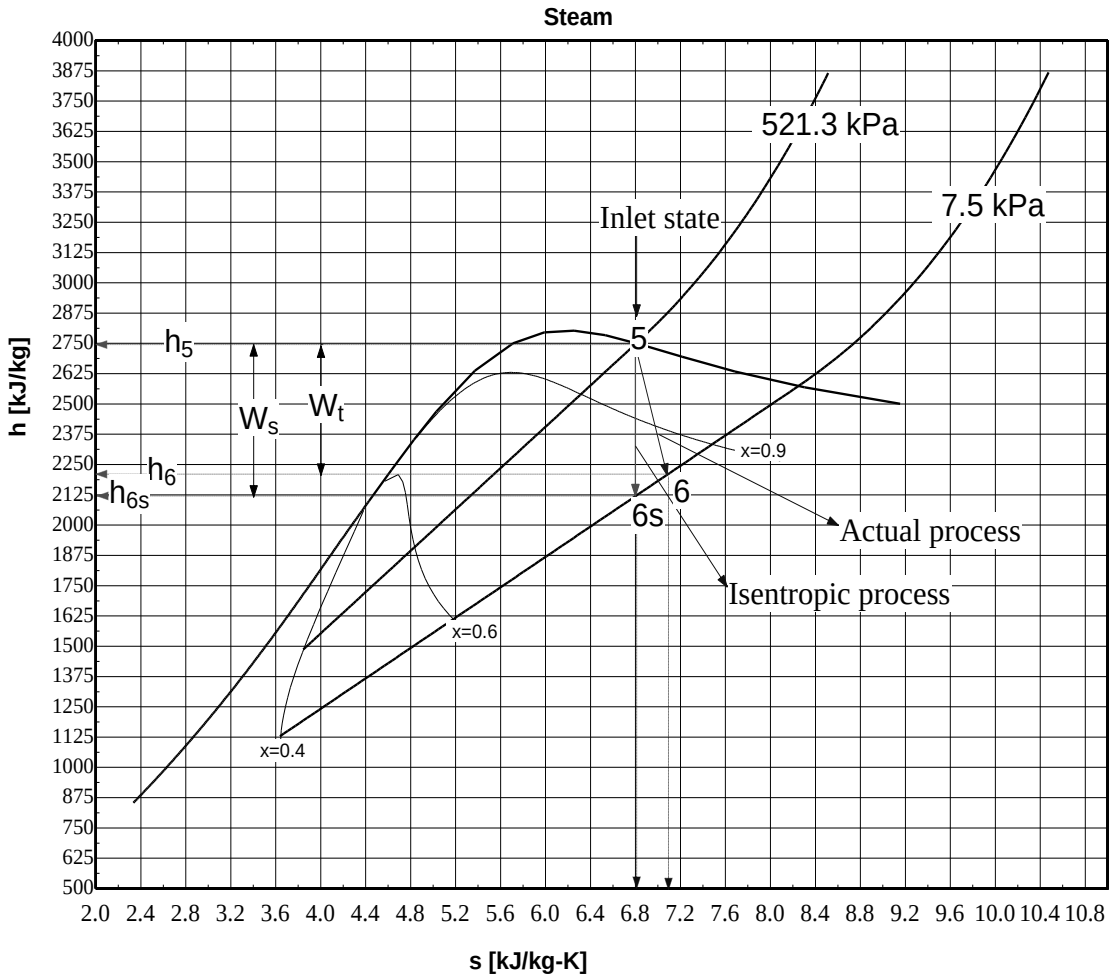

Figure 2.8: h-s diagram for turbine operation with inlet and exit pressures of 521.3 kPa and 7.5 kPa respectively

The actual turbine power is calculated using the actual enthalpy of the geothermal fluid at state 6 by help of Eq. 2.23

$$W_{gen} = W_{tur} \times \eta_{gen} \quad [2.23]$$

Equation 2.24 shows the expression for exergy balance in the turbine,

$$E_5 = E_6 + W_{tur} + I_{tur\text{-}gen} \quad [2.24]$$

where $I_{tur\text{-}gen}$ is the exergy loss in the steam turbine, and exergetic efficiency is expressed in Eq. 2.25,

$$\eta_{E,tur\text{-}gen} = \frac{W_{tur}}{E_5 - E_6} \quad [2.25]$$

IV. Condenser

The primary purpose of the condenser is to condense the exhaust steam leaving the turbine for reuse in the cycle and to maximize turbine efficiency by maintaining proper vacuum. The circulating water system supplies cooling water to the turbine condensers and thus acts as the vehicle by which heat is rejected from the steam cycle to the environment.

Figure 2.9 illustrates the temperature distribution in the condenser. The circulating-water inlet temperature should be sufficiently lower than the steam-saturation temperature. To get reasonable values of ΔT_o or Total Temperature Difference (TTD) it is usually recommended that ΔT_i should be between 11 and 20 °C and that ΔT_0, should not be less than 2.8 °C (El-Wakil, 1984). The enthalpy drop and turbine work per unit pressure drop is much greater at the low-pressure end than the high-pressure end of a turbine.

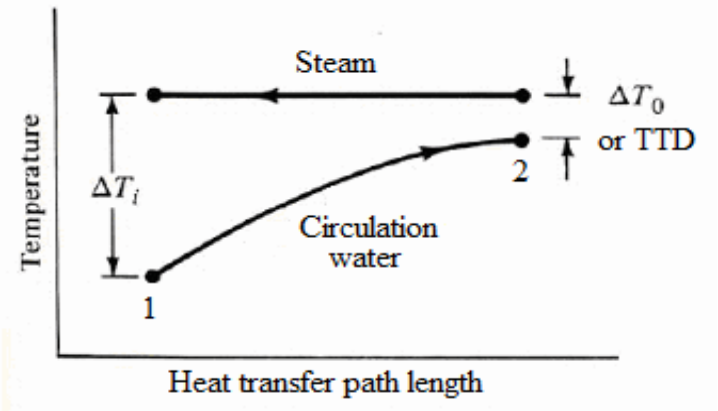

Figure 2.9: Condenser temperature distribution. (Source: Siregar, 2004)

There exist two types of condensers, which are direct contact and surface condensers. The most common type used in geothermal power plants (GPPs) is direct-contact condensers (Siregar, 2004) which is the one used in Olkaria II geothermal power plant. The condenser pressure is 7.5 kPa. Its performance is vital to the efficiency of the power plant itself because as the operating pressure of the condenser is lowered (vacuum increased) the enthalpy drop of the expanding steam in the turbine will also increase. Lowering the condenser pressure has an effect of increasing turbine output, reducing steam flow for a given plant output and increasing the plant exergy efficiency

For a given circulating water flow rate, the water temperature into the condenser determines the operating pressure of the condenser. As this temperature increases, the condenser pressure will also increase. Increase in pressure will hence decrease the plant output and efficiency. Therefore, to ensure increased plant output and efficiency the inlet water temperature to condenser should be lowered. The typical condensate temperature attained in practice is 45-50°C, corresponding to a condenser pressure of 9.6-12.5 kPa (El-Wakil, 1984; Moghaddam, 2006).

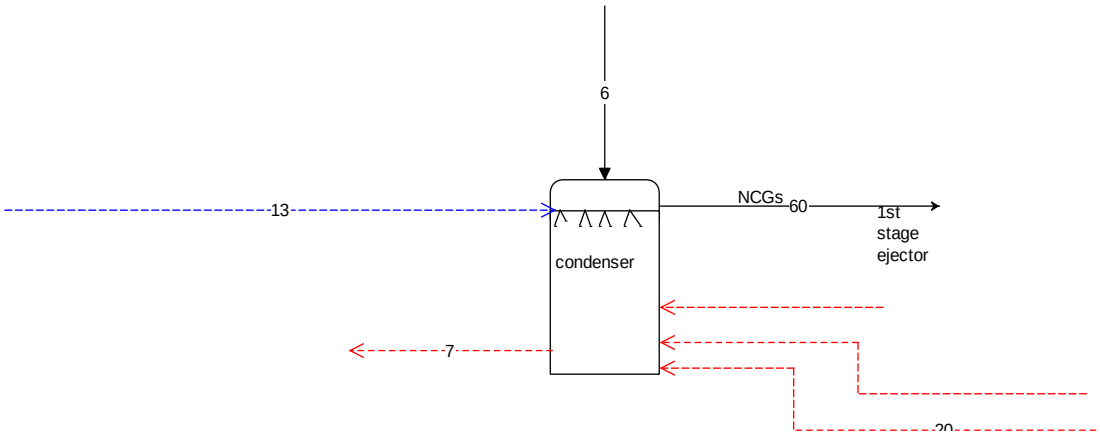

Figure 2.10: Condenser inlets and outlets

Heat rejected in the condenser is expressed as

$$Q_{cond} = \dot{m}_6 h_6 - \dot{m}_{60} h_{60} - \left[\dot{m}_{l,6} + \left(\dot{m}_{s,6} - \dot{m}_{s,60} \right) \right] h_7 \qquad [2.26]$$

Note, for direct contact condensers

$$\dot{m}_{cw} \text{ or } \dot{m}_{13} = \frac{\left(Q_{cond} - \dot{m}_{62} \times \left(h_7 - h_{62} \right) \right)}{h_7 - h_{13}} \qquad [2.27]$$

Equation 2.28 shows the expression for exergy balance in the condenser,

$$E_6 + E_{13} + E_{20} = E_7 + E_{60} + I_{cond} \quad [2.28]$$

where I_{cond} is the exergy loss in the condenser, and the exergetic efficiency is given by Eq. 2.29,

$$\eta_{E,cond} = \frac{E_{7cw} - E_{13} - E_{20cw}}{E_6 + E_{20,\ steam} - E_{7,steam}} \quad [2.29]$$

V. Cooling Tower

Power plants generate large quantities of waste heat that is often discarded through cooling towers to the environment. A cooling tower is an evaporative heat transfer device in which atmospheric air cools warm water, with direct contact between the water and the air, by evaporating part of the water (Siregar, 2004).

Equation 2.30 shows the expression for the coefficient of performance (COP) of the cooling tower,

$$COP = \frac{E_{10} - E_{11}}{W_{fans} + W_{pumps}} \quad [2.30]$$

where W_{fans} and W_{pumps} is the electric power consumed by the fans and pumps respectively.

VI. Non-Condensable Gas Removal System

For the case of steam jet ejectors (SJES) the exergy balance is expressed by Eq. 2.31,

$$I_{sjet1} = E_{60} + E_{4a} - E_{61} \quad [2.31]$$

where I_{sjet1} is the exergy loss in the ejector, and Eq. 2.32 shows the expression for the exergetic efficiency,

$$\eta_{E,sjet1} = \frac{E_{60} + E_{4a} - I_{sjet1}}{E_{60} + E_{4a}} \quad [2.32]$$

VII. Inter and After Condenser

By condensing the vapour prior to the next stage, the vapour load is reduced. This allows smaller NCG removal systems to be used and reduce steam consumption. (Birgenheier et al., 1993; Swandaru, 2006)

Inter condenser heat load is expressed as,

$$Q_{ic}=\dot{m}_{s,61}\times h_{s,61}+\dot{m}_{NCG,61}\times h_{NCG,61}- \dot{m}_{s,62}\times h_{s,62}-\dot{m}_{NCG,62}\times h_{NCG,62}-\left[\left(\dot{m}_{s,61}-\dot{m}_{s,62}\right)\right]\times h_{20} \quad [2.33]$$

Using the value of Eq. 2.33, cooling water mass flow rate is expressed in Eq. 2.34,

$$\dot{m}_{cw}=\frac{Q_{ic}}{\left(h_{20}-h_{19}\right)} \quad [2.34]$$

Equation 2.35 shows the expression for exergy loss at the inter-condenser, I_{ic} whereas Eq. 2.36 shows the expression for exergetic efficiency.

$$I_{ic}=E_{61}+E_{19}-E_{62}-E_{20} \quad [2.35]$$

$$\eta_{E,ic}=\frac{E_{61}+E_{19}-I_{ic}}{E_{61}+E_{19}} \quad [2.36]$$

After condenser heat load is expressed as,

$$Q_{ac}=\dot{m}_{s,63}\times h_{s,63}+\dot{m}_{NCG,63}\times h_{NCG,63}-\dot{m}_{s,31}\times h_{s,31}-\dot{m}_{NCG,63}\times h_{NCG,25} \quad [2.37]$$

where Q_{ac} is the heat transferred in the after condenser.

Using Eq. 2.37, the cooling water mass flow rate is expressed as in Eq. 2.38,

$$\dot{m}_{cw,2}=\frac{Q_{ac}}{\left(h_{25}-h_{24}\right)} \quad [2.38]$$

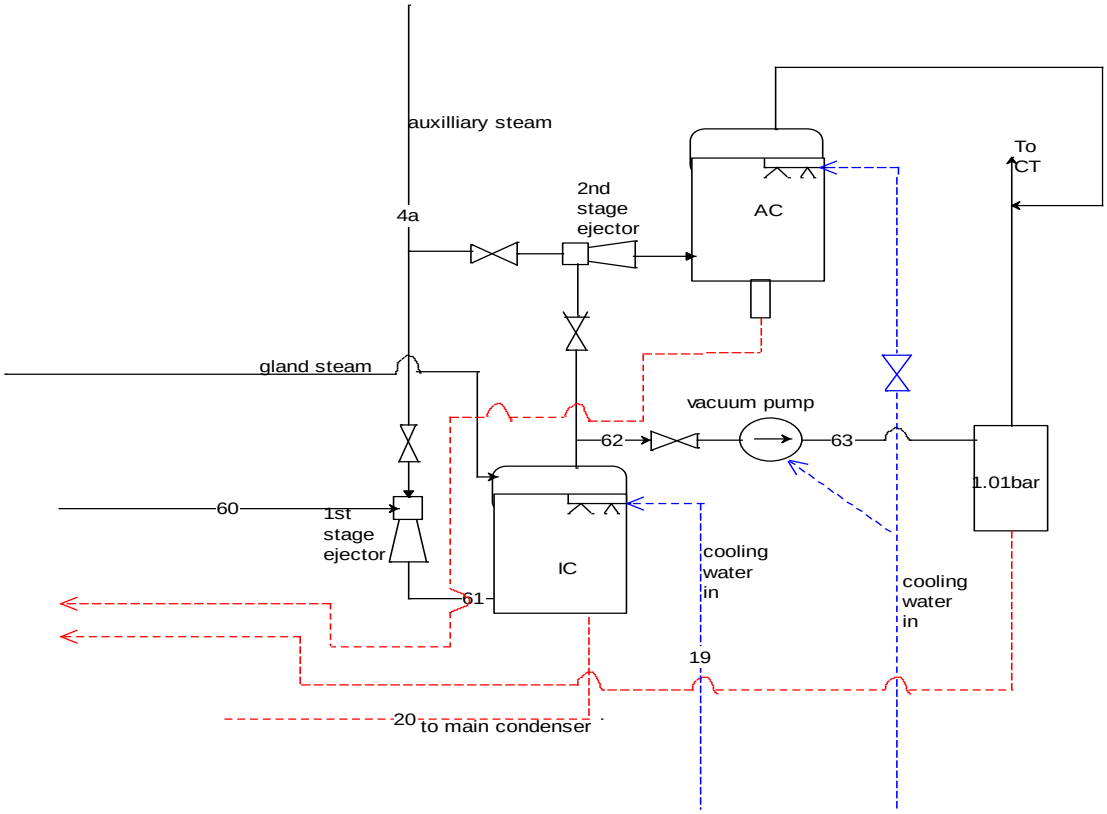

Figure 2.11: Gas extraction system

Equation 2.39 shows the expression for exergy loss in the after condenser, I_{ac} whereas the exergetic efficiency is given by Eq. 2.40.

$$I_{ac}=E_{63}+E_{24}-E_{31}-E_{25} \quad [2.39]$$

$$\eta_{E,ac}=\frac{E_{63}+E_{24}-I_{ac}}{E_{63}+E_{24}} \quad [2.40]$$

2.2.2 Absorption Chiller

2.2.2.1 Principle of operation of absorption chiller

Absorption chillers powered by waste geothermal energy can be used to serve as an intermediate cooling system between the cooling tower and the condenser. This will facilitate further cooling of the water from the cooling tower before inlet into the condenser. The system has the capacity to cool water to a temperature as low as 10^{o}C.

At point 21 in Fig.2.12 the solution rich in refrigerant and a pump forces the liquid through a solution heat exchanger (SHX) to the desorber numbered 23. The process increases the temperature in the SHX.

The added thermal energy in the desorber by the process boils off the refrigerant from the solution. The refrigerant vapor (27) flows to the condenser, where heat is rejected as the refrigerant condenses. The condensed liquid (28) flows through the refrigerant heat exchanger (RHX) where more heat is rejected. The condensed liquid then flows through a flow restrictor (Expansion Valve 2, EV2) to the evaporator (30) thus lowering its pressure. This change in pressure allows the evaporator temperature to be low enough for the refrigerant to absorb heat from the water being cooled (12). The change in pressure also allows the condenser temperature to be high enough for the refrigerant to reject heat to the cooling water (16) at normal available temperatures. The heat from the cooling water (evaporator load) evaporates the refrigerant, which flows back to the absorber through the RHX (32). At the desorber exit (24) the steam consisting of absorbent solution, is cooled in the SHX before flowing back to absorber (26).

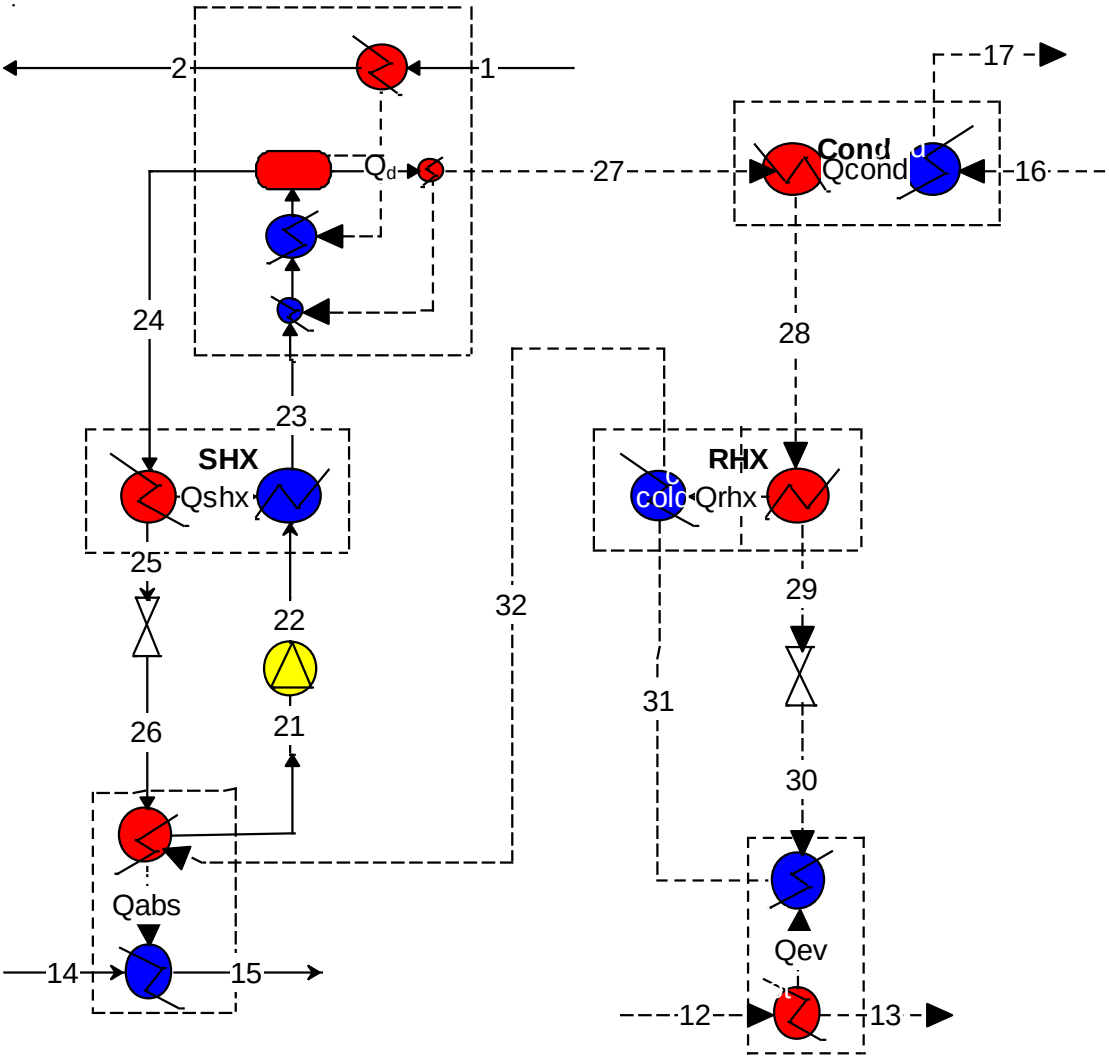

Figure 2.12: Absorption Refrigeration System

In order to perform estimation of equipment sizing and performance of the absorption chiller, the following assumptions were considered; there is no pressure change except through the flow restrictors and pumps, the solution pump is adiabatic and is used to maintain the constant solution level in the desorber, the pump is isentropic, there are no jacket heat losses, the system is operating in a steady state and only two pressures exist i.e., high pressure zone and low pressure zone

For mass balance, each component is treated as a control volume with inlet and outlet of flows. It is considered that the total mass flow rate into system is equal to the total mass flow rate out of the system as shown in Eq.2.4, whereas the energy balance is expressed in Eq. 2.41.

$$Q=\dot{m}\times\left(h_a-h_b\right) \quad [2.41]$$

where $\dot{m}$ is mass flow rate, h is enthalpy and a and b are state points

For heat exchangers Eq. 2.42 will be applicable, where ΔT_{lm} is expressed in Eq. 2.43.

$$Q=UA\Delta T_{lm} \quad [2.42]$$

where

$$\Delta T_{lm}=\frac{\left(T_{h,1}-T_{c,2}\right)-\left(T_{h,2}-T_{c,1}\right)}{\ln\frac{\left(T_{h,1}-T_{c,2}\right)}{\left(T_{h,2}-T_{c,1}\right)}} \quad [2.43]$$

U=coefficient of heat transfer of the material used for the heat exchanger tubes, in this case copper

A=Area of the heat exchanger system

ΔT_{lm} = Logarithmic Mean Temperature Difference

Where, h and c are referred as hot and cold sides, respectively. The subscript 1 and 2 refer to either end of heat exchanger.

In modeling of absorption refrigeration system both mass and energy balance equations form the basis of other expressions. The subscript numbers in the equation refers to state points in Fig.2.12.

2.2.2.2 Absorption chiller components modeling

I. Absorber

Pressure drop is assumed to be zero and solution exit as saturated liquid.

Mass balance for the absorber is given by Eq. 2.44, whereas energy balance is expressed as in Eq. 2.45

$$\dot{m}_{21}=\dot{m}_{26}+\dot{m}_{32} \quad [2.44]$$

$$Q_{abs}=\dot{m}_{26}h_{26}+\dot{m}_{32}h_{32}-\dot{m}_{21}h_{21}=\dot{m}_{14}\left(h_{15}-h_{14}\right) \quad [2.45]$$

Equation 2.46 shows the expression for heat transfer rate,

$$Q_{abs}=U.A_{abs}.LMTD_{abs} \quad [2.46]$$

where subscript *abs* refers to absorber and Eq. 2.47 shows the expression for logarithmic mean temperature difference,

$$LMTD_{abs}=\frac{(T_{26}-T_{15})-(T_{21}-T_{14})}{\ln\frac{(T_{26}-T_{15})}{(T_{21}-T_{14})}} \quad [2.47]$$

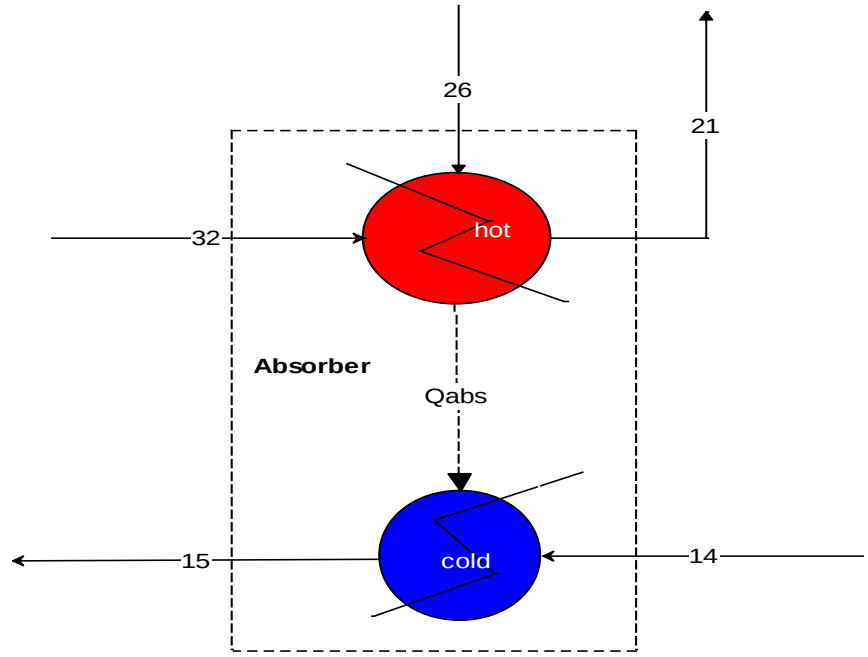

Figure 2.13: Absorber subsystem

II. Desorber

Mass balance for the desorber is expressed by Eq. 2.48, whereas energy balance is given by Eq. 2.49.

$$\dot{m}_{23}=\dot{m}_{24}+\dot{m}_{27} \quad [2.48]$$

$$Q_d=\dot{m}_{24}h_{24}+\dot{m}_{27}h_{27}-\dot{m}_{23}h_{23}=\dot{m}_1(h_1-h_2) \quad [2.49]$$

Equation 2.50 shows the expression for heat transfer rate in the desorber,

$$Q_d=U.A_d.LMTD_d \quad [2.50]$$

where subscript d refers to desorber and Eq. 2.51 shows the expression for the logarithmic mean temperature difference,

$$LMTD_d = \frac{(T_1 - T_{24}) - (T_2 - T_{27})}{\ln \frac{(T_1 - T_{24})}{(T_2 - T_{27})}} \quad [2.51]$$

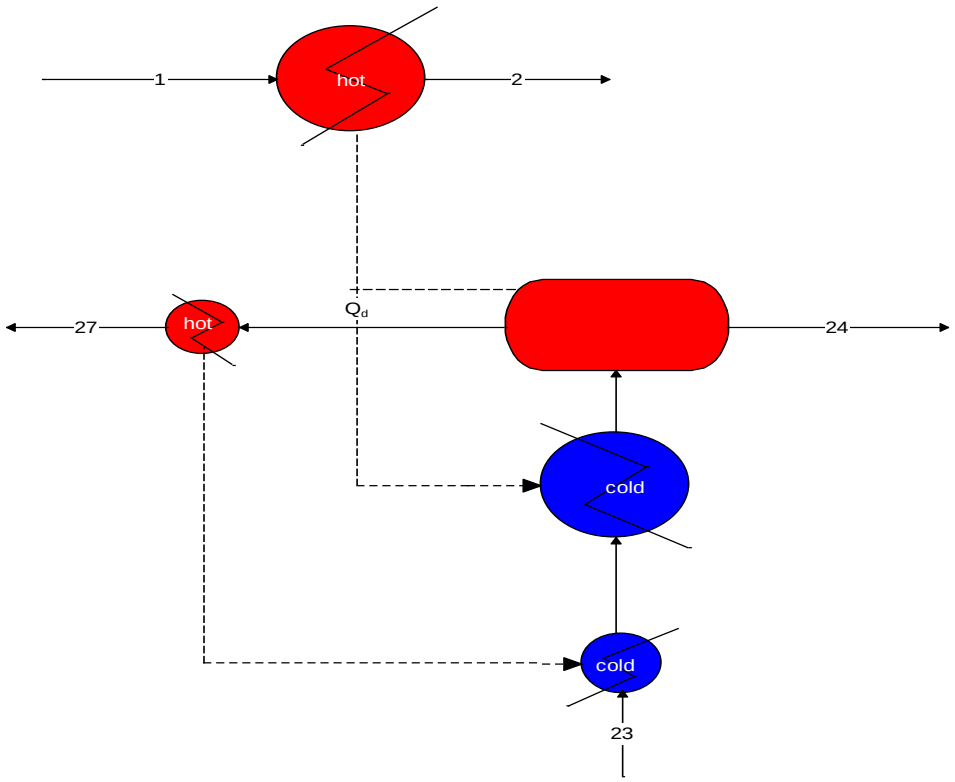

Figure 2.14: Desorber subsystem

III. Condenser

The condenser was modeled as a heat exchanger, and zero pressure drop was assumed. The refrigerant was assumed to leave the condenser as saturated liquid.

Mass balance for the condenser is expressed by Eq. 2.52 whereas energy balance is given by Eq. 2.53,

$$\dot{m}_{27} = \dot{m}_{28}. \quad [2.52]$$

$$Q_c = \dot{m}_{27} h_{27} - \dot{m}_{28} h_{28} = \dot{m}_{16} (h_{17} - h_{16}) \quad [2.53]$$

Equation 2.54 shows the expression for heat transfer rate,

$$Q_c = U.A_c.LMTD_c \quad [2.54]$$

where subscript c refers to condenser and Eq. 2.55 shows the expression for the logarithmic mean temperature difference,

$$LMTD_c = \frac{(T_{28}-T_{16})-(T_{27}-T_{17})}{\ln\frac{(T_{28}-T_{16})}{(T_{27}-T_{17})}} \quad [2.55]$$

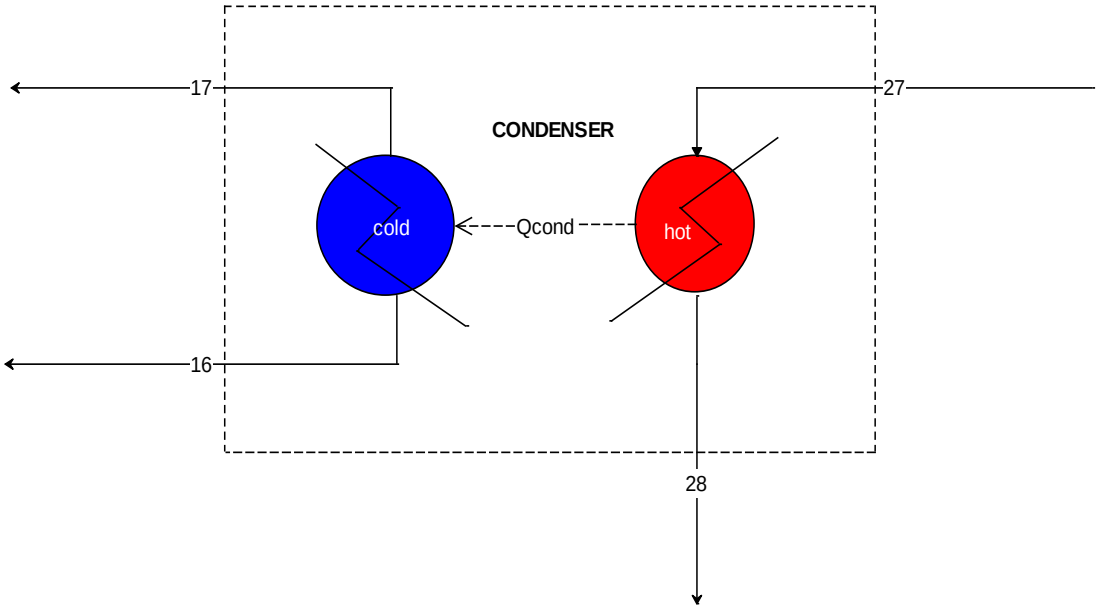

Figure 2.15: Condenser subsystem

IV. Evaporator

Modeling of the evaporator was similar to that of the condenser. It was assumed that there was no pressure drop and the quality of the refrigerant vapor at exit was one.

Mass balance for the evaporator is expressed by Eq. 2.56, whereas energy balance is given by Eq. 2.57,

$$\dot{m}_{30} = \dot{m}_{31} \quad [2.56]$$

$$Q_e = \dot{m}_{31}h_{31} - \dot{m}_{30}h_{30} = \dot{m}_{12}(h_{12}-h_{13}) \quad [2.57]$$

Equation 2.58 shows the expression for heat transfer rate,

$$Q_e = U.A_e.LMTD_e \quad [2.58]$$

where subscript e refers to evaporator and Eq. 2.59 shows the expression for the logarithmic mean temperature difference,

$$LMTD_e = \frac{(T_{12}-T_{31})-(T_{13}-T_{30})}{\ln\frac{(T_{12}-T_{31})}{(T_{13}-T_{30})}} \quad [2.59]$$

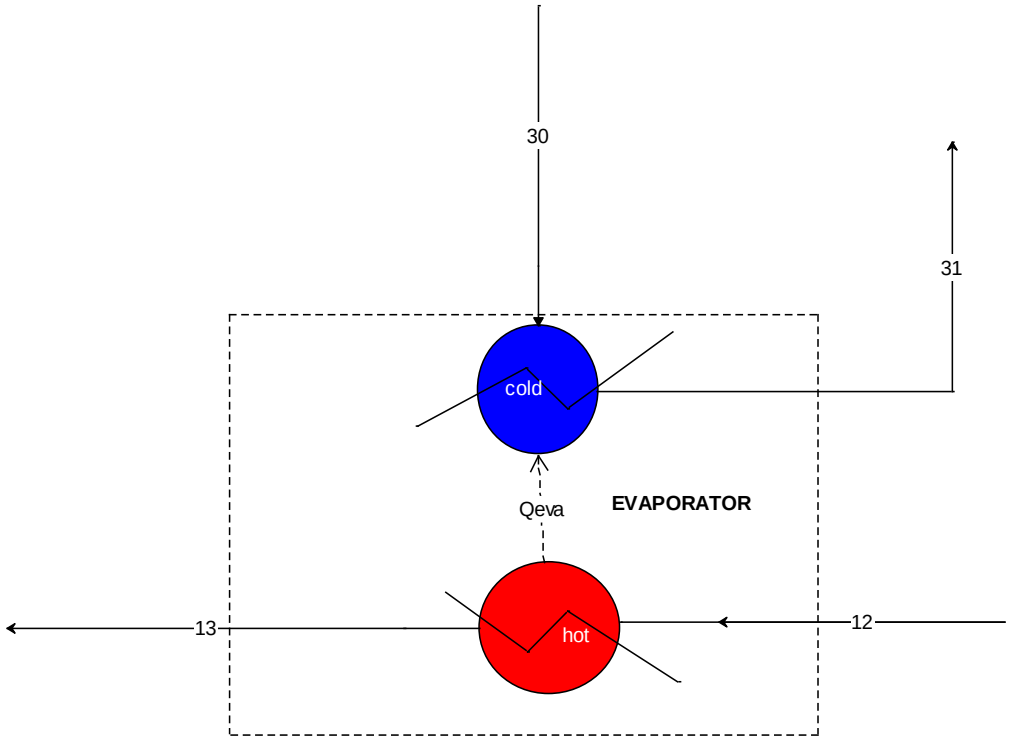

Figure 2.16: Evaporator subsystem

V. Solution heat exchanger

Mass balance for the solution heat exchanger is given by Eq. 2.60 whereas the energy balance is expressed in Eq. 2.61,

$$\dot{m}_{22}=\dot{m}_{23}=\dot{m}_{24}=\dot{m}_{25}. \quad [2.60]$$

$$Q_{SHX}=\dot{m}_{23}h_{23}-\dot{m}_{22}h_{22}=\dot{m}_{24}(h_{24}-h_{25}) \quad [2.61]$$

Equation 2.62 shows the expression heat transfer rate,

$$Q_{SHX}=U.A_{SHX}.LMTD_{SHX} \quad [2.62]$$

where subscript SHX refers to solution heat exchanger and Eq. 2.63 shows the expression for the logarithmic mean temperature difference,

$$LMTD_{SHX} = \frac{(T_{24}-T_{23})-(T_{25}-T_{22})}{\ln\frac{(T_{24}-T_{23})}{(T_{25}-T_{22})}} \quad [2.63]$$

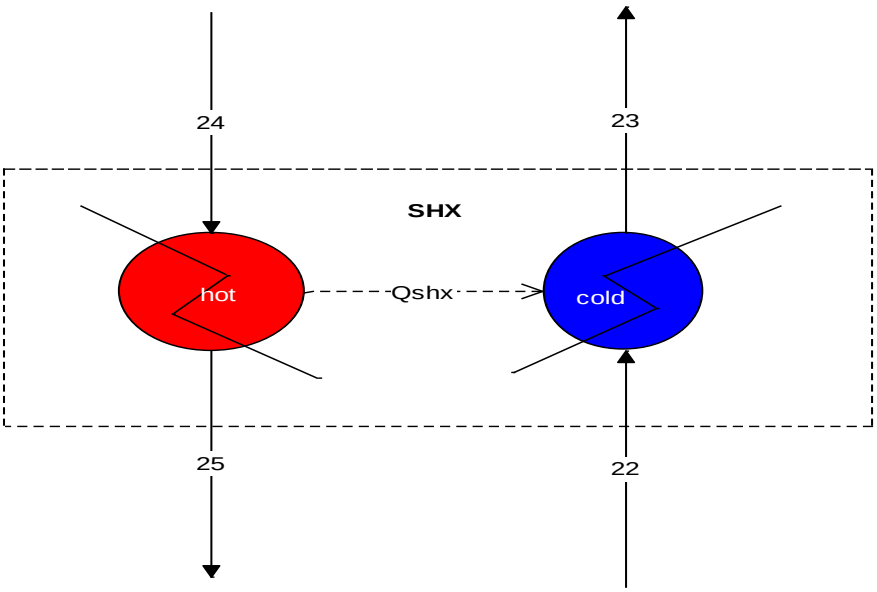

Figure 2.17: Solution Heat Exchanger subsystem

VI. Refrigerant heat exchanger

Mass balance for the refrigerant heat exchanger is given by Eq. 2.64,

$$\dot{m}_{28}=\dot{m}_{29}=\dot{m}_{30}=\dot{m}_{31} \quad [2.64]$$

Energy balance for the refrigerant heat exchanger is expressed as in Eq. 2.65,

$$Q_{RHX}=\dot{m}_{28}h_{28}-\dot{m}_{29}h_{29}=\dot{m}_{30}(h_{32}-h_{31}) \quad [2.65]$$

Heat transfer rate is determined by Eq. 2.66,

$$Q_{RHX}=U.A_{RHX}.LMTD_{RHX} \quad [2.66]$$

where subscript RHX refers to refrigerant heat exchanger and Eq. 2.67 shows the expression for the logarithmic mean temperature difference,

$$LMTD_{RHX} = \frac{(T_{28}-T_{32})-(T_{29}-T_{31})}{\ln\frac{(T_{28}-T_{32})}{(T_{29}-T_{31})}} \quad [2.67]$$

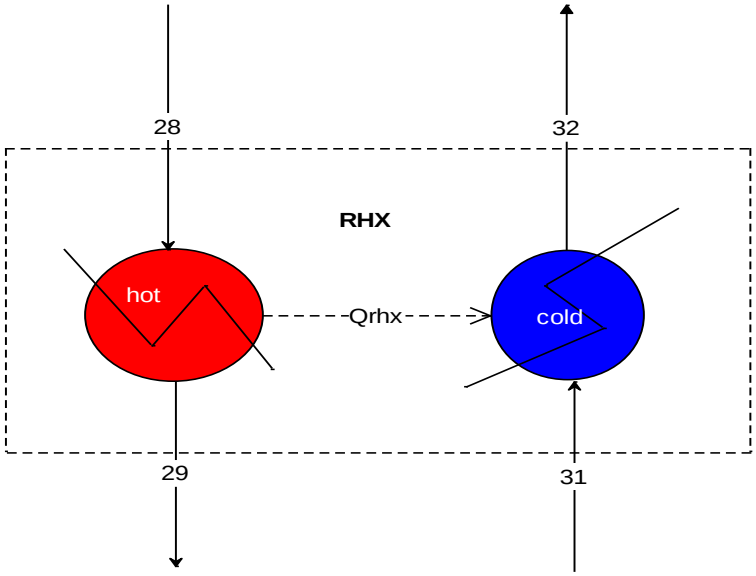

Figure 2.18: Refrigerant Heat Exchanger subsystem

VII. Pump

A pump is used between states 21 and 22 in the single effect model as shown in Fig. 2.12. The pumps require only one input, the exit pressure. Pump efficiency may also be included, but the default value of 100% was used because of the negligible effect on the overall cycle of choosing a different efficiency. The work of the pump is less than 0.1% of the heat duties of the other components (Fox and Mcdonald, 1992). This means that all of the work by the pump is added directly to the enthalpy of the working fluid as expressed in Eq. 2.68.

$$h_{in} = h_{out} + W_{pump} \quad [2.68]$$

VIII. Valves

The other pressure change devices needed to model the cycle are valves. Equation 2.69 shows that there is no enthalpy change across the device. For the single effect cycle there is one refrigerant and one solution expansion valve (EV). The valve model is self-explanatory; one only needs to give the exit pressure or some equivalent (i.e. pressure ratio).

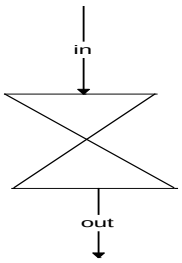

Figure 2.19: Expansion Valve

$$h_{in} = h_{out} \quad [2.69]$$

2.2.2.3 Performance Evaluation of the system

Equation 2.70 shows that in an absorption chiller the sum of heat transferred in the condenser and absorber is approximately equal to the sum of heat transmitted in the desorber and evaporator. The coefficient of performance (COP) of the absorption system as expressed in Eq. 2.71 is the ratio of the heat transferred in the evaporator to the heat transferred in the desorber.

$$|Q_c + Q_{abs}| = |Q_d + Q_e| \quad [2.70]$$

$$COP = \frac{Q_e}{Q_d} \quad [2.71]$$

Chapter Three

Methodology

3.1 Collection of model parameters

The Parameters, which were considered during data collection, were pressure, mass flow rate and temperature at various state points. These model parameters are outlined in detail in Appendix B and were collected from actual plant operation log sheets which included the turbine log sheets, auxiliary log sheets and occurrence books. Others were obtained through observation of the field operating conditions while those that could not be directly measured due to fiber communication breakdown to control room were software estimated.

3.2 Absorption chiller model

In this research the absorption chiller has been modelled to suite the application. The models were based on a simple steady state and the main equations were formulated on the basis of mass and energy balance as expressed in Eq. 2.4 and 2.41. Besides the basic thermodynamic principles of mass and energy balance, Eq. 2.42 and 2.43 and effectiveness type of heat exchanger models are used for most of the chiller system. The desorber and absorber were modelled as adiabatic flash drum for two-phase mixture where the mixture i.e., the absorbent and refrigerant are in equilibrium and the exiting vapour in the desorber is pure water.

A single effect absorption refrigeration system that uses water as the refrigerant and lithium Bromide as the absorbent has been adopted. Compared to other absorbents, lithium bromide has great affinity for water vapor. The absorption refrigeration system was connected between the cooling tower and the condenser as shown in Fig. 2.5. The desorber was connected to brine that was discharged from the separator to provide the needed thermal heat for the system. The cooling water from cooling tower was channeled to the evaporator then discharged to the main plant condenser.

The model parameters that were measured included pressure, temperature and mass flow rate of the fluid at the absorber and condenser state points for cooling water inflow and outflow as well as the temperature, mass flow rate and pressure for heat source at the desorber state points within the system. The measured parameters served

as inputs to the modelled system for simulation on Engineering Equation Solver (EES). These parameters were essential for calculating the coefficient of performance of the absorption refrigeration system.

Efficiency of an absorption refrigeration system is easily expressed by a Coefficient of Performance (COP), which is defined as the ratio between the amount of heat/energy absorbed from the environment by the evaporator and the heat/energy supplied to the desorber to operate the cycle, the pump and fans if available. As the energy supplied to the absorption system, is very small compared to the amount of heat supplied to the desorber, the amount of work was excluded from the calculation. The heat energy was calculated from the brine discharged from the separator. A refrigeration cycle is optimized, when it can give more of a cooling effect for the same amount of heat that is supplied to the system in order to complete an operation cycle.

Equation 3.1 shows the expression for the COP of the absorption chiller,

$$COP_{chiller} = \frac{Q_{evaporator}}{Q_{desorber} + W_{solution}} \qquad [3.1]$$

3.3 Code development and Simulation

Each subsystem was considered within the power plant as a control volume with distinct inflow and outflow. For a steady-flow process, the balance equations for mass, energy, entropy and exergy were applied. This was to help evaluate work and heat interaction, the rate of exergy decrease, the rate of irreversibility, as well as the energy and exergy efficiencies. For mass, energy, entropy and exergy balance Eq. 2.4 to 2.8 were used. Once the equations were formulated, EES codes were developed using Eq. 2.9 as the guiding equation and simulated to determine the output parameters as shown in Fig 3.1.

The flow diagram of exergy balance module is shown in Fig. 3.1. As it is demonstrated, exergy balance module mainly consists of two sub-modules namely exergy losses and exergetic efficiencies.

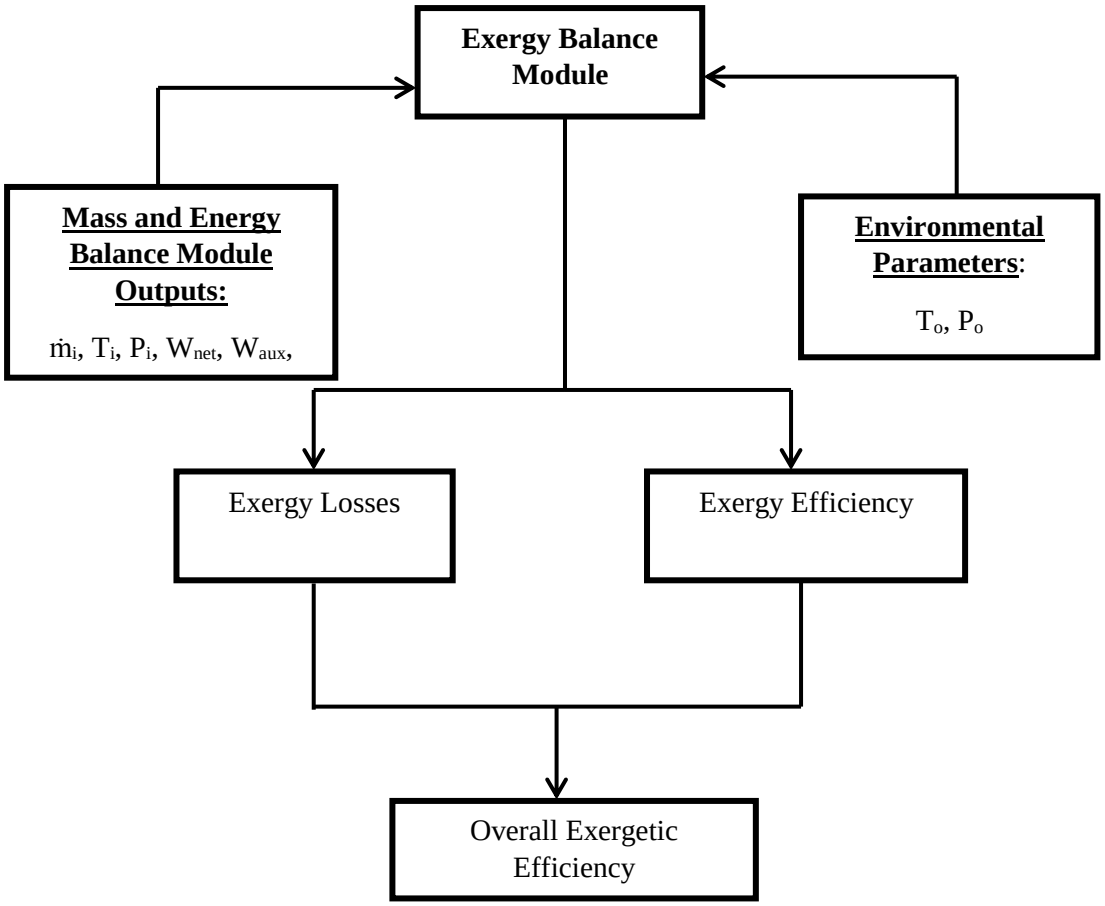

Figure 3.1: Exergy flow simulation process. (Source: Ozcan, 2010)

During the code development for the exergy balance modules the input parameters were environmental parameters (dead state temperature and pressure), and mass and energy balance outputs that included; Mass flow rate, temperature and pressure output at each state of the plant for unknown values, auxiliary power of pumps and fans, turbine power output, net power output and generator power output.

The thermodynamical definitions and equations of exergy balance are given in Chapter 2. The module first calculates exergy of each state by Eq. 2.9 considering input parameters explained above. Then exergy losses/destroyed and exergetic efficiencies of each component of the plant is computed as expressed in Eq. 2.6 and 2.10 respectively. The module results with the determination of overall exergetic efficiency of the plant as given in Eq. 2.11.

Simulation for the proposed geothermal power plant with a hybridized cooling system was conducted based on the new design parameters. Using the Engineering Equation Solver, mathematical models formulated were simulated to compute the output

properties of the system. Iterations were run at varying cooling water temperatures to establish the optimum operating conditions of the hybridized system. Aqueous lithium bromide solutions have a tendency to crystalize when passing through an expansion valve into the absorber. To prevent crystallization the chiller system parameters were designed appropriately. Hence, during simulation the temperature margin between critical point and crystallization temperature was maintained at minimum of 10^{o}C temperature difference. Plots for various operating conditions were generated using EES software. The simulation results for the plant with hybridized cooling system was then compared with the current plant in Olkaria II in terms of power output and overall energy and exergy efficiencies.

3.4 Economic analysis module

The module uses mass and energy module and economical parameters such as interest, electricity sale price, operation and maintenance costs, Absorption refrigeration system cost as inputs as shown in Fig. 3.2. The mass and energy modules are essential in the determination of area of each subsystem. Based on these inputs the total cost of the investment was computed. The amount of power gained annually after simulation of the proposed plant design was multiplied with the sale price of electricity to determine the annual net revenue. By subtracting the annual operation and maintenance cost the annual cash flow was estimated. Using the discounted payback period analysis tool with an interest rate of 16% (Rotich, 2015) and operation and maintenance cost estimated at 0.00763 US $/kWh (Energy Regulation Commission, 2009), the payback period for the investment was computed as shown in Table 4.9. According to Ngugi (2012) the payback period of a geothermal investment is assumed to vary between 5 – 12 years.

In estimating the discounted cash inflow, Eq.3.2 was used.

$$\text{Discounted cash inflow} = \frac{\text{Actual cash inflow}}{(1+i)^n} \qquad [3.2]$$

where i is the interest rate and n is the period to which the cash inflow relates and Eq. 3.3 expresses the discounted payback period.

$$\text{Discounted Payback Period} = A + \frac{B}{C} \qquad [3.3]$$

where A is the last period with a negative discounted cumulative cash flow, B is the absolute value of discounted cumulative cash flow at the end of the period and C is the discounted cash flow during the period after A.

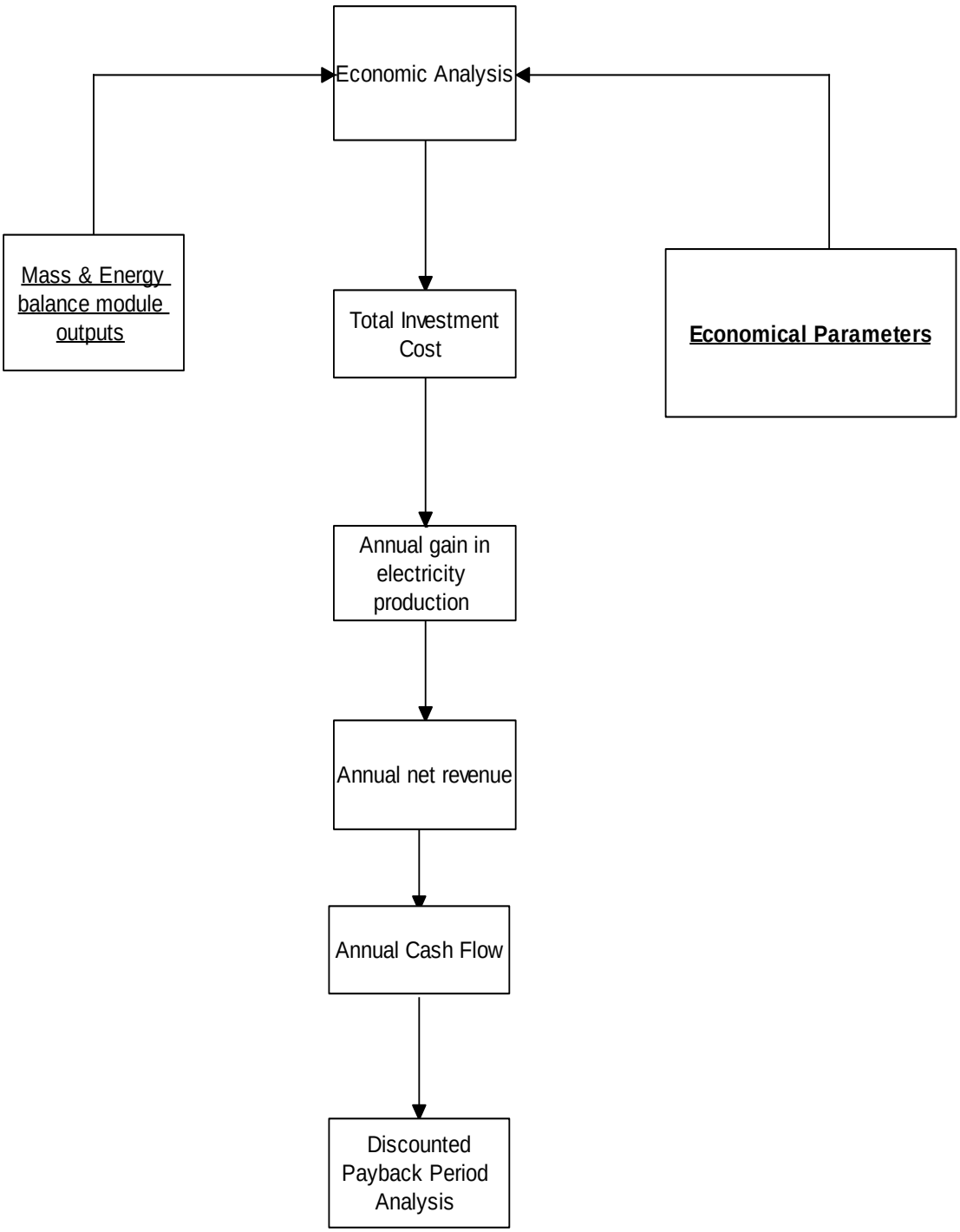

Figure 3.2: Flow diagram illustrating economical analysis module

Chapter Four

Results and Discussions

4.1 Simulation

The objective of simulation was to carry out an exergy analysis of Olkaria II power plant as well as evaluate the effect of condenser pressure on power output by varying cooling water temperature. The simulation results were classified into two categories explained as section 4.1.1 and 4.1.2.

4.1.1 Exergy analysis results for the current system design

Table 4.1 gives the simulation results of performance of each subsystem in terms of exergy wasted, exergy destroyed and exergetic efficiency. Table 4.2 outlines the energy and exergy efficiency of the power plant as well as the coefficient of performance of the cooling tower.

Table 4.1: Exergy wasted, destroyed and efficiency for specific subsystem.

Subsystem	Total exergy (MW)	Total Desired exergy output (MW)	Total Exergy wasted (MW)	Total Exergy destroyed (MW)	Exergetic efficiency (%)
Separator	196.6	174.78	21.5	0.34	88.9
Transmission lines for unit 3	56.0	55.19	0.85	0	98.5
Steam scrubber	53.97	53.24	0.54	0.188	98.8
Turbine	53.24	37.5	8.04	7.7	83.6
Condenser	8.04	5.0	0.15	2.89	39.7

Table 4.2: Other subsystems efficiencies.

Coefficient of performance (COP) of Cooling Tower	5.6
Energy Efficiency of turbine	18.2%
Overall Exergetic efficiency of Plant as a function of steam into transmission lines	58.4%
Overall Exergetic efficiency of Plant as a function of geo-fluid	49.9%

The total exergy available for Olkaria II power plant is 196.6 MW. Of this available exergy 21.5 MW exit as brine. The brine is re-injected back into the ground. Therefore, 175 MW is what is contained in the steam that is supplied to the plant.

For the case of unit 3, the total exergy into the transmission line is 56 MW out of which 0.85 MW is wasted while 1.31 MW is tapped for steam ejectors. 54 MW of exergy is available at the steam scrubbers of which 0.54 MW is wasted while 0.19 MW is destroyed leaving 53.2 MW as the total exergy available at the turbines inlet. In the turbine the exergy drop amounts to 45.2 MW against a gross work developed by the turbine of 37.5 MW for a steam flow rate of 71.1 kg/s. 7.7 MW of exergy is destroyed in the turbine which accounts for 14% of total exergy into the turbine. From the simulation results the exergy and energy efficiency of unit 3 turbine was found to be 83.6% and 18.2% as shown in Table 4.1 and 4.2 respectively. Exergy of turbine steam exhausted into the condenser amounts to 8.04 MW, accounting for 15% of the exergy entering the turbines.

The power output of unit 3 amounted to 35.6 MW for a condenser pressure of 9.7 kPa and a constant cooling water flow rate of 2194 kg/s with an average temperature of 25^{o}C. The power output is dependent on the condenser operating parameters such as pressure. By condensing the steam exhausted from the turbine an enthalpy drop is created within the turbine which give rise to turbine power output. Results show that out of the 8.04 MW supplied exergy into the condenser 2.89 MW is lost while 0.15 MW is wasted thus leaving 5 MW as the desired exergy in the condenser. Exergy efficiency of the condenser was found to be 39.7% while the gas extraction system efficiency stood at 24%. The efficiency of the condenser is greatly dependent on the ability to condense more steam to avoid steam build-up. The efficiency of gas extraction system to extract more non condensable gases to avoid build-up of pressure that lowers the vacuum also influences the condenser efficiency. The COP of the cooling towers was found to be 5.6.

Based on the exergy analysis of each subsystem, the overall exergy efficiency was evaluated as a function of the geo-fluid into the separator and the steam into the transmission line. The efficiencies were found to be 49.9% and 58.4% respectively.

4.1.2 Exergy analysis for unit 3 system with hybrid system using absorption chiller.

Table 4.3: Exergy wasted, destroyed and efficiency for unit 3 specific subsystems.

Subsystem	Total exergy (MW)	Total Desired exergy output (MW)	Total Exergy wasted (MW)	Total Exergy destroyed (MW)	Exergetic efficiency (%)
Separator	196.62	174.78	21.5	0.34	88.9
Transmission line for unit 3	56.0	55.18	0.85	0	98.5
Steam scrubbers	53.97	53.24	0.54	0.188	98.8
Turbine	53.23	39.13	6.8	7.3	84.3
Condenser	7.34	4.9	0.14	2.3	65.2

Table 4.4: Other subsystems efficiencies.

	Efficiency
Coefficient of performance (COP) of Cooling Tower	16.9
Overall Energy Efficiency	20.3%
Overall Exergetic efficiency of Plant as a function of steam into transmission lines	65.2%
Overall Exergetic efficiency of Plant as a function of geo-fluid	55.7%

Adoption of the hybrid cooling system showed some positive results in terms of power output, condenser and turbine exergy efficiencies, turbine energy efficiency and coefficient of performance of cooling tower. Simulation results in Table A.2 show that by lowering cooling water temperature from 25^{o}C to 16^{o}C the exergy drop in the turbine increased from 45.2 MW to 46.4 MW resulting in power output increasing from 35.6 MW to 37.2 MW. This accounts for 4.4% increase in power output. Tables 4.6 shows that the condenser exergy efficiency increased from 39.7% to 65.2% for a condenser pressure of 5.93 kPa. The coefficient of performance (COP) of the cooling tower also increased to 16.9 from 5.6.

The exergy destroyed in the turbine decreased by 0.4 MW accounting for 0.75% of exergy into the turbine while exergy destroyed in the condenser dropped by 0.59 MW accounting for 7.3% of exergy into the condenser. These results clearly show that by lowering the condenser pressure from 9.7 kPa to 5.9 kPa the condenser exergy

efficiency increases leading to an increase in power output for constant auxiliary power consumption.

In comparison to what was done by Tasha (2009) this system shows an improved efficiency. The simulation results from Tasha showed that by lowering the condenser pressure from 11. 178 kPa to 8.651 kPa an extra power of 131 kW was achieved for a single flash system. In our case by lowering the condenser pressure from 9.7 kPa to 5.93 kPa and extra power of 1.6 MW was achieved for a single flash system.

4.2 Absorption chiller sizing

Using the expression in Eq. 2.42 for each of the chiller component, their areas were computed as shown in Table 4.5. From the table it is clear that the absorber covers the largest area followed by the evaporator while refrigerant heat exchanger covers the least area. Heat exchanger area is dependent on the heat transfer rate, coefficient of heat transfer and the logarithmic mean temperature difference within the component. In sizing the heat exchanger one aims to achieve a higher heat transfer rate while ensuring that the area is considerably small. The essence of this approach is to lower the cost of manufacture and therefore the price.

Table 4.5: Required area of the absorption chiller components.

Component	Area (m^2)
Absorber	2840
SHX	226
Desorber	970
Condenser	919
RHX	93
Evaporator	2163

From the data collected as shown in Table B.1 in appendix B it was clear that the power output during the earlier morning hour (0800 h) was higher compared to other periods of the day. This was attributed to decreased temperatures of the cooling water hence lowered condensing pressure that ultimately translated to increased power output. Based on this fact, the absorption chiller was adopted to ensure lowered cooling water temperature before it entered the condenser.

4.3 Comparison of efficiencies between the current system design and the hybridized cooling system

Table 4.6: Specific subsystem.

Subsystem	Total Desired Exergy		Total Exergy wasted (KW) Unit 3		Total Exergy destroyed (KW) Unit 3		Exergetic efficiency Unit 3 (%)	
	Current	HS	current	HS	current	HS	current	HS
Separator	174.78	174.78	21.5	21.5	0.34	0.34	88.9	88.9
Trans-mission lines	55.19	55.18	0.85	0.85	0	0	98.5	98.5
Steam scrubbers	53.24	53.24	0.54	0.54	0.188	0.188	98.8	98.8
Turbine	37.5	39.13	8.04	6.8	7.7	7.3	83.6	84.3
Condenser	5.0	4.9	0.15	0.14	2.89	2.3	39.7	65.2

Table 4.7: Other subsystems efficiencies.

	Efficiency (Unit 3)	
	Current	Hybrid System (HS)
Coefficient of performance (COP) of Cooling Tower	5.6	16.9
Overall Energy Efficiency	18.2%	20.3%
Overall Exergetic efficiency of Plant as a function of steam into transmission lines	58.4%	65.2%
Overall Exergetic efficiency of Plant as a function of geo-fluid	49.9%	55.7%

4.4 Operating graphs for the power plant with hybridized cooling system

The simulation result show that cooling water temperature from the cooling tower which is also referred to as refrigerant load temperature of 25^{o}C gives a cooling water temperature of 16^{o}C for an evaporator temperature of 9^{o}C ($\Delta T_{cooling}$). Figure 4.1 show that this refrigerant load temperature at constant evaporator temperature gives a condenser pressure of 5.93 kPa. Figure 4.2 shows that with a condenser pressure of 5.93 kPa the exergy efficiency of the condenser is estimated to be 65.2%.

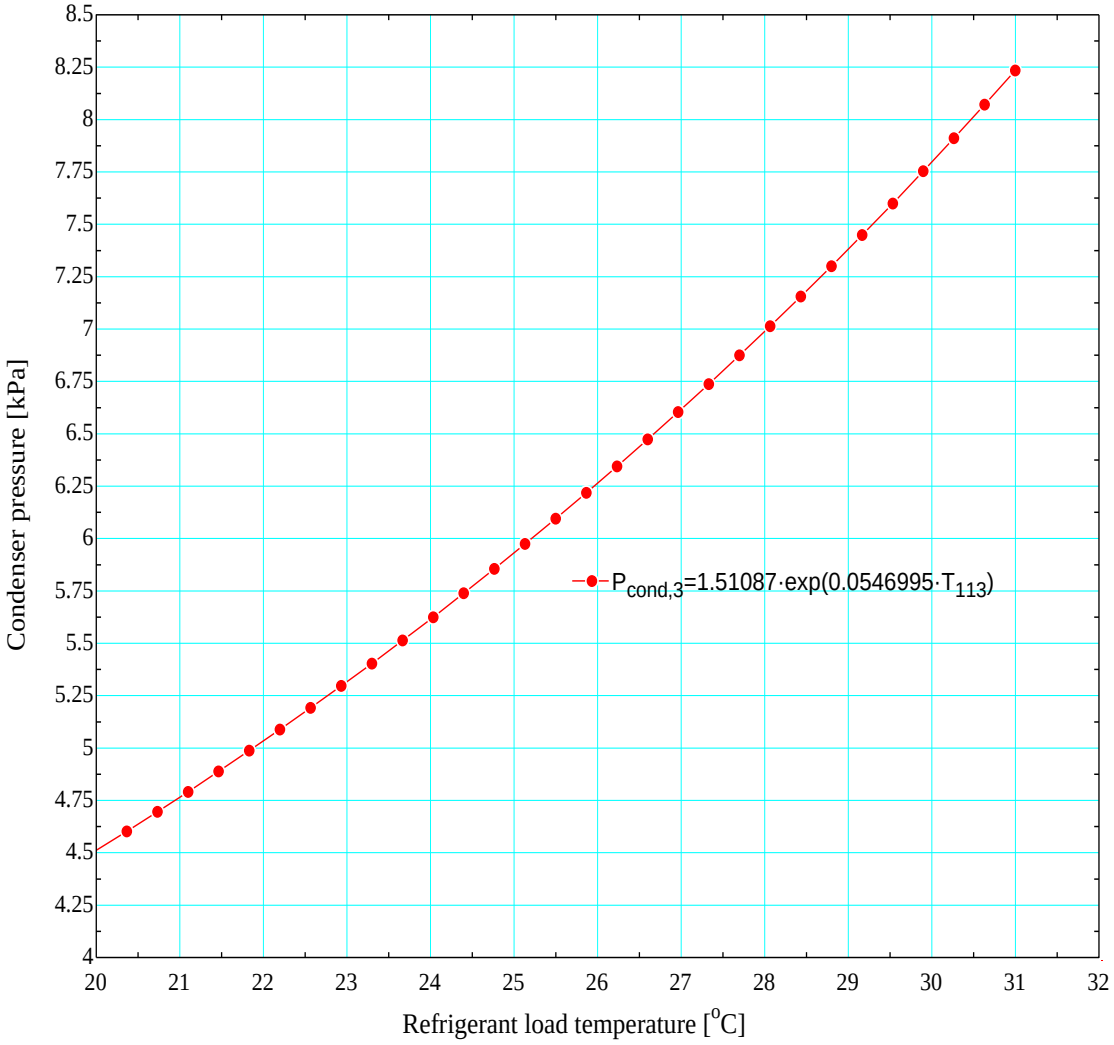

Figure 4.1: A Graph of Condenser pressure (kPa) against refrigerant load temperature (ºC).

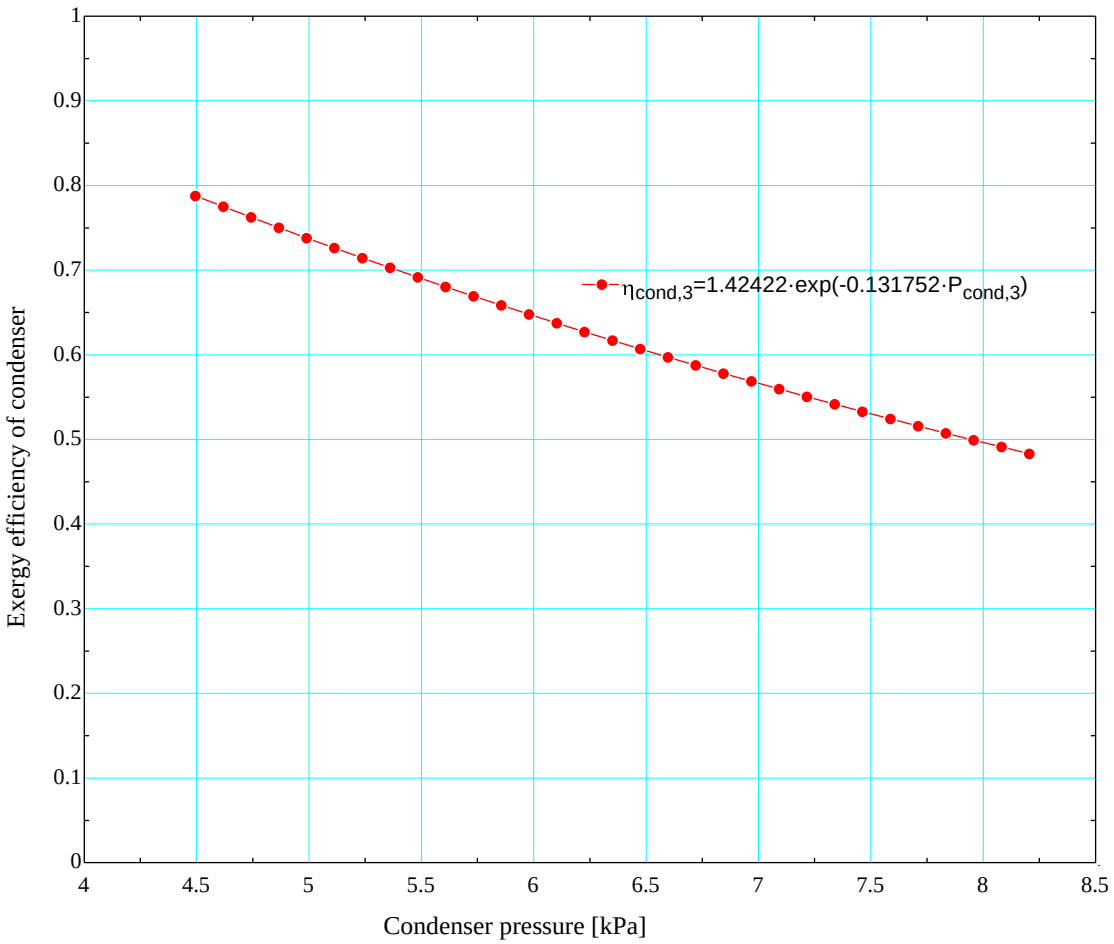

Figure 4.2: A Graph of condenser exergy efficiency against Condenser pressure.

To establish the relationship of condensing pressure on cooling water temperature, temperature was varied between 11-22^{o}C. The lower temperature is limited by the refrigerant temperature (T_{31}) into the evaporator. Since the refrigerant temperature was set at 10^{o}C, low cooling water temperature was limited to 11^{o}C to avoid a zero or negative value for the logarithmic mean temperature difference. The simulation was done at constant steam load and cooling water flow rate. Figure 4.3 shows the behavior of this dependence where condensing pressure increases with increasing temperature of the cooling water.

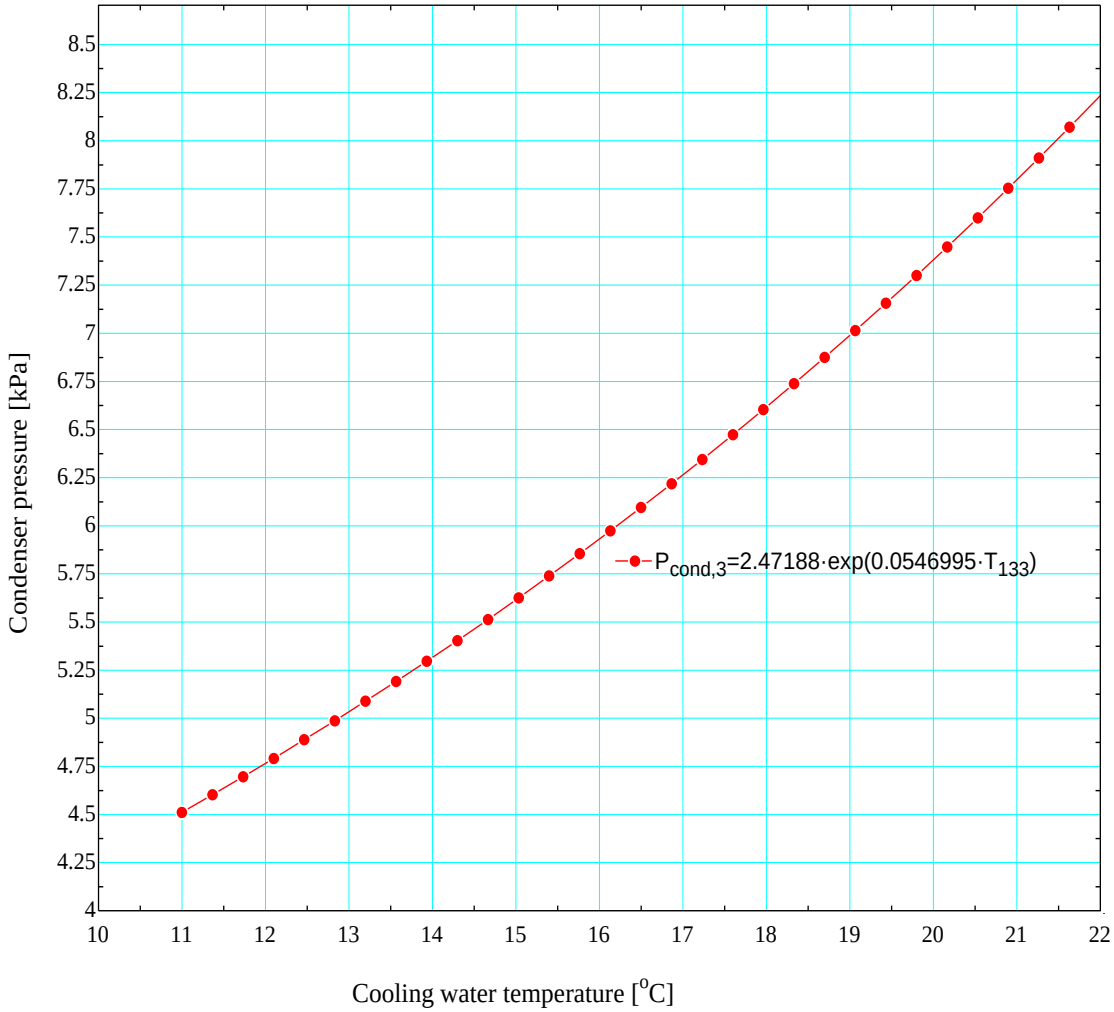

Figure 4.3: A Graph of Condenser pressure against cooling water temperature.

Figure 4.4 shows the dependency of turbine energy and exergy efficiencies on condenser pressure. Turbine energy efficiency is a function of steam load into the turbine, inlet enthalpy and exit enthalpy at the turbine. The changes in condenser pressure affect the turbine exhaust enthalpy. An increase in condenser pressure leads to an increase in turbine exhaust enthalpy which eventually leads to a decrease in output energy of the turbine. In this senario the steam mass flow rate and inlet enthalpy into the turbine were maintained at a constant rate. Turbine exergy efficiency is a function of steam into and out of the turbine, inlet and outlet enthalpies, inlet and outlet entropies. An increase in condenser pressure equally leads to a decrease in turbine exergy efficiency.

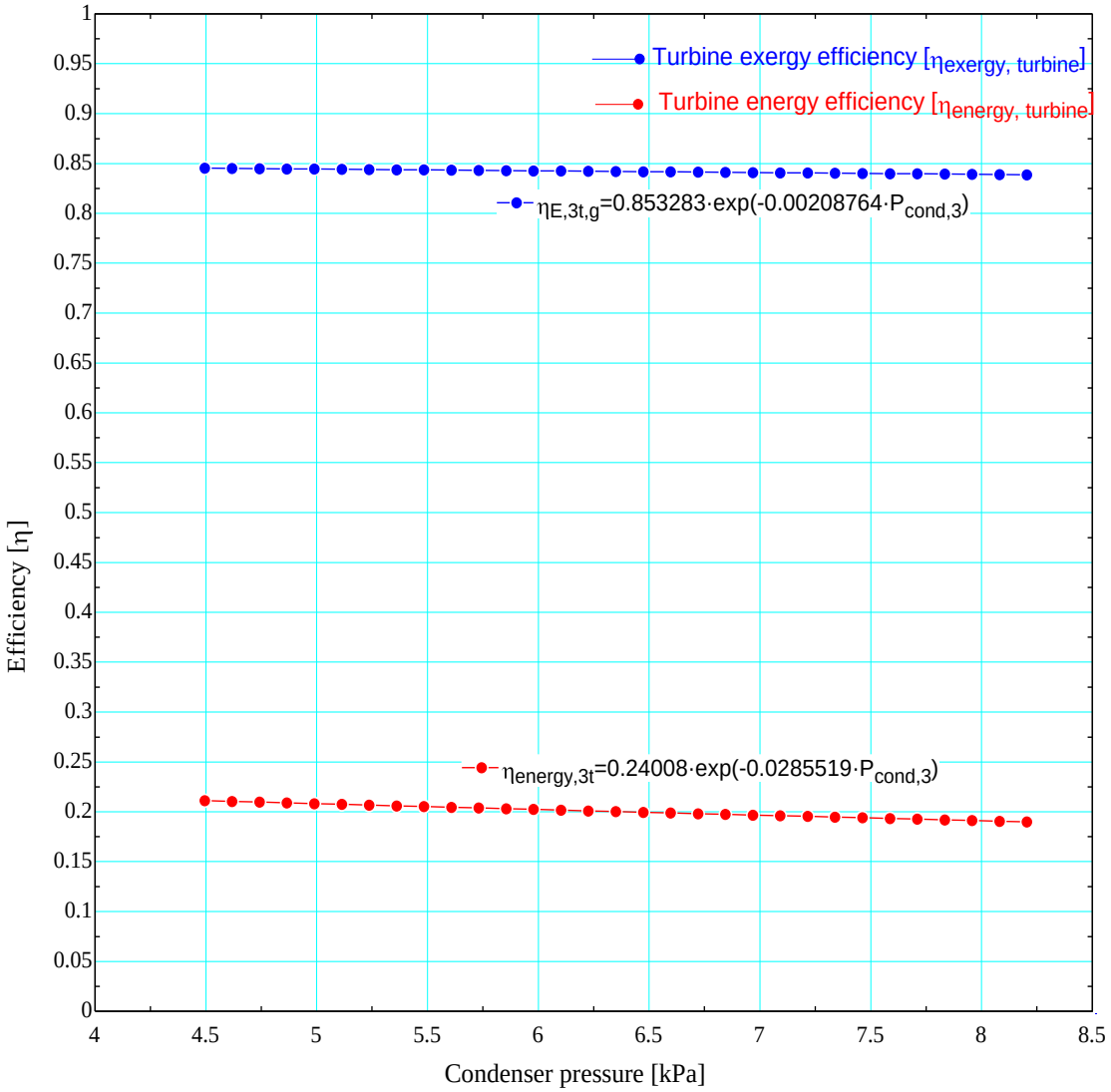

Figure 4.4: Graph of turbine energy and exergy efficiency against condensing pressure.

Geothermal power plants strongly depend on the cold end operating conditions where the condenser is the key of the heat exchanger system. The operating conditions of the condenser depends on the cooling system which gives the inlet condition of condenser parameters. One of that parameter is the cooling water temperature which greatly influences the condenser pressure and eventuary the power output. From Fig. 4.3, it is clear that a decrease in the cooling water temperature result in a decrease in condenser pressure. A decrease in condenser pressure results in an increase in turbine output power as shown graphically in Fig. 4.5. This statement clearly agrees with the theoritical studies performed earlier. This study explains why the power output decrease during hot months when daytime temperatures are usually very high.

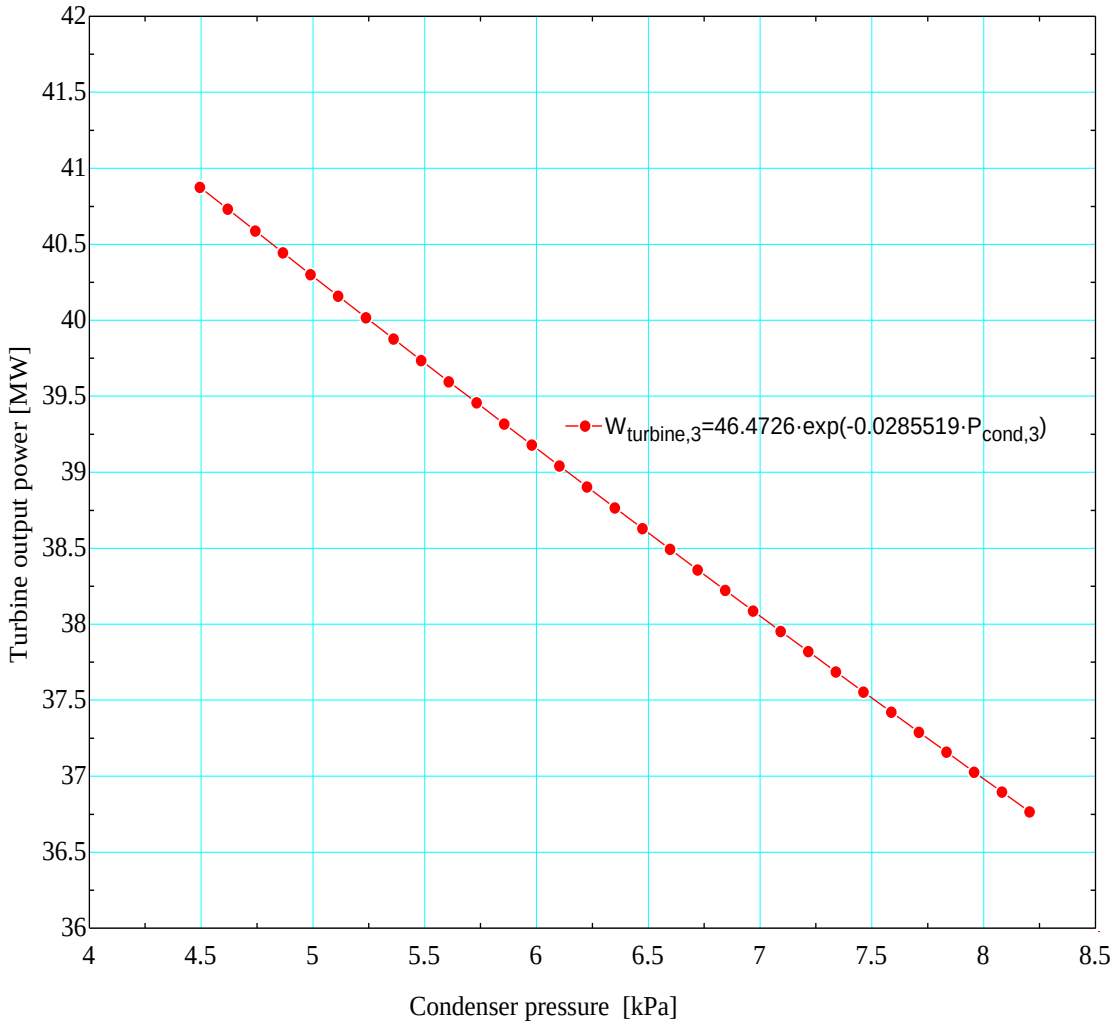

Figure 4.5: A Graph of turbine power output against condenser pressure.

Condensation of steam exiting the turbine is essential for any geothermal power plant. For effective condensation the temperature of water used for cooling should be as low as practically viable. By improving condensation process, the exergy efficiency of the condenser is improved and this improves the exergy efficiency of the turbine. Sum total of these improvements is depicted by increased overall exergy efficiency of the power plant. Graphical variations of overall exergy efficiency and condenser pressure are shown in Fig. 4.6.

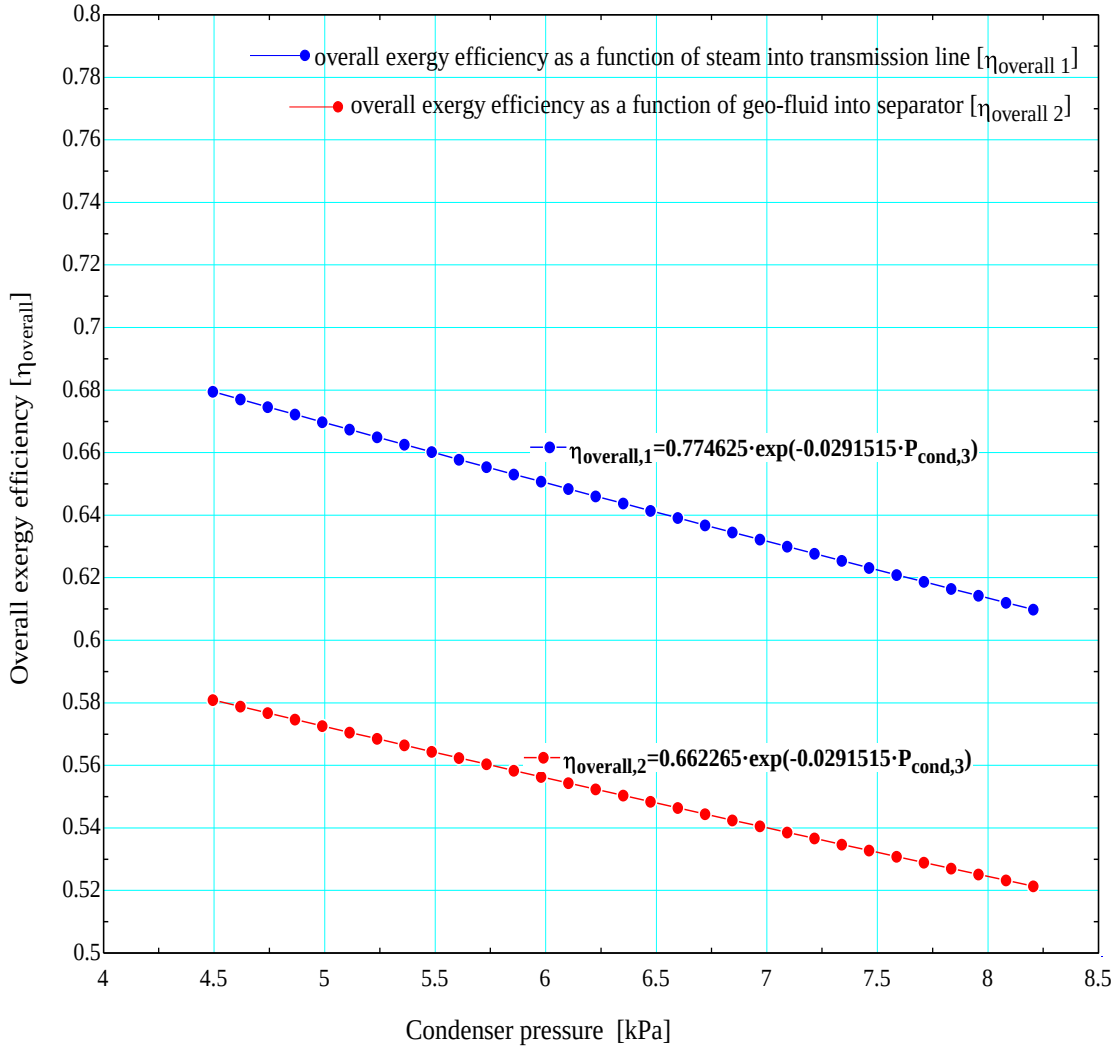

Figure 4.6: Graph of overall exergy efficiency against condenser pressure.

Figure 4.7 shows the effect of varying the mass flow rate on condenser heat transfer rate at different condenser pressures. The figure shows that for a given condenser pressure, an increase in the mass flow rate leads to an increase in the condenser heat transfer rate.

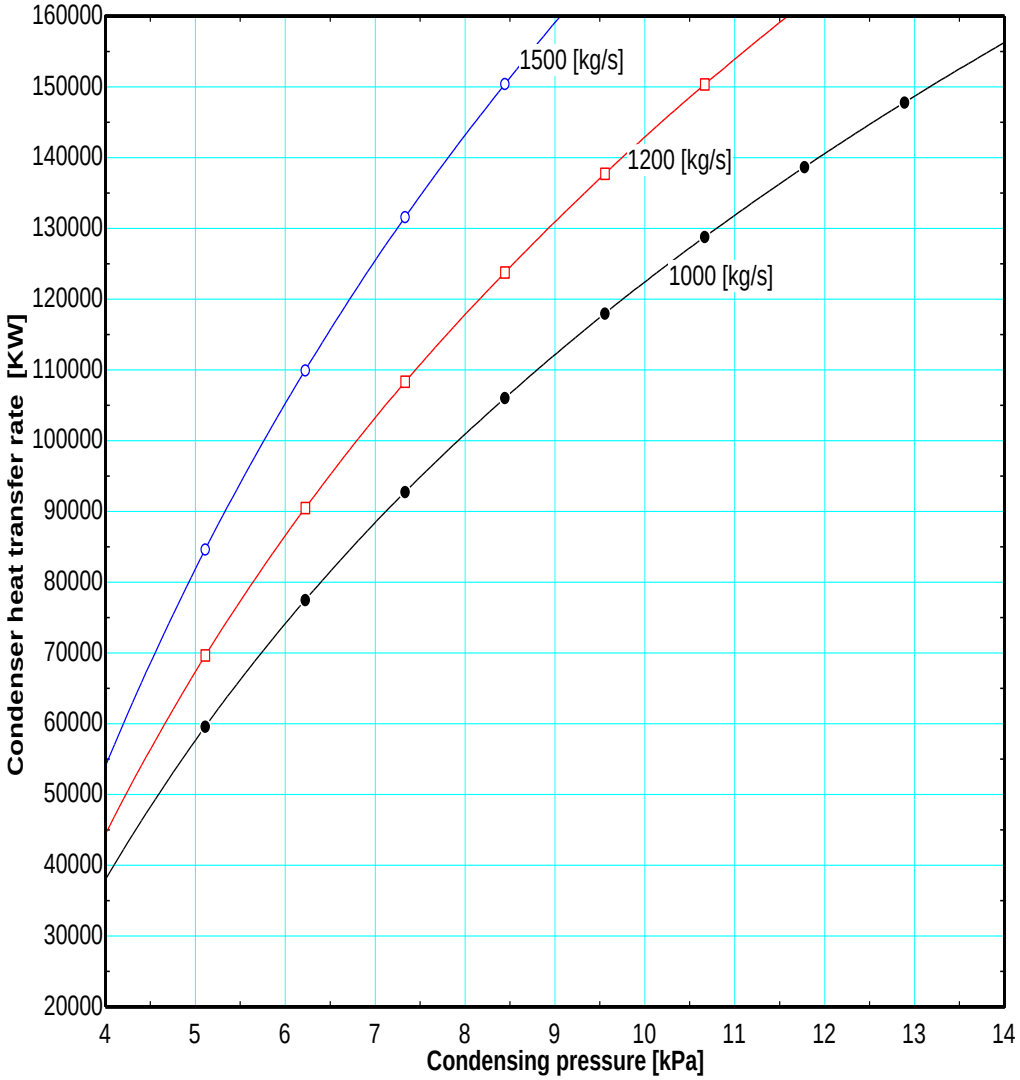

Figure 4.7: A Graph of condenser heat transfer rate against Condensing pressure for different cooling water flow rates.

Since the condenser performance depends on the cooling water temperature, the water temperature for the proposed plant design will depend on the evaporator temperature. Increased evaporator temperature lowers the cooling water temperature. Figure 4.8 shows how the condenser efficiency is affected by the evaporator temperature.

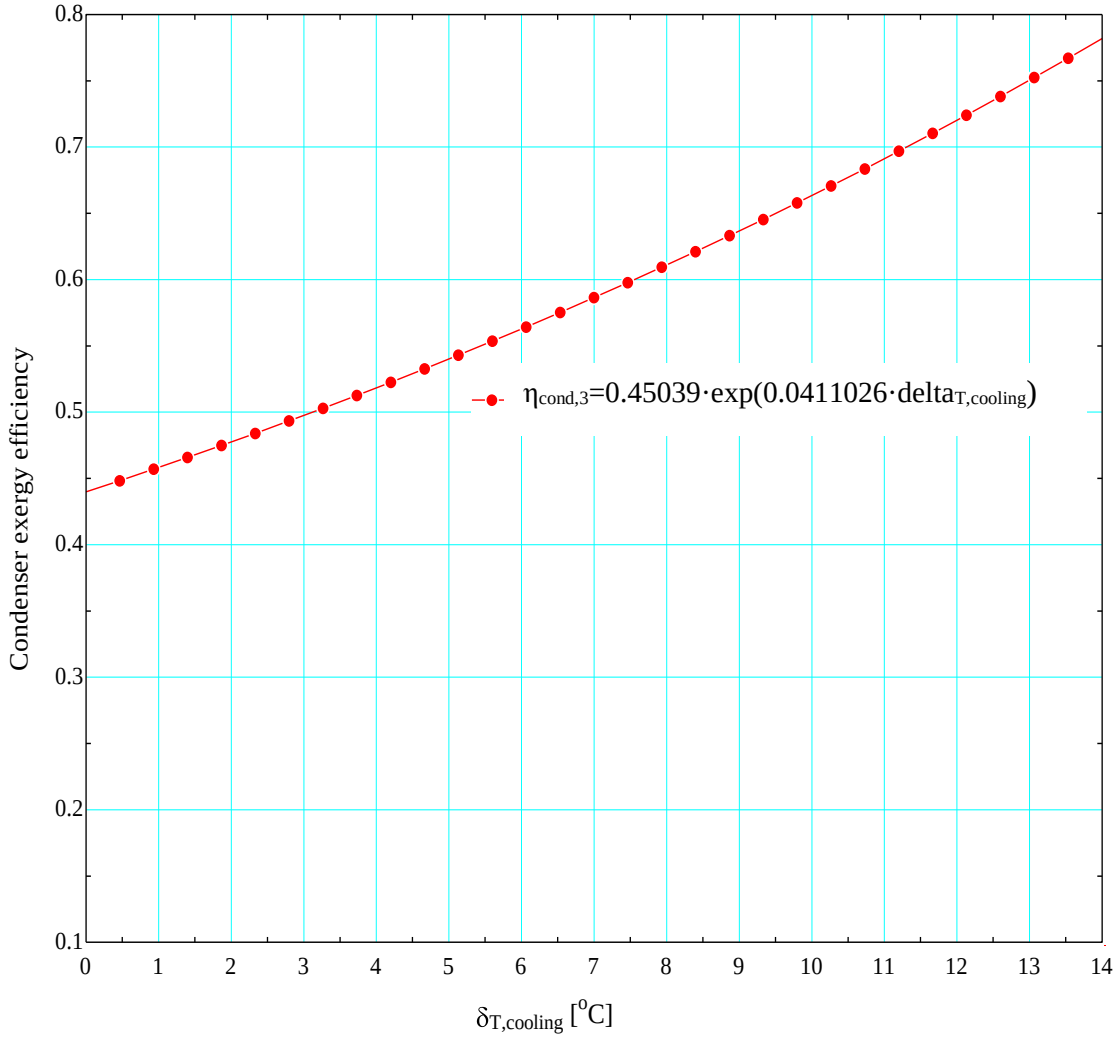

Figure 4.8: Graph of condenser exergy efficiency against evaporator temperature changes.

An increase in the refrigerant load temperature results in an increase in enthalpy of cooling water out of the evaporator. This leads to a decrease in evaporator heat transfer rate as shown in Eq. 2.57. Since absorption chiller coefficient of performance is dependent on evaporator heat transfer rate as shown in Eq. 2.71, its decrease results in lower coefficient of performance of chiller as graphically shown in Fig.4.9.

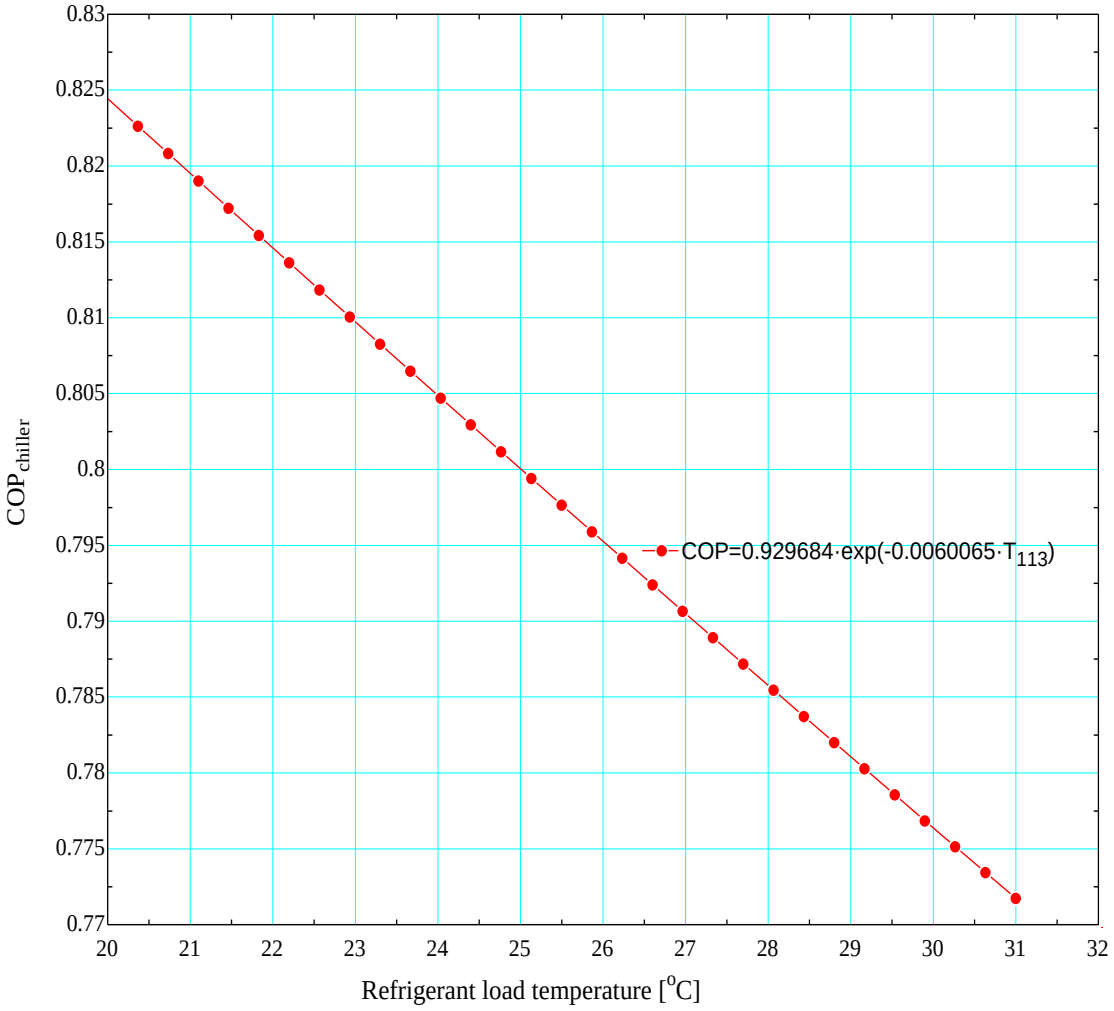

Figure 4.9: Graph of Absorption chiller COP against refrigeration load inlet temperature.

The effect of environmental condition on the energy and exergy efficiency of geothermal power plants was studied by varying the ambient temperature at variable condenser pressures and both energy and exergy efficiencies outputs were recorded. In Fig. 4.10, it was shown that at variable condenser pressures the exergy and energy efficiency decreased. The decrease for energy efficiency was much higher than exergy efficiency for the same temperature range.

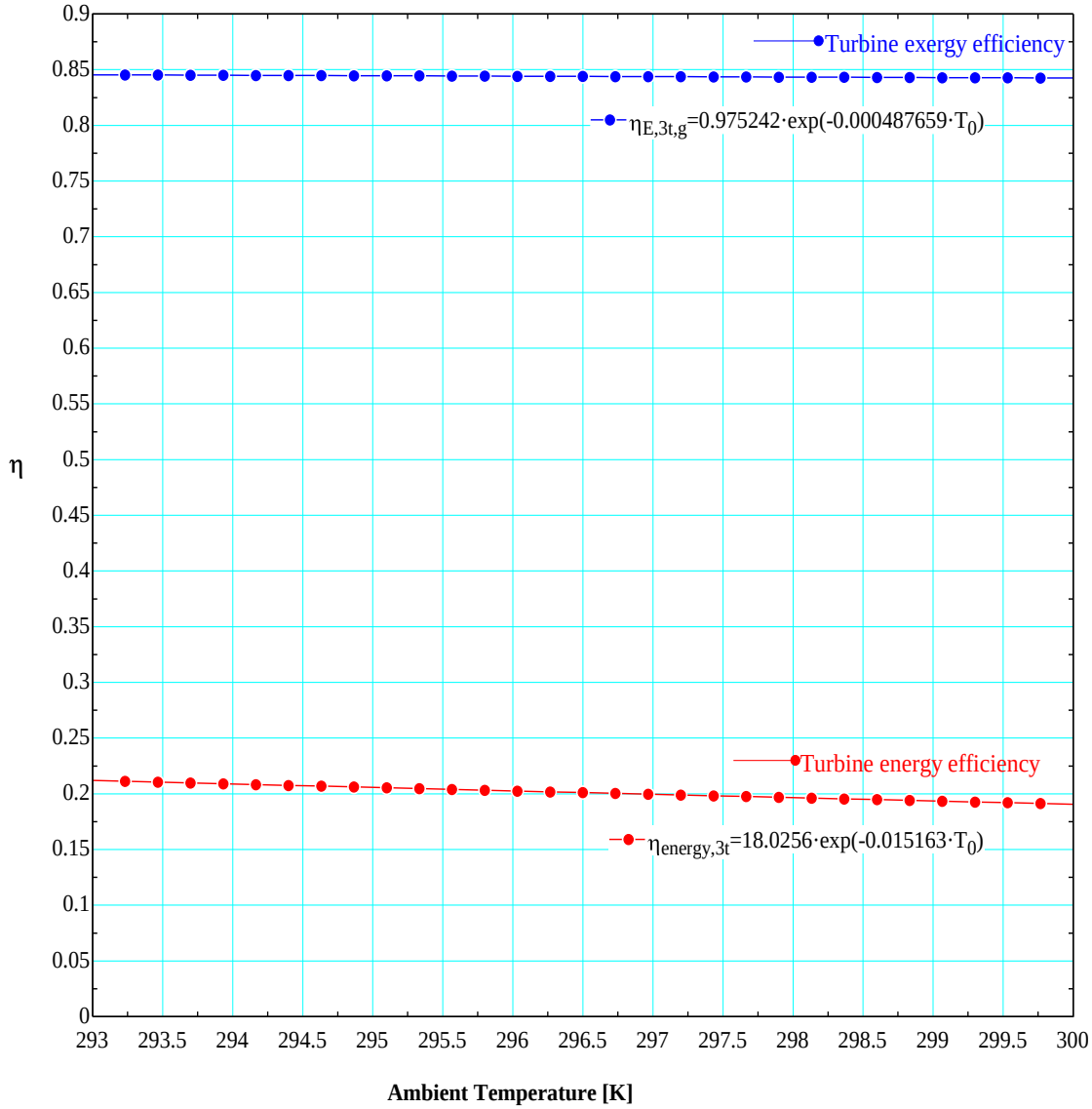

Figure 4.10: Effect of ambient temperature on energy and exergy efficiency at variable condenser pressure for a geothermal power plant.

From Fig. 4.11 it is noted that at constant condenser pressure and specified cooling water flow rate, increase in cooling water temperature results in a decrease in condenser heat transfer rate. However, for specified cooling water temperature and at constant condenser pressure, heat transfer rate increases as the cooling water flow rate increases.

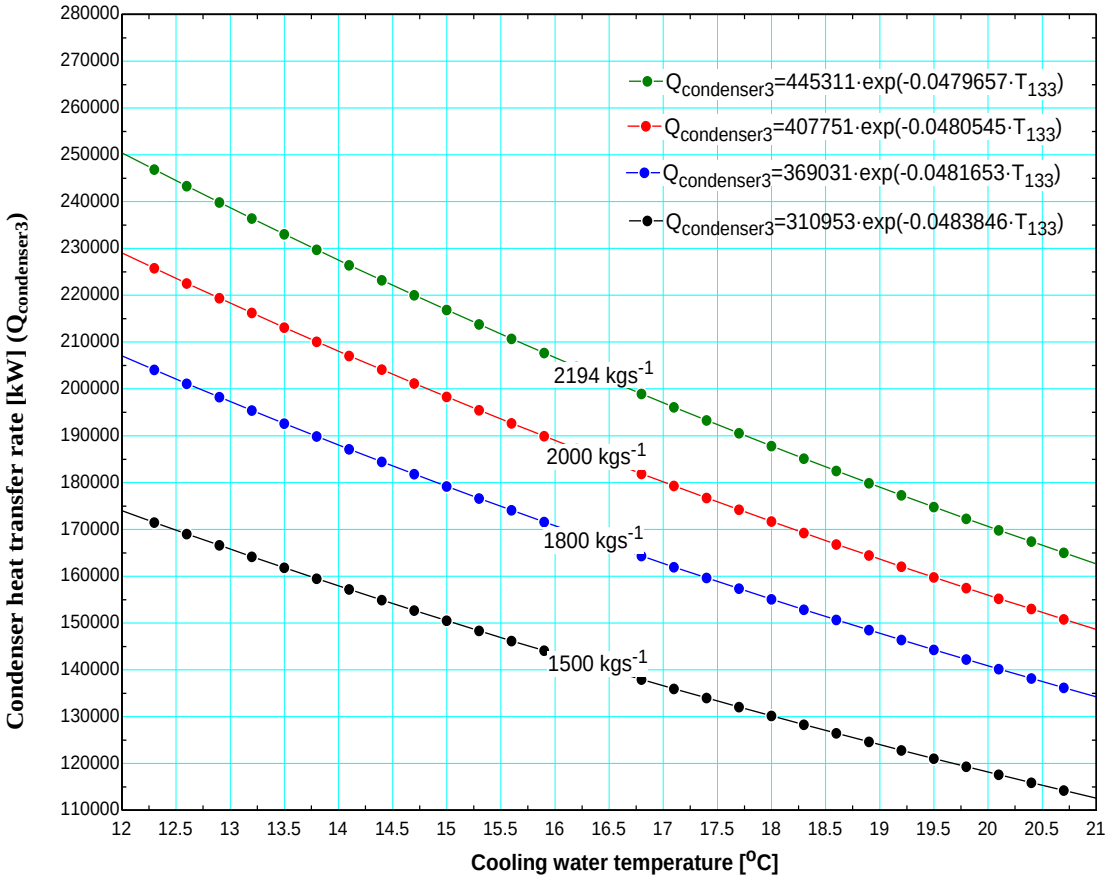

Figure 4.11: Condenser heat transfer rate due to cooling water temperature and flow rate changes at constant condenser pressure of 5 kPa.

4.5 Economic Analysis

The essence of any project is to be profitable. The financial structure, conditions and related costs are important factors influencing the levelized cost of energy and profitability of the project (Ozcan, 2010). It is therefore important to carry out an in-depth analysis on the likely profitability of the intended project before investing in it. In the case of our study we shall base the economic analysis on discounted payback time analysis.

The discounted payback period is calculated using a return that is greater than 0%. However, in practice most analysts have used the simple payback period with a no-return requirement (i.e i = 0%). This is aimed at screening the project to determine if the project requires further consideration. This approach has been criticized since it gives a false picture of an investment's viability. For this reason discounted payback

period has been preferred for this kind of analysis as it incorporates the time value for money.

In this analysis the lifespan of the plant was set at 25 years with the cash flow from the sale of electricity estimated at 0.07 $/KWh (Mugambi, 2014). The cash flow was assumed to be constant per annum. According to Rotich (2015) report, the interest rate offered to investors in the energy sector stand at 16%.

Table 4.8 shows an estimation of the total capital investment for the single effect lithium bromide-water ARS. With the cost of investment estimated at $ 4,107,644 (Matches, 2014) and a constant cash flow of 0.07 $/KWh, the sale of the power gained (1600 KW) could pay for the investment after a period of 9.4 years as shown in Table 4.9. The operation and maintenance (O and M) costs were included based on a proposed figure of 0.00763 US $/KWh (Energy Regulation Commission, 2009). It is worth noting that the costs estimate for (O and M) used were for the year 2009 and it is likely that the cost may be higher based on the current year. The total cost of investment is therefore likely to be higher. This assumption is likely to increase the payback period to more than 9.4 years.

The payback period is also likely to decrease if the proposed system was to be incorporated on a plant that is already operating. This is because some of the civil works could be avoided. However, this estimated payback period would be a clear picture of a new plant.

Table 4.8: Estimation of total capital investment for single effect lithium bromide-water ARS Source: Adopted from (Matches, 2014; Tesha, 2009).

Cost components	**SF H_2O/ LiBr – 45 MW**
I. Capital Investment (CI)	
1. Direct cost (DC)	
a. Heat exchangers	$ 1,406,500
b. Pumps (Horizontal, ANSI, 1-stage)	$ 6,300
c. Piping system [5% of (a+b)]	$ 70,640
d. Electrical control and monitoring system [30% of (a+b+c)]	$ 445,032
e. Civil, structural and architectural work [20% of a+b+c+d]	$ 385,694
f. Service facilities (hot source and cold sink connection)[25% of a+b+c+d]	$ 482,118
g. Contingencies [20% of a+b+c+d]	$ 385,694
Total direct cost	**$ 3,181,978**
2. Indirect cost (IDC)	
i. Engineering and supervision [15% of DC]	$ 462,833
ii. Construction cost incl. contractor's profit [15% of DC]	$ 462,833
Total indirect cost	**$ 925,666**
Total capital investment	**$ 4,107,644**

Table 4.9: Payback period analysis

For i = 16%

Year	Cash Flow (US $)	Present Value factor	Discounted Cash Flow (US $)	Cumulative Discounted Cash Flow (US $)
0	-4107644	1	-4107644	-4107644
1	874178	0.862069	753601.7	-3354042
2	874178	0.743163	649656.7	-2704386
3	874178	0.640658	560048.8	-2144337
4	874178	0.552291	482800.7	-1661536
5	874178	0.476113	416207.5	-1245329
6	874178	0.410442	358799.6	-886529
7	874178	0.35383	309310	-577219
8	874178	0.305025	266646.5	-310572
9	874178	0.262953	229867.7	-80704.7
10	874178	0.226684	198161.8	117457.1
11	874178	0.195417	170829.2	288286.3
12	874178	0.168463	147266.5	435552.8
13	874178	0.145227	126953.9	562506.7
14	874178	0.125195	109443	671949.7
15	874178	0.107927	94347.42	766297.1
16	874178	0.093041	81333.98	847631.1
17	874178	0.080207	70115.5	917746.6
18	874178	0.069144	60444.4	978191
19	874178	0.059607	52107.24	1030298
20	874178	0.051385	44920.04	1075218
21	874178	0.044298	38724.17	1113942
22	874178	0.038188	33382.9	1147325
23	874178	0.03292	28778.37	1176104
24	874178	0.02838	24808.94	1200913
25	874178	0.024465	21387.01	1222300
Discounted Payback Period				**9.4 Years**

Chapter Five

5.1 Conclusions

The research presents the effect of varying cooling water temperature on condenser pressure and ultimately power output. The effect of lowering cooling water temperature on condenser pressure and power output has been assessed and the following conclusions have been made.

Firstly, by lowering cooling water temperature from 25^{o}C to 16^{o}C the condenser pressure is reduced from 9.7 kPa to 5.9 kPa for unit 3 and this pressure decrease is accompanied by additional power output of 1.6 MWh. The idea of lowering cooling water temperature is to ensure that more steam is condensed within the condenser thus creating a higher cooling water temperature difference. The higher temperature difference offered a higher efficiency of the condenser.

Secondly, the adoption of an absorption refrigeration system as the secondary cooling system minimized the influence of environmental effect on cooling efficiency. The system yielded cooling water temperature of 16^{o}C that resulted to a decrease in exergy destroyed in the condenser and turbine by 0.59 MW and 0.4 MW respectively. Overall exergy efficiency of the plant as a function of steam into transmission line increased from 62.2% to 65.2%.

Thirdly, an investment of $4,107,644 to gain an extra 1.6 MWh seemed to be economically feasible based on the payback period of approximately 9.4 years based to the recommended period of 5 to 12 years.

5.2 Recommendations

There is need to do an optimization on the absorption chiller using exergy flow analysis. The optimization should be geared towards reducing the area of the heat exchangers without affecting its efficiency. Since the price of the absorption chiller is dependent on area of each component, therefore, a reduction in surface area will lead to a lowered investment cost. There is also need to investigate the use of other materials besides iron, copper and aluminum that will maintain the component efficiency but lower the cost of manufacture. There is also need to study the possibility of using an absorption chiller as opposed to the cooling tower as primary

and sole cooling system. In this way the cost of investing in the cooling tower will be eliminated.

A detailed analysis should be conducted to assess the potential of using the brine to power a binary plant to generate more electricity. Then, comparisons should be made with one studied above in terms of power gained and payback period of investment.

References

Acir, A., Bilgnsoy, A. K., and Coskun, H. (2012). Investigation of varying dead state temperature on energy and exergy efficiencies in thermal power plant. *Journal of the energy institute*, 85(1).

Align, M. (2001). *Exergy analysis of Mindanao I and Mindanao II geothermal power plant*, Philippines. Diploma course project, Geothermal Institute, University of Auckland.

Bertani, R. (2015). *Geothermal Power Generation in the World 2010-2014 Update Report* .Proceedings World Geothermal Congress 2015,April 19-25, Melbourne, Australia.pp 1-19.

Betttagli, N.,and Bidin, G. (1996). Landerello-Farinello-Valle Secolo geothermal area: Exergy analysis of the transportation network and of the electric power plant, *Geothermics,* 25(1). pp 3-16.

Bharathan, D., andNix, G. (2001). *Evaluation of an Absorption Heat Pump to mitigate plant capacity reduction due to ambient temperature rise for an air-cooled ammonia and water system,* Geothermal Resource Council Transactions, 25. pp 563-567.

Birgenheier, D. B., and Butzbach, L. T. (1993). *Designing Steam-Jet Vacuum Systems*. Chemical Engineering, 100 (7).

Dorj, P. (2005). *Thermoeconomics analysis of a new geothermal utilization CHP plant in Tsetserleg Mongolia*. MSc. Thesis, United Nations University Geothermal Training Programme, Reykjavik, Iceland, Report no. 2.

Dutta, A., Das, A. K., and Chakrabarti, S. (2013). Study on the effect of cooling water temperature rise on the loss factor and efficiency of a condenser for a 210 MW thermal power plant. *International journal of emerging technology and advanced engineering*. 3(3). pp 485-489.

El-Wakil, (1984). *Geothermal Plant Technology*, McGraw-Hill Inc, New York.

Energy Regulation Commission, (2009). Least cost power development plan.

Fox, R.W., and Mcdonald, A.T. (1992). *Introduction to Fluid Mechanics, 4th edition*, John Wiley and Sons, New York.

Gong, M., and Wall, G. (1997). *On exergetics, economics and optimization of technical processes to meet environmental conditions*. Conference proceedings of Thermodynamic analysis and improvement of energy systems, June 10-13, Beijing, China. pp 453-460.

Holdmann, G., andErickson, D. (2006). *Absorption chiller for the Chana Hot Springs Aurora Ice Museum.* Conference proceedings of Geothermal Conference (GHC) Bulletin,November 14, 2007, Geo-Heat Center Oregon Institute 0f Technology, USA. pp 1-20.

Izquierdo, M. (2008). Air conditioning using an air-cooled single effect lithium bromide absorption chiller: Results of a trial conducted in Madrid in August 2005. *Applied Thermal Engineering*, 28(8-9). pp 1074-1081.

Kececiler, A., Acar, H.,and Dogan, A. (2000). Thermodynamic analysis of the absorption refrigeration system with geothermal energy: an experimental study. *Energy Conversion and Management*. 41(1). pp 37-48.

Kozubal, E., andKutscher, C. (2003). *Analysis of a Water-Cooled Condenser in Series with an Air-Cooled Condenser for a Proposed 1-MW Geothermal Power Plant*, GRC Transactions, 27.Davis, California: Geothermal Resource Council. pp 580-600.

Kwambai, C. B. (2005). *Exergy analysis of Olkaria I power plant, Kenya*. Report of United Nations University Geothermal Training Programme, Reykjavik, Iceland, Report No. 5. pp 1-37.

Matches, (2014). *Matches' process equipment cost estimates*. http://www.matche.com/EquipCost/index.htm

Mehdi, S., and Amir, V. (2012). *The Effect of Ambient Temperature to Power Plant Efficiency*. 2nd International Conference on Mechanical, Production and Automobile Engineering, April 28-29, Singapore. pp 1-5.

Moghaddam, A.R. (2006). *A conceptual Design of A Geothermal Combined Cycle and Comparison with a Single-Flash Power Plant for Well NWS-4, Sabalan, Iran.* Report of the United Nations University Geothermal Training Programme, June 16, Reykjavik, Iceland, Report No:18. pp 391-428.

Mostafavi, M., and Agnew, B. (1996).The impact of ambient temperature on lithium-bromide/water absorption machine performance. *Applied Thermal Engineering*, 16(6). pp 515-522.

Mugambi, M. (2014). High power costs loom in KPLC's bid for review of tariffs. Business Daily Report. Posted on May 9.

Ngugi, K. P. (2012). *What does geothermal cost? -The Kenya experience*. Report of the United Nations University Geothermal Training Programme, October 31-November 22, Reykjavik, Iceland.pp 1-12.

Ozcan, Y.N. (2010). *Modeling, Simulation and Optimization of Flashed-Steam Geothermal Power Plants from the point of view of Non-condensable Gas Removal Systems.* Ph.D. Thesis, United Nations University Geothermal Training Programme, June 7, Reykjavik, Iceland.

Rosen, M., and Dincer, I. (2001). Exergy as the confluence of energy, environment and sustainable development. *International Journal on Exergy*, 1. pp 3-13.

Rosen, M.A. (1999). Second law analysis, approaches and implications. *International Journal of Energy Research*, 23. pp. 415-429.

Rotich, H. (2015). Medium Term Debt Management Strategy. Report of the National Treasury, Republic of Kenya, February 8, Nairobi, Kenya. pp 1-56.

Sharma, P., Rajput, SPS.,and Pandey, M. (2011). Exergetic optimization of inlet cooling water temperature of cross flow steam condensers. *International journal on emerging technologies*. 2 (1). pp. 144-147.

Siregar, P. H. H. (2004). *Optimization of Electrical Power Production Process for the Sibayak Geothermal Field, Indonesia*. Report of the United Nations University Geothermal Training Programme, September 20, Reykjavik, Iceland. Report No: 16. pp. 1-27.

Swandaru, R. B (2006). *Thermodynamic Analysis of Preliminary Design of Power Plant Unit I Patuha, West Java, Indonesia,* Report of the United Nations UniversityGeothermal Training Programme, June 11, Reykjavik, Iceland, Report No: 7. pp. 1-30.

Tesha. (2009). *Absorption refrigeration system as an integrated condenser cooling unit in a geothermal power plant*. Report of the United Nations University Geothermal Training Programme, May 10, Reykjavik, Iceland, Report No: 1. pp. 1-20.

Vosough, A., falahat, A., vosough, S., Esfehani, N, H., Behjat, A., and Naseri, R, R. (2011). Improvement Power Plant Efficiency with Condenser Pressure. *International Journal of Multidisciplinary Sciences and Engineering*, 2 (3). pp. 1-6.

Woodruff, E.B., Lammers, H.B., and Lammers, T.F. (1998). *Steam Plant Operation. Seventh Edition*. McGraw-Hill. New York.

Zhang, F., Bock, J., Jacobi, M., and Wu, H., (2007). *Simultaneous heat and mass transfer in a wetted heat exchanger, part I: experiments*. 14th International Refrigeration and Air Conditioning Conference, July 16-19, 2012, Purdue, USA. pp. 1-10.

Appendices

Appendix A - Simulation results

Table A.1. Simulation results of the mass, energy and exergy balance of Olkaria II Geothermal Power Plant.

State Points (unit no)	ṁ (kg/s)	h (kJ/kg)	s (kJ/kg-K)	T (^oC)	P (kPa)	E_x (KW)
Environmental condition		83.93	0.2962	293.2 [K]	86	
1	206.9	659.7	1.906	156.4	562.5	21488
3	227.4	2754	6.782	156.4	562.5	174780
3(1)	57.16	2754	6.782	156.4	562.5	43933
3(2)	72.36	2754	6.782	156.4	562.5	55616
3(3)	72.9	2754	6.782	156.4	562.5	56031
4(1)	54.17	2751	6.801	151.7	531.3	41193
4(1)a	2.99	2741		151.7	427	2180
4(2)	69.4	2752	6.795	150	541.3	52960
4(2)a	2.96	2741		150	420	2151
4(3)	71.1	2751	6.805	153.1	526	53966
4(3)a	1.8	2741		153.1	423	1310
5(1)	53.63	2750	6.808	150.3	521.3	40636
5(2)	68.71	2750	6.813	148	512.8	51899
5(3)	70.39	2750	6.811	151.3	516.3	53239
6(1)	48.27	2209	7.114	41.13	6.959	6095
6(2)	61.84	2211	7.118	44.5	6.997	7854
6(3)	63.35	2210	7.116	44.97	6.997	8044
7(1)	2266	162.9	0.5576	38.9	6.959	5106
7(2)	2316	163.3	0.5589	39	6.997	5194
7(3)	2372	163.3	0.5589	39	6.997	5676
9(1)	12.3	162.9	0.5576	38.9	190	29.09
9(2)	16.39	163.3	0.5589	39	180	39.18
9(3)	23.54	163.2	0.5589	39	163	56.27
10(1)	2254	162.9	0.5576	38.9	190	5330
10(2)	2300	163.3	0.5589	39	180	5498
10(3)	2349	163.3	0.5589	39	163	5615
11(1)	2318	103.0	0.3609	24.57	126	1493
11(2)	2347	113.2	0.3949	27.2	126	901.7
11(3)	2397	104.9	0.3670	25.0	126	518.7
12(3)	2194	104.9	0.3669	25.0	126	474.8
13(1)	2111	103	0.3609	24.57	126	136
13(2)	2111	113.2	0.3949	27	126	811
13(3)	2194	104.9	0.3673	25	126	209.1
19(1)	107.4	103	0.3609	24.57	3.089	15.84

State Points (unit no)	ṁ (kg/s)	h (kJ/kg)	s (kJ/kg-K)	T (°C)	P (kPa)	E_x (KW)
19(2)	144.1	113.2	0.3949	27	3.567	49.59
19(3)	115.6	104.8	0.3669	25	3.169	20.39
20(1)	107.4	167.1	0.5709	39.9	7.342	284.5
20(2)	144.1	172.9	0.5896	41.3	7.908	436.7
20(3)	115.6	158.7	0.5441	37.9	6.594	246.3
60(1)	0.362	13.69	0.5507	41.13	6.959	-52.43
60(2)	0.4638	16.6	0.5589	44.5	6.997	-66.94
60(3)	0.4751	17	0.5602	44.97	6.997	-68.57
61(1)	0.362	2.819 ncg	0.5364	28.4	6.227 ncg	772.7
61(2)	0.4638	11.05 ncg	0.5135	38.07	8.107 ncg	668.4
61(3)	0.4751	2.975 ncg	0.5784	28.4	43	644

Table A.2. Simulation results of the mass, energy and exergy balance of Olkaria II Geothermal Power Plant with HS of Cooling.

State Points (unit no)	ṁ (kg/s)	h (kJ/kg)	T (°C)	P (kPa)	E_x (KW)	s(kJ/kg-K)
Environmental condition		83.93	293.2 [K]	86		0.2962
1	206.9	659.7	156.3	562.5	21488	1.906
2	206.9	151.3	93.7	562.5		
3	227.4	2754	156.3	562.5	174780	6.782
3(3)	72.9	2754	156.3	562.5	56031	6.782
4(3)	71.1	2751	153.1	526	53966	6.805
4(3)a	1.8	2741	153.1	526	1310	6.878
5(3)	70.39	2750	151.3	516.3	53239	6.811
6(3)	63.35	2194	36	5.945	6806	7.128
7(3)	2372	159.1	38	6.63	5086	0.5455
9(3)	23.54	159.1	38	163	50.48	0.5455
10(3)	2349	159.1	38	163	5031	0.5455
11(3)	4985	104.8	25	126	1079	0.367
12(3)	2194	104.8	25	126	474.8	0.367
13(3)	2194	67.1	16	126	67.76	0.2387
14	1227	104.9	25	126		
15	1227	188.5	45	126	5229	0.6385
16	1361	104.9	25	126		
17	1361	167.6	40	126	3770	0.5722
19(3)	115.6	67.18	25	3.169	13.32	0.2387
20(3)	115.6	188.4	45	9.59	488.5	0.6385
21	157	76.05	35	1.228		
22	157	76.05	35	9.59		
23	157	134.9	62.6	9.59		

State Points (unit no)	ṁ (kg/s)	h (kJ/kg)	T (^oC)	P (kPa)	E_x (KW)	s(kJ/kg-K)
24	122.2	281.8	108.8	9.59		
25	122.2	206.1	64.1	9.59		
26	122.2	206.1	65.1	1.228		
27	34.85	2638	74.4	9.59		
28	34.85	188.4	45	9.59		
29	34.85	141.6	33.8	9.59		
30	34.85	141.6	10	1.228		
31	34.85	2519	10	1.228		
32	34.85	2566	35	1.228		
60(3)	0.4751	9.296	36	5.945	-73.09	0.5664
61(3)ncg	0.4751	2.975	28.6	5	-77.76	0.5784
63(3)ncg	0.4751	7.028			-46.94	0.3709

Appendix B - Collected data

The measured performance values for Olkaria II power plant are shown in Table B.1. The measurements are based on readings taken for the month of June-2013 on average

Table B.1: Average daily measured values for the month of June-2013

Items	Units	Unit 1			Unit 2			Unit 3		
		0800	1200	1600	0800	1200	1600	0800	1200	1600
Unit load	MW	24.7	23.7	23.4	35.5	34.3	34.0	35.7	35.4	35.6
Vent station steam pressure	bar	4.4	4.3	4.3	4.4	4.4	4.4	4.4	4.1	4.1
Main steam flow	t/h	195.7	195.0	194.3	-	-	-	252.7	256.8	258.1
Main steam temperature (scrubber inlet)	^{O}C	151.9	151.6	151.5	-	-	-	153.4	153.0	153.0
Main steam pressure (scrubber inlet)	bar	4.3	4.3	4.3	4.4	4.4	4.4	4.2	4.2	4.2
Main steam temperature (turbine inlet; LH)	^{O}C	146.7	146.2	146.2	151.1	150.7	150.7	151.5	151.1	151.0
Main steam temperature (turbine inlet; RH)	^{O}C	151.9	151.4	151.4	151.7	151.3	151.3	151.3	150.8	150.8
Main steam pressure (turbine inlet; LH)	bar	4.2	4.2	4.2	4.2	4.1	4.1	4.2	4.1	4.1

Items	Units	Unit 1			Unit 2			Unit 3		
		0800	1200	1600	0800	1200	1600	0800	1200	1600
Auxiliary steam flow	t/h	10.8	10.8	10.7	10.8	10.7	10.5	6.5	6.4	6.4
Ejector steam supply Header Pressure	bar-a	4.3	4.2	4.3	4.2	4.2	4.2	4.3	4.2	4.2
Turbine steam chest pressure	bar-g	4.211	4.165	4.195	3.835	3.797	3.827	3.392	3.459	3.47
Turbine exhaust steam temperature	^{o}C	40.1	41.3	42	43.6	44.8	45.0	44.3	45.8	44.8
Hotwell water temperature	^{o}C	38.2	40.0	38.5	37.2	40.5	39.5	37.2	39.5	40.5
Hotwell discharge Header pressure	bar	1.9	1.9	1.9	1.8	1.8	1.8	1.7	1.6	1.6
Hotwell discharge Header temperature	^{o}C	37.3	39.1	39.6	42.7	44.5	44.9	37.0	39.6	40.3
CT to condenser water flow	t/h	3964	3389	3663	2861	1699	1780	-	-	-
CT to condenser water temperature	^{o}C	23.3	25.0	25.4	26.1	27.7	27.9	23.6	26.5	25.0
After condenser inner pressure	mbar	-407	-407	-407	-407	-203	-250	-5.6	-4.6	-

Items	Units	Unit 1			Unit 2			Unit 3		
		0800	1200	1600	0800	1200	1600	0800	1200	1600
Condensate Reinjection pump Discharge header pressure	bar	11.6	11.7	11.6	12.0	12.0	11.9	11.5	11.5	11.5
Condensate Reinjection pump Discharge flow	t/h	44.2	44.6	44.4	58.9	58.9	59.2	84.7	84.8	-
Inter-condenser inlet Gas Header pressure	mbar	52.5	59.7	74.6	68.7	82.1	92.4	47.0	53.0	-
Inter-condenser (A) inlet pressure	mbar	186.2	193.4	199.1	158	163.7	168.2	163	168.9	-
Inter-condenser (B) inlet pressure	mbar	140.6	149.1	149.3	114.5	126.8	125.9	163	168.9	-
Inter-condenser (C) inlet pressure	mbar	185.3	194.1	196.4	-	-	-	947	969	-
Inter-condenser (A) outlet temperature	^{o}C	37.1	39.6	40.1	41.9	44.5	44.4	34.3	36.7	-
Inter-condenser (C) outlet temperature	^{o}C	28	34.7	36.8	46.0	45.2	42.6	23.6	26.3	-

Items	Units	Unit 1			Unit 2			Unit 3		
		0800	1200	1600	0800	1200	1600	0800	1200	1600
After condenser outlet temperature	^{o}C	28.8	34.7	36.8	46.0	45.2	47.3	23.6	26.5	-
Inter-condenser outlet pressure	mbar	188.0	193.6	196.7	253.0	261.3	266.0	158	163.9	-
Inter-condenser outlet temperature	^{o}C	37.0	38.9	35.2	45.5	44.1	43.7	35.6	37.7	-
Vacuum pump/After-condenser outlet temperature	^{o}C	40.9	44	44.3	50.7	52.7	52.7	31.8	35.1	-
CCWP Discharge strainer Differential pressure	bar-g	0.26	0.265	0.274	0.24	0.244	0.233	0.13	0.141	-
CCW flow to cooling tower	t/h	360	359	355	332	330	329	312	315.0	-
CCW flow to inter/After-condenser	t/h	381.9	390.8	386.4	518.1	519.4	514.9	344	341.9	-
CCW discharge temperature to CT	^{o}C	25	26.7	27.1	28	29.4	30	23.3	25.1	-

Note**:**

Some of the data not captured in the table was missing due to breakdown of fiber communication to control room. Also some points had no gauges for measuring data due to manufacture’s design of plant hence some values had to be assumed.

Table B.2: Daily steam status report as at 20.05.2013

Well No	Last monito-red date	Status Open=1 Shut=0	Enthalpy kJ/kg (well-head)	Water t/hr	Steam To Plant t/hr	MWe (well-head)	Separa-tor Pressur e (bar-g)
OW-701 (Connected to 727)	12-Dec	1	2106.1	14.4	30.6	4.08	4.6
OW-705 (Connected to 725)	12-Dec	1	1616	19.45	27.32	3.64	4.7
OW-706		1	1837.4	38.65	47.75	6.37	4.4
OW-707		0	-	47.2	0	0	-
OW-709	12-Dec	1	2029.1	20.35	39.8	5.31	4.3
OW-710		1	1544.90 3	41.7	17.49	2.33	5.3
OW-711		1	1391	18.1	28.98	3.86	4.4
OW-712	12-Dec	1	1845.4	20.1	24.82	3.31	4.4
OW-713	12-Dec	1	2361.14	7.92	34.31	4.57	4.75
OW-714	13-Jan	1	1894	111.4 7	94.86	13.15	4.6
OW-715		1	1539.8	52.2	27.85	3.71	4.1
OW-716		1	1894	9.3	42	5.6	4.6
OW-719		1	1635.98 4	79	35.7	4.76	4.9
OW-720		1	2260.6	13.85	16.97	2.26	4.82
OW-721	12-Dec	1	2078.4	16.5	35.4	4.72	4.6
OW-725 (Connected to 705)	12-Dec	1	1616	75.44	61.45	8.19	4.7
OW-726		1	1635.98 4	48.9	47	6.27	4.9
OW-727	12-Dec	1	2106.1	12.65	30.1	4.01	4.6
OW-728		1	2260.6	30.1	51.48	6.86	4.82
OW-32		1	2000	65.75	103.1	13.75	4.8
OW-35A		1	1332.6	2	21.8	2.91	4.2
TOTAL/MEAN (AT WELLHEAD and SEPARATOR)			1757	745.0 3	818.78	109.68	4.625
ADD: Estimated flow from Olkaria I field					0		
LESS: Steam flow to Oserian Plant 202					24.65		
Available steam for power plant					794.13		
Provision of 5% transmission losses T/HR					39.71		
Steam expected at Plant Interface T/HR					754.42		

Appendix C - Analysed data

Analyzed data for mean values based on measurements for Olkaria II power plant operating parameters taken for June-2013

Table C.1: Geothermal Field Parameters

	Units	value
Wellhead pressure	Bar-g	5.035
Separator pressure	Bar-g	4.6225
Geo-fluid flow rate	Kg/s	434.3
Brine flow rate	Kg/s	206.9
Steam flow rate	Kg/s	227.4
Dryness fraction of geo-fluid		0.5236
Enthalpy of geo-fluid	kJ/kg	1757

Table C.2.Power plant parameters

Items	Units	Design Values	Unit 1	Unit 2	Unit 3
			Mean Values	Mean Values	Mean Values
Unit load	MW	35	23.9	34.6	35.6
Vent station steam pressure	Bar	-	4.3	4.4	4.2
Main steam flow	T/H	-	195	-	256
Main steam temperature (scrubber inlet)	^{o}C	-	151.7	-	153.1
Main steam pressure (scrubber inlet)	Bar-g	-	4.3	4.4	4.2
Main steam temperature (turbine inlet; LH)	^{o}C	150.3	146.4	150.8	151.5
Main steam temperature (turbine inlet; RH)	^{o}C	150.3	151.6	151.4	151
Main steam pressure (turbine inlet; LH)	Bar-g	4.8	4.2	4.1	4.1
Main steam pressure (turbine inlet; LH)	Bar-g	4.8	4.2	4.1	4.1

Items	Units	Design Values	Unit 1	Unit 2	Unit 3
			Mean Values	Mean Values	Mean Values
Condenser vacuum pressure	Bar-a	0.075	0.074	0.097	0.073
Auxiliary steam flow	T/H	6.14	10.77	10.67	6.43
Ejector steam supply Header Pressure	Bar-a	-	4.27	4.20	4.23
Turbine gland steam pressure	Bar	-	0.34	0.22	0.22
Turbine steam chest pressure	Bar-g	-	4.19	3.82	3.44
Turbine exhaust steam pressure	Bar-a	0.075	0.066	0.07	0.07
Turbine exhaust steam temperature	oC	-	41.13	44.5	44.97
Hotwell water temp	^{o}C	-	38.9	39.0	39.0
CT to condenser water temperature	^{o}C	-	24.57	27.2	25
Inter-condenser inlet Gas Header pressure	mbar	-	62.27	81.07	50
Inter-condenser (A) inlet pressure	mbar	-	192.9	163.3	165.9
Inter-condenser (B) inlet pressure	mbar	-	146.33	122.4	165.9
Inter-condenser (C) inlet pressure	mbar	-	191.93	-	958.6
Inter-condenser (A) outlet temperature	^{o}C	-	38.93	43.6	35.5
Inter-condenser (B) outlet temperature	^{o}C	-	33.93	27.3	36.15
Inter-condenser (C) outlet temperature	^{o}C	-	33.17	44.6	24.95
After condenser outlet temperature	^{o}C	-	33.43	46.17	25.05
Inter-condenser outlet pressure	mbar	-	192.77	260.1	160.85

Items	Units	Design Values	Unit 1	Unit 2	Unit 3
			Mean Values	Mean Values	Mean Values
Inter-condenser outlet temperature	^{o}C	-	37.03	44.43	36.65
Vacuum pump/After-condenser outlet temperature	^{o}C	-	43.07	52.03	33.45
CCWP Discharge Header Pressure	Bar-g	-	2.17	1.90	2.535
CCWP Discharge strainer Differential pressure	Bar-g	-	0.266	0.239	0.1385
CCW flow to cooling tower	T/H	-	358	330.3	313.4
CCW flow to inter/After-condenser	T/H	-	386.37	518.75	343
CCW discharge temperature to CT	^{o}C	-	26.27	29.13	24.2

Note: Some of the design values were not captured because they depended on the user choices. Also, the mean values were taken based on the data available.

Appendix D - Models

Model 1

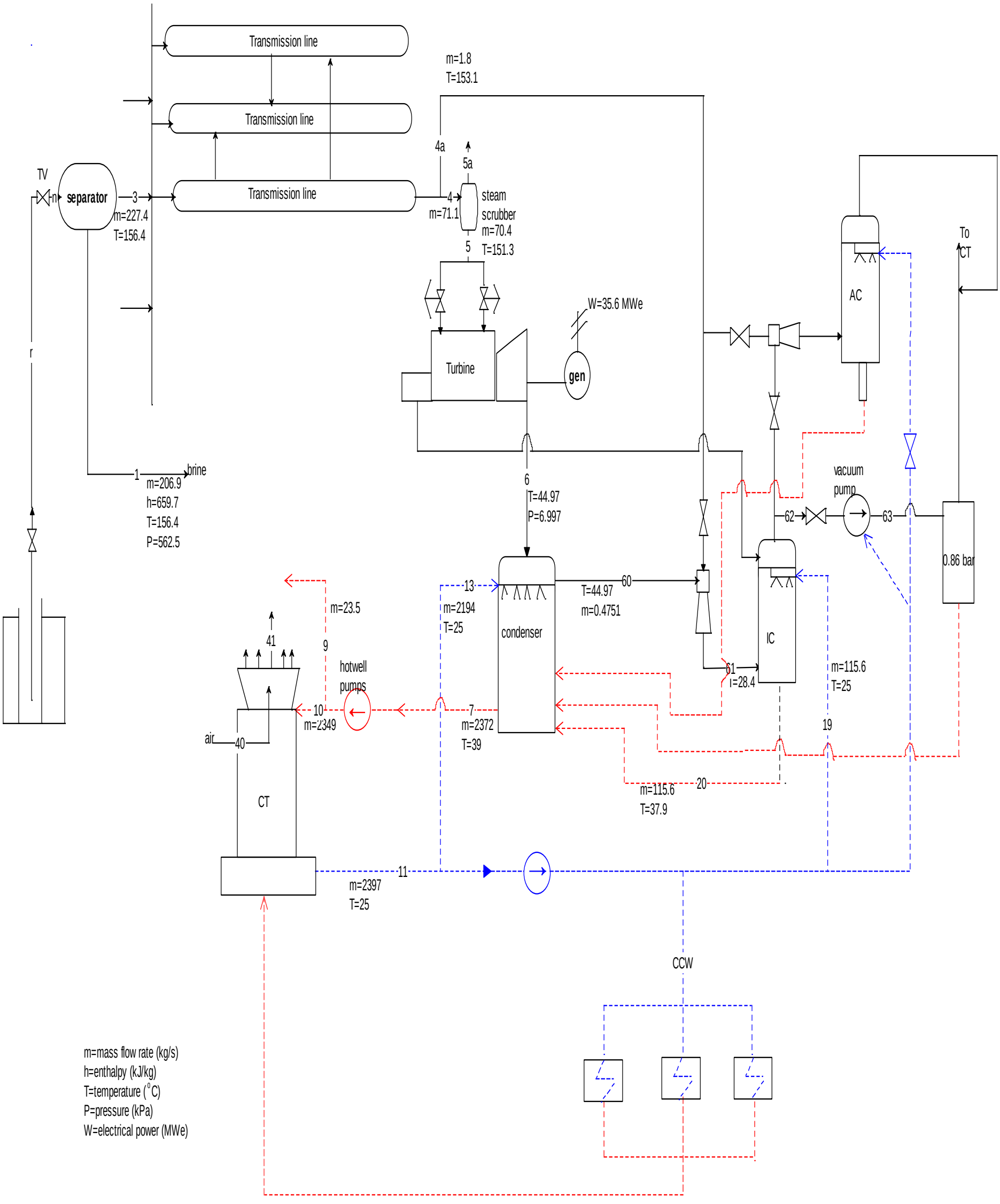

Figure D.1. Flow chart diagram for Olkaria II power plant (unit 3)

Model 2

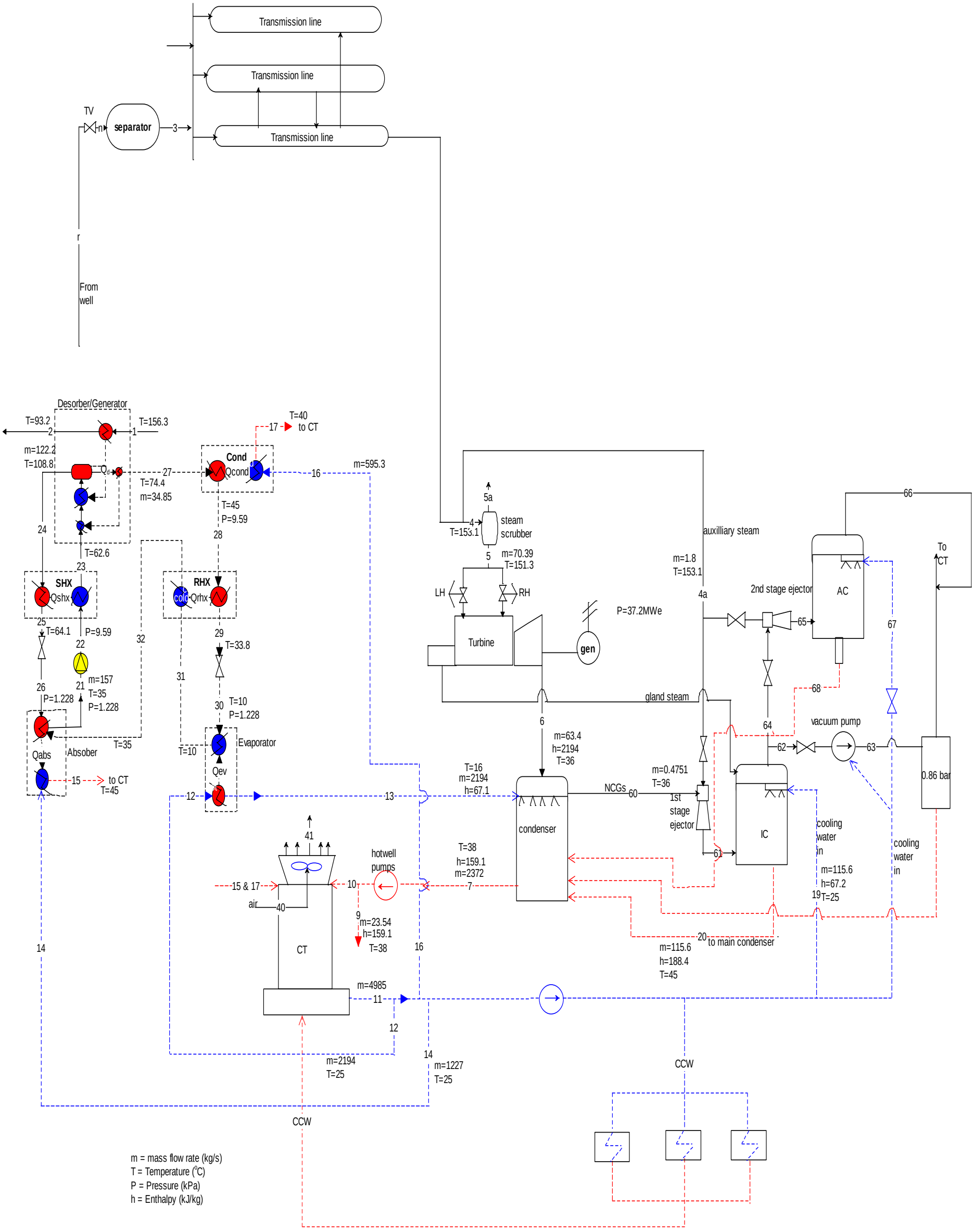

Figure D.2. Flow chart diagram for the proposed plant design for Olkaria II with hybridized cooling system (unit 3)

Appendix E - Sample Exergy Analysis Codes for Olkaria II Power Plant

{********ENIVIRONMENTAL CONDITION**********}**
T_0=293.15 [K]
P_0= 86
h_0=enthalpy (water,P=P_0,T=20)
s_0=entropy (water,P=P_0,T=20)

{********HEAT SOURCE**********}**

m_dot_r=434.3[kg/s]**{mass flow rate from all the wells feeding Olkaria II}**
h_r=1757 [kJ/kg] **{average enthalpy of the geo-fluid into the separators}**

{********SEPARATOR**********}**

P_sep=562.5 **{abslute pressure in the separator}**
P_n=P_sep**{pressure of geo-fluid into separator}**
P[1]=P_sep**{pressure of brine from the separator}**
P[3]=P_sep**{pressure of steam from separator}**

E_n=E[1]+E[3]+I_sep **"exergy loss determination, I_sep"**
E_n=m_dot_n*((h_n-h_0)-T_0*(s_n-s_0)) **{exergy of geo-fluid}**
h_n=h_r
s_n=entropy(steam,P=P_n,x=x_n)
m_dot_n=m_dot_r **{Total mass flow into Olkaria II separators}**

x_n= m_dot[3]/m_dot_n **{quality of dryness fraction of geo-fluid into the separator}**

E[1]=m_dot[1]*((h[1]-h_0)-T_0*(s[1]-s_0)) **{exergy of brine from separator}**
h[1]=enthalpy(water,P=P[1],x=0) **{enthalpy of brine from separator}**
s[1]=entropy(water,P=P[1],x=0)
m_dot[1]=m_dot_n-m_dot[3] **"Total mass flowrate of brine from all separators"**

E[3]=m_dot[3]*((h[3]-h_0)-T_0*(s[3]-s_0)) **{exergy of steam from separator into transmission line}**
h[3]=enthalpy(steam,P=P[3],x=1) **{enthalpy of steam from separator}**
s[3]=entropy(steam,P=P[3],x=1)
T[3] = temperature(water, P=P[1], h=h[1]) **{Temperature of steam into transmission lines}**
m_dot[3]=227.4**"Total mass flowrate of steam from all separators"**

eta_E_sep=E[3]/E_n **"exergetic efficiency of the separator"**

{********TRANSMISSION**********}**

E[33]=m_dot[33]*(h[3]-h_0-T_0*(s[3]-s_0))**{Estimated Exergy of steam into unit 3 transmission line}**
m_dot[33]=m_dot[43]+m_dot_43a
Loss_Transmission3=E[33]-(E[43]+E_43a)

eta_transmission3= (E[43]+E_43a)/E[33]

eta_transmission= Average (eta_transmission1, eta_transmission2, eta_transmission3) **{Average exergy efficiency of transmission}**
Loss_Transmission= Loss_Transmission1+Loss_Transmission2+Loss_Transmission3 **{Total exergy lost due to transmission}**

{********STEAM SRUBBER**********}**

E_4_total=E[41]+E[42]+E[43] **{total exergy of steam into olkaria II steam scrubbers}**
E_5a=E_51a+ E_52a+ E_53a

"UNIT 3"

E[43]=E[53]+E_53a+I_scrubber3

E[43]=m_dot[43]*(h[43]-h_0-T_0*(s[43]-s_0))
m_dot[43]=71.1 **{mass flow rate of auxilliary steam into unit 3 steam scrubber}**
h[43]=enthalpy(steam,P=P[43],x=1)
s[43]=entropy(steam,P=P[43],x=1)
P[43]=526 **{Pressure into unit 3 steam scrubber}**

E_53a=m_dot_53a*(h[43]-h_0-T_0*(s[43]-s_0))
m_dot_53a=0.01*m_dot[43]

eta_E_scrubber3=E[53]/E[43]**"exergetic efficiency of unit 3 steam scrubber"**

I_scrubber=I_scrubber1+ I_scrubber2+ I_scrubber3 **{Total exergy destroyed in the steam scrubbers}**
eta_E_scrubber=Average(eta_E_scrubber1,eta_E_scrubber2,eta_E_scrubber3) **{Average exergetic efficiency of Olkaria 2 steam scrubbers}**

{********TURBINE**********}**

x[5]=1 **{Estimated quality of dryness fraction of steam into turbines}**
eta_t=0.85 **{estimated efficiency of all turbines}**
eta_g=0.95 **{Estimated efficiency of the generator}**

"Design performance for all turbines"

W_d=W_s*eta_t **{Turbine design work}**
W_s=m_dot_5d*(h_5d-h_6dis) **{ turbine Isentropic work}**

h_6dis=enthalpy(steam,P=P_6d,s=s_5d)
m_dot_5d=72.9
P_5d=581.3
P_6d=7.5
s_5d= entropy(steam,P=P_5d,x=1)
h_5d=enthalpy(steam,P=P_5d,x=1)
E_6d=m_dot_5d*(h_6d-h_0-T_0*(s_6d-s_0))
h_6d=h_5d-w_d/m_dot_5d
s_6d=entropy (water,x=x_6d,P=p_6d)
x_6d=(h_6d-h_6f)/(h_6g-h_6f)
h_6f=enthalpy (water,x=0,P=p_6d)
h_6g=enthalpy (Steam,x=1,P=p_6d)

"UNIT 3"
x[53]=1
eta_3t=0.85

P[53]=516.3 **{inlet pressure into unit 3 turbine}**
P[63]=Pressure(steam, T=T_cond3, x=0)**{7.57 Design turbine exhaust pressure}**

"Isentropic Performance"
s[53]=s_63is
E_63is=m_dot[53]*(h_63is-h_0-T_0*(s_63is-s_0))
h_63is=enthalpy(steam,P=P_63actual,s=s[53])
W_3s=m_dot[53]*(h[53]-h_63is) **{ turbine Isentropic work}**

"Actual performance"

I_3t_g =E[53]-E[63]-W_3t **{Exergy loss at the turbine}**

E[53]=m_dot[53]*(h[53]-h_0-T_0*(s[53]-s_0)) **{Exergy inlet into unit 3 turbine}**
s[53]= entropy(steam,P=P[53],x=x[53])
h[53]=enthalpy(steam,P=P[53],x=x[53])
m_dot[53]=m_dot[43]-0.01*m_dot[43]**{Mass flow rate of steam into turbine}**

E[63]=m_dot[63]*(h[63]-h_0-T_0*(s[63]-s_0)) **{Exergy outlet from unit 3 turbine}**
h[63]=h[53]-eta_3t*(h[53]-h_63is)
s[63]=entropy(steam,P=P[63],h=h[63])

SSC3=m_dot[53]*1000/W_3actual **{specific steam consumption for unit 3 turbine}**

W_3actual=35600**{Generator power output}**
W_3t=W_3actual/eta_g**{Actual turbine work}**
P_63actual=P_cond3
m_dot[63]=m_dot[53]*0.9

eta_E_3t_g=W_3t/(E[53]-E[63]) **{Exergetic efficiency of unit 3 turbine}**

eta_energy_3t=W_3t/(m_dot[53]*h[53]) **{Energy efficiency of unit 3 turbine}**

eta_energy_t=Average(eta_energy_t1,eta_energy_2t,eta_energy_3t) **{Average energy efficiency of Olkaria 2 turbines}**
eta_E_t_g=Average(eta_E_t_g1, eta_E_2t_g, eta_E_3t_g) **{Average exergy efficiency of Olkaria 2 turbines}**

{********CONDENSER**********}**

"UNIT 3"

E[63]+E[133]+E[203]=E[73]+E[603]+I_cond3 **{Exergy loss at the condenser, I_cond}**

E[133]=m_dot[133]*(h[133]-h_0-T_0*(s[133]-s_0)) **{Exergy of cooling water into unit 3 condenser}**
s[133]=entropy(water,h=h[133],T=T[133])

E_73cw=(m_dot[133]+m_dot[203])*(h[73]-h_0-T_0*(s[73]-s_0)) **{Exergy of cooling water out of unit 3 condenser}**
s[73]=entropy(steam,T=T[73],x=0)
h[73]=enthalpy(steam, T=T[73], x=0)
E_73steam=(m_dot[63]+m_dot_43a)*(h[73]-h_0-T_0*(s[73]-s_0))**{Exergy of steam out of unit 3 condenser}**
E[73]=E_73cw+E_73steam **{Total exergy out of condenser into hotwell pumps}**
P[73]=Pressure(steam,T=T[73],x=0)
P_cond3=P[73]
T_cond3 = Temperature(steam,P=P[73],x=0)

m_dot[133]=(Q_condenser3-m_dot[203]*(h[73]-h[203]))/(h[73]-h[133])
m_dot[63]+m_dot[133]+m_dot[203]=m_dot[73]+m_dot[603] **{Gain in m_dot[73]}**

m_dot[133]=2194 **{mass flow rate of colling water into unit 3 condenser}**
T[63]=44.97 **{exhaust temperature of unit 3 turbine}**
T[73]=39**{39.2}{Temperature of condensate from unit 3 condenser}**
T[133]=25 **{Temperature of cooling water into unit 3 condenser}**

LF3=T[73]-T[133] **{Loss factor}**

eta_condenser3=(E_73cw-E[133]-E_203cw+E[603])/(E[63]+E_203s-E_73steam)**{Exergy efficiency of unit 3 condenser}**

eta_condenser=Average(eta_condenser1,eta_condenser2,eta_condenser3) **{Exergy efficiency of all condenser}**

{********STEAM EJECTORS**********}**

ncg=.0075 **{Assumed that NCG = 0.75% of steam by mass}**

E_4a_total=E_41a+E_42a+E_43a **{total exergy of auxilliary steam from olkaria II transmissions line to ncg ejectors}**
"UNIT 3"
E_43a=m_dot_43a*(h_43a-h_0-T_0*(s_43a-s_0)) **{Exergy of motive steam into unit 3 ejector}**
h_43a=enthalpy(steam,P=P_43a,x=1)
s_43a=entropy(steam,P=P_43a,x=1)
m_dot_43a=1.8 **{mass flow rate of auxilliary steam into unit 3 ejector}**
P_43a=423

E[603]=m_dot[603]*(h[603]-h_0-T_0*(s[603]-s_0))**{Exergy of ncg into unit 3 ejector}**
h[603]=enthalpy(CarbonDioxide,T=T[63],P=P_63actual)
s[603]=entropy(CarbonDioxide,T=T[63],P=p_63actual)
P[603]=Pressure(CarbonDioxide,T=T[63],h=h[603])
m_dot[603]=ncg*m_dot[63] **{mass flow rate of NCG from condenser 3}**
E[603]+E_43a=E[613]+I_sjet3

m_dot_613ncg=m_dot[603]**{mass flow rate of ncg into unit 3 intercondenser}**
h_613ncg=enthalpy(carbondioxide,P=P_613ncg,T=T_613ncg)
s_613ncg=entropy(carbondioxide,P=P_613ncg,T=T_613ncg)
E_613ncg=m_dot_613ncg*(h_613ncg-h_0-T_0*(s_613ncg-s_0))**{Exergy of ncg into unit 3 intercondenser}**
T[53]=151.3 **{Temperature of steam into unit 3 turbine}**
h_613s=enthalpy(steam,P=P[613],x=1)
s_613s=entropy(steam,P=P[613],x=1)
E_613s=m_dot_43a*(h_613s-h_0-T_0*(s_613s-s_0))**{Exergy of steam into unit 3 intercondenser}**
E[613]=E_613ncg+E_613s**{Total exergy of ncg+motive steam into unit 3 intercondenser}**

E[193]=m_dot[193]*(h[193]-h_0-T_0*(s[193]-s_0))**{Exergy of cooling water into unit 3 intercondenser}**
h[193]=enthalpy(water,p=p_0,T=T[133])
s[193]=entropy(water,p=p_0,T=T[133])
P[193]=Pressure(water,x=0,T=T[193])

E_203s=0.7*(h[203]-h_0-T_0*(s[203]-s_0))**{Exergy of steam out of unit 3 intercondenser to cooling tower}**
s[203]=entropy(water,x=0,T=T[203])
h[203]=enthalpy(water,x=0,T=T[203])
E_203cw=m_dot[193]*(h[203]-h_0-T_0*(s[203]-s_0))**{Exergy of cooling water out of unit 3 intercondenser to cooling tower}**
P[203]=Pressure(water,h=h[203],T=T[203])
m_dot[203]=m_dot[193] **{mass flow rate of cooling water from unit 3 intercondenser to cooling tower}**
E[203]=E_203s+E_203cw**{Total exergy of steam+cooling water out of unit 3 intercondenser to cooling tower}**

E_633ncg=m_dot[633]*(h_633ncg-h_0-T_0*(s_633ncg-s_0)){exergy of ncg from unit 3 vacuum pump into CT}
h_633ncg=enthalpy(carbondioxide,T=T[633],p=16.1)
s_633ncg=entropy(carbondioxide,T=T[633],p=16.1)
E_633s=1.1*(h_633s-h_0-T_0*(s_633s-s_0)) {exergy of steam from unit 3 vacuum pump to CT}
h_633s=enthalpy(steam,x=1,P=P[633])
s_633s=entropy(steam,x=1,P=P[633])
m_dot[633]=m_dot_613ncg
E[633]=E_633s+E_633ncg

T[203]=37.9{condensate drain temperature of ejector 3 intercondenser}
T[193]=T[113]{Temperature of cooling water into unit 3 intercondenser}
P[613]=43 {Pressure of ncg + motive steam into unit 3 inter-condenser}
P_613ncg=5{pressure of ncg into unit 3 intercondenser}
T_613ncg=28.57 {temperature of ncg into unit 3 intercondenser}

T[603]=T[63]{temperature of ncg from condenser}
T[633]=36.15
P[633]=16.1
m_dot[193]=115.6 {mass flow rate of ejector 3 cooling water}

eta_ges3=((E_633ncg-E[603])+(E_203cw-E[193]))/(E_43a-(E_633s-E_203s))
eta_sjet3=E[613]/(E[603]+E_43a)
{Ratio of exergy gained by NCG and cooling water to exergy lost by the motive steam}

eta_ges=Average(eta_ges1,eta_ges2,eta_ges3)

{**********COOLING TOWER**********}

W_fans=rating_fan*4
W_pump1=rating_pump_hotwell*1*0.6
W_pump2=rating_pump_CCW*0.6
W_pump3=rating_pump_condensate_reinjec*0.6
rating_pump_hotwell=400{KW}
rating_pump_CCW=75{KW}
rating_pump_condensate_reinjec=45{KW}
rating_fan=149.1{KW}
W_pumps=W_pump1+W_pump2+W_pump3
P_CT_mid=P_0+40

"UNIT 3"
E[103]=m_dot[103]*(h[103]-h_0-T_0*(s[103]-s_0))
s[103]=s[73]
h[103]=h[73]

E[113]=m_dot[113]*(h[123]-h_0-T_0*(s[123]-s_0))
h[113]=h[133]

s[113]=entropy(water,x=0,T=T[113])
m_dot[113]= m_dot[133]+m_dot[193]+m_dot_CCW3

E[123]=m_dot[123]*(h[123]-h_0-T_0*(s[123]-s_0))
h[123] = enthalpy(water, T=T[123], P=P[123])
s[123]=entropy(water,h=h[123],T=T[123])
h[133] =enthalpy(water, T=T[133], P=P[133])
m_dot[123] = m_dot[133]**{mass flow rate of cooling water out of CT}**

m_dot[93]=m_dot[73]-m_dot[103]**{Gain in m_dot[103], mass flow rate of condensate into unit 3 CT}**
E[93]=m_dot[93]*(h[93]-h_0-T_0*(s[93]-s_0))**{Exergy of reinjection from unit 3}**
s[93]=entropy(water,x=0,T=T[93])
h[93]=h[73]

T[103]=T[93] **{Temperature of condasate into unit 3 CT}**
P[93]=P[103]
P[113]=P[123]
T[123]=T[113]
P[123] = P_CT_mid
P[133]= P[123] **{Pressure of cooling water into unit 3 condenser}**

T[93]=T[73]
P[103]=163
m_dot[93]=23.54**{mass flow rate of unit 3 reinjection}**
T[113]=25 **{Temperature of cooling water out of unit 3 CT}**
m_dot_CCW3=87.06 **{mass flow rate of unit 3common cooling water}**

COP_cooling3=(E[103]-E[113])/(W_fans+W_pumps) **{Coefficient of Performance of unit 3 CT}**

COP_cooling=Average(COP_cooling1,COP_cooling2,COP_cooling3)

{********OVERALL EXERGY EFFICIENCY OF PLANT**********}**

Auxilliary_power=3*(W_pumps+W_fans)
W_actual=W_1actual+W_2actual+W_3actual
W_net=W_actual-Auxilliary_power
eta_overall1=W_net/E[3] **{efficiency as a function of tota steam into the transmission}**
eta_overall2=W_net/E_n **{efficiency as a function of geo-fluid}**

COMBINED CODES FOR UNIT 3 WITH ADOPTION OF A CHILLER SYSTEM

{********ENIVIRONMENTAL CONDITION**********}**
T_0=293.15 [K]
P_0= 86
h_0=enthalpy (water, P=P_0, T=20)
s_0=entropy (water, P=P_0, T=20)

{********HEAT SOURCE**********}**

m_dot_r=434.3[kg/s] **{mass flow rate from all the wells feeding Olkaria II}**
h_r=1757 [kJ/kg] **{average enthalpy of the geo-fluid into the separator}**

{********SEPARATOR**********}**

P_sep=562.5 **{abslute pressure in the separator}**
E_n=E_1+E_3+I_sep **{exergy loss determination, I_sep}**

E_n=m_dot_n*((h_n-h_0)-T_0*(s_n-s_0)) **{exergy of geo-fluid}**
h_n=h_r
s_n=entropy (steam,P=P_n,x=x_n)
P_n=P_sep **{pressure of geo-fluid into separator}**
m_dot_n=m_dot_r
x_n= m_dot_3/m_dot_n **{quality of dryness fraction of geo-fluid into the separator}**

E_1=m_dot_1*((h_1-h_0)-T_0*(s_1-s_0)) **{exergy of brine from separator}**
h_1=enthalpy (water,P=P_1,x=0) **{enthalpy of brine from separator}**
s_1=entropy (water,P=P_1,x=0)
P_1=P_sep **{pressure of brine from the separator}**
m_dot_1=206.9 **{mass flowrate of brine from separator}**

E_3=m_dot_3*((h_3-h_0)-T_0*(s_3-s_0)) **{exergy of steam from separator into transmission line}**
s_3=entropy (steam,P=P_3,x=1)
h_3=enthalpy (steam,P=P_3,x=1) **{enthalpy of steam from separator}**
P_3=P_sep **{pressure of steam from separator}**
m_dot_3=227.4 **{mass flowrate of steam from separator}**
T_3 = temperature (water, P=P_1, h=h_1)
T_3=T_1

x_2=0

eta_E_sep=E_3/E_n **"exergetic efficiency of the separator"**

{********TRANSMISSION**********}**

m_dot_33=72.9 **{mass flow rate to unit 3 transmission line}**
E_33=m_dot_33*(h_3-h_0-T_0*(s_3-s_0))**{Estimated Exergy of steam into unit 3 transmission line}**
eta_transmission= (E_43+E_43a)*3/E_3 **{exergy efficiency of transmission}**
Loss_Transmission=E_33-E_43-E_43a **{exergy lost due to transmission}**

{********STEAM SRUBBER**********}**

"UNIT 3"
E_43=E_53+E_53a+I_scrubber
E_53a=m_dot_53a*(h_43-h_0-T_0*(s_43-s_0))
m_dot_53a=0.01*m_dot_43

P_53a=531.3 **{Pressure in unit 3 steam scrubber}**

E_43=m_dot_43*(h_43-h_0-T_0*(s_43-s_0))
m_dot_43=m_dot_33-1.8 **{mass flow rate of auxilliary steam into unit 3 steam scrubber}**
h_43=enthalpy (steam,P=P_43,x=1)
s_43=entropy (steam,P=P_43,x=1)
P_43=526 **{Pressure into unit 3 steam scrubber}**
eta_E_scrubber3=E_53/E_43**"exergetic efficiency of unit 3 steam scrubber"**

eta_E_scrubber=Average
(eta_E_scrubber1,eta_E_scrubber2,eta_E_scrubber3)**{Average exergetic efficiency of Olkaria 2 steam scrubbers}**

{********TURBINE**********}**

x_5=1 **{Estimated quality of dryness fraction of steam into turbines}**
eta_t=0.85 **{estimated efficiency of all turbines}**

"UNIT 3"
x_53=1
P_53=516.3 **{inlet pressure into unit 3 turbine}**
P_63=7.5 **{Design turbine exhaust pressure}**

"Isentropic Performance"
s_53=s_63is
E_63is=m_dot_53*(h_63is-h_0-T_0*(s_63is-s_0))
h_63is=enthalpy (steam,P=P_63actual,s=s_53)
W_3s=m_dot_53*(h_53-h_63is) **{turbine Isentropic work}**

"Design performance"
W_d=W_s*eta_t **{Turbine design work}**
W_s=m_dot_5d*(h_5d-h_6dis) **{turbine Isentropic work}**
h_6dis=enthalpy (steam,P=P_6d,s=s_5d)

m_dot_5d=72.9
P_5d=566
P_6d=7.5
s_5d= entropy (steam,P=P_5d,x=1)
h_5d=enthalpy (steam,P=P_5d,x=1)
E_6d=m_dot_5d*(h_6d-h_0-T_0*(s_6d-s_0))
H_6d=h_5d-W_d/m_dot_5d
S_6d=entropy (water,x=x_6d,P=P_6d)
X_6d= (h_6d-h_6f)/(h_6g-h_6f)
h_6f=enthalpy (water,x=0,P=P_6d)
h_6g=enthalpy (Steam,x=1,P=P_6d)

"Actual performance"
eta_g=0.95 **{Estimated efficiency of the generator}**
h_63gactual=enthalpy (Steam,x=1,P=P_63actual)
h_63factual=enthalpy (water,x=0,P=P_63actual)

s_53= entropy (steam,P=P_53,x=x_53)
h_53=enthalpy (steam,P=P_53,x=x_53)
h_63actual=h_53-eta_t*(h_53-h_63is)
m_dot_53=m_dot_43-0.01*m_dot_43 **{Mass flow rate of steam into turbine}**
W_3t= (x_53*m_dot_53*(h_53-h_63actual))**{Actual turbine work}**
W_3actual=W_3t*eta_g **{Generator power output}**

I_3t_g =E_53-E_63actual-W_3t **{Exergy loss at the turbine}**
E_53=m_dot_53*(h_53-h_0-T_0*(s_53-s_0)) **{Exergy inlet into unit 3 turbine}**
E_63actual=m_dot_63*(h_63actual-h_0-T_0*(s_63actual-s_0)) **{exergy of steam into unit 3 condenser}**
s_63actual=entropy (steam,h=h_63actual,P=P_63actual)
P_63actual=P_cond3 **{Pressure at turbine exit}**
SSC3=m_dot_53*1000/W_3actual **{specific steam consumption for unit 3 turbine}**

eta_E_3t_g= (W_3t)/(E_53-E_63actual) **{Exergetic efficiency of unit 3 turbine}**
eta_energy_3t=W_3t/(m_dot_53*h_53) **{Energy efficiency of unit 3 turbine}**
W_turbine3=W_3t/1000 [MW]

eta_energy_t=Average (eta_energy_1t, eta_energy_2t, eta_energy_3t) **{Average energy efficiency of Olkaria II turbines}**
eta_E_t_g=Average (eta_E_1t_g, eta_E_2t_g, eta_E_3t_g) **{Average exergy efficiency of Olkaria II turbines}**

{********CONDENSER**********}**

"UNIT 3"
E_63actual+E_133+E_203=E_73+E_603+I_cond3 **{Exergy loss at the condenser, I_cond}**
E_133=m_dot_133*(h_133-h_0-T_0*(s_133-s_0)) **{Exergy of cooling water into unit 3 condenser}**
s_133=entropy (water,T=T_133,x=0)
h_133 =enthalpy (water, T=T_133, x=0)

E_73cw= (m_dot_133+m_dot_203)*(h_73-h_0-T_0*(s_73-s_0)) **{Exergy of cooling water out of unit 3 condenser}**
h_73=enthalpy (steam,P=P_73,x=0)
s_73=entropy (steam,P=P_73,x=0)
E_73s=(m_dot_63+m_dot_43a)*(h_73-h_0-T_0*(s_73-s_0))**{Exergy of steam out of unit 3 condenser}**
E_73=E_73cw+E_73s **{Total exergy out of condenser into hotwell pumps}**
P_cond3=pressure(steam,T=T_cond3,x=1) **{Pressure of condenser}**
P_73=Pressure(water, T=T_73, x=0) **{Pressure of condansate into hotwell pumps}**
T_cond3 = T_133 + delta_T_cond **{temperature inside the condenser}**
T_63=Temperature(steam,P=P_63actual, s=s_63actual) **{Temperature of turbine exhaust}**
Q_condenser3=m_dot_73*h_73-m_dot_133*h_133-m_dot_203*h_203
m_dot_63+m_dot_133+m_dot_203=m_dot_603+m_dot_73**{Gain in m_dot_73}**
m_dot_63=0.9*m_dot_53 **{mass flow rate of steam exiting the turbine}**

m_dot_133=2194 **{mass flow rate of cooling water into unit 3 condenser}**
T_73=38**{Temperature of condensate from unit 3 condenser}**
T_133=T_123-delta_T_cooling**{Temperature of cooling water into unit 3 condenser}**
delta_T_cond = 20[C]

LF3=T_73-T_133 **{Loss factor}**
eta_cond3=(E_73cw-E_133-E_203cw)/(E_63actual+E_203s-E_73s) **{Exergy efficiency of unit 3 condenser}**

eta_condenser=Average(eta_condenser1,eta_condenser2,eta_condenser3) **{Exergy efficiency of all condenser}**

{********STEAM EJECTORS**********}**

ncg=.0075 **{Assumed that NCG = 0.75% of steam by mass}**

"UNIT 3"
E_43a=m_dot_43a*(h_43a-h_0-T_0*(s_43a-s_0)) **{Exergy of motive steam into unit 3 ejector}**
h_43a=enthalpy(steam,P=423,x=1)
s_43a=entropy(steam,P=423,x=1)

E_603=m_dot_603*(h_603-h_0-T_0*(s_603-s_0))**{Exergy of ncg into unit 3 ejector}**
h_603=enthalpy (CarbonDioxide,T=T_63,P=P_63actual)
s_603=entropy (CarbonDioxide,T=T_63,P=P_63actual)
P_603=Pressure(CarbonDioxide,T=T_63,h=h_603)
m_dot_603=ncg*m_dot_63 **{mass flow rate of NCG from condenser 3}**
E_603+E_43a=E_613+I_sjet3

m_dot_613ncg=m_dot_603**{mass flow rate of ncg into unit 3 intercondenser}**
h_613ncg=enthalpy(carbondioxide,P=P_613ncg,T=T_613ncg)

s_613ncg=entropy(carbondioxide,P=P_613ncg,T=T_613ncg)
E_613ncg=m_dot_613ncg*(h_613ncg-h_0-T_0*(s_613ncg-s_0))**{Exergy of ncg into unit 3 intercondenser}**
T_53=151.3 **{Temperature of steam into unit 3 turbine}**
h_613s=enthalpy(steam,P=43,x=1)
s_613s=entropy(steam,P=43,x=1)
E_613s=m_dot_43a*(h_613s-h_0-T_0*(s_613s-s_0))**{Exergy of steam into unit 3 intercondenser}**
E_613=E_613ncg+E_613s**{Total exergy of ncg+motive steam into unit 3 intercondenser}**

E_193=m_dot_193*(h_193-h_0-T_0*(s_193-s_0))**{Exergy of cooling water into unit 3 intercondenser}**
h_193=enthalpy(water,p=P_0,T=T_133)
s_193=entropy(water,p=P_0,T=T_133)
P_193=Pressure(water,x=0,T=T_193)

E_203s=(m_dot_43a+m_dot_603)*(h_203-h_0-T_0*(s_203-s_0))**{Exergy of steam out of unit 3 intercondenser to cooling tower}**
s_203=entropy(water,x=0,T=T_203)
h_203=enthalpy(water,x=0,T=T_203)
E_203cw=m_dot_193*(h_203-h_0-T_0*(s_203-s_0))**{Exergy of cooling water out of unit 3 intercondenser to cooling tower}**
P_203=Pressure(water,h=h_203,x=0)
m_dot_203=m_dot_193 **{mass flow rate of cooling water from unit 3 intercondenser to cooling tower}**
E_203=E_203s+E_203cw**{Total exergy of steam+cooling water out of unit 3 intercondenser to cooling tower}**

E_633ncg=m_dot_633*(h_633ncg-h_0-T_0*(s_633ncg-s_0))**{exergy of ncg from unit 3 vacuum pump into CT}**
h_633ncg=enthalpy(carbondioxide,T=33.45,p=16.1)
s_633ncg=entropy(carbondioxide,T=33.45,p=16.1)
E_633s=1.1*(h_633s-h_0-T_0*(s_633s-s_0)) **{exergy of steam from unit 3 vacuum pump to CT}**
h_633s=enthalpy(steam,x=1,p=16.1)
s_633s=entropy(steam,x=1,p=16.1)
m_dot_633=m_dot_613ncg
E_633=E_633s+E_633ncg

T_203=T_193+delta_T_cond**{condensate drain temperature of ejector 3 intercondenser}**
T_193=T_113**{Temperature of cooling water into unit 3 intercondenser}**
P_613ncg=5**{pressure of ncg into unit 3 intercondenser}**
T_613ncg=28.57 **{temperature of ncg into unit 3 intercondenser}**
T_603=T_63**{temperature of ncg from condenser}**
m_dot_43a=1.8 **{mass flow rate of auxilliary steam into unit 2 steam ejector}**
m_dot_193=115.6 **{mass flow rate of ejector 3 cooling water}**

eta_ges3=((E_633ncg-E_603)+(E_203cw-E_193))/(E_43a-(E_633s-E_203s))
eta_sjet3=E_613/(E_603+E_43a) **{Ratio of exergy gained by NCG and cooling water to exergy lost by the motive steam}**

eta_ges=Average(eta_ges1,eta_ges2,eta_ges3)**{Average exergy efficiency of all ncg ejectors}**

{********COOLING TOWER**********}**

W_fans=rating_fan*3 **{Power consumed by fans}**
W_pump1=rating_pump_hotwell*1*0.6
W_pump2=rating_pump_CCW*0.6
W_pump3=rating_pump_condensate_reinjec*0.6
rating_pump_hotwell=400**{KW}**
rating_pump_CCW=75**{KW}**
rating_pump_condensate_reinjec=45**{KW}**
rating_fan=149.1**{KW}**
W_pumps=W_pump1+W_pump2+W_pump3**{Power consumed by pumps}**
P_CT_mid=P_0+40

"UNIT 3"
E_103=m_dot_103*(h_103-h_0-T_0*(s_103-s_0)) **{exergy of condensate into CT}**
s_103=s_73
h_103=h_73

E_113=m_dot_113*(h_123-h_0-T_0*(s_123-s_0))**{exergy of cooling water out of CT}**
h_113=enthalpy(water,x=0,T=T_113)
s_113=entropy(water,x=0,T=T_113)
m_dot_113= m_dot_123+m_dot_14+m_dot_16+m_dot_193+m_dot_CCW3

E_123=m_dot_123*(h_123-h_0-T_0*(s_123-s_0))**{exergy of cooling water into chiller evaporator}**
h_123 = enthalpy(water, T=T_123, P=P_123)
s_123=entropy(water,h=h_123,T=T_123)
m_dot_123 = m_dot_133**{mass flow rate of cooling water out of CT}**

E_15=m_dot_15*(h_15-h_0-T_0*(s_15-s_0)) **{exergy of condensate out of absorber into CT}**
s_15=entropy(water,T=T_15,P=P_15)
E_17=m_dot_17*(h_17-h_0-T_0*(s_17-s_0))
s_17=entropy(water,T=T_17,P=P_17)

m_dot_93=m_dot_73-m_dot_103**{Gain in m_dot_103, mass flow rate of condensate into unit 3 CT}**
E_93=m_dot_93*(h_93-h_0-T_0*(s_93-s_0))**{Exergy of reinjection from unit 3}**
s_93=entropy(water,x=0,T=T_93)
h_93=h_73

T_103=T_93 **{Temperature of condensate into CT}**

P_93=P_103
P_113=P_123
T_123=T_113**{Temperature of cooling water out of unit 3 CT}**
P_123 = P_CT_mid
P_133= P_123

T_93=T_73 **{Temperature of condansate for reinjection}**
P_103=163
m_dot_93=23.54**{mass flow rate of unit 3 reinjection}**
T_113=25 **{Temperature of cooling water out of CT}**
m_dot_CCW3=87.06 **{mass flow rate of unit 3common cooling water}**

COP_cooling3=(E_103+E_15+E_17-E_113)/(W_fans+W_pumps) **{Coefficient of Performance of unit 3 CT}**

COP_cooling=Average(COP_cooling1,COP_cooling2,COP_cooling3)

{********CHILLER**********}**

d_x = 15 **{change in concentration of solution after separation in the desorber}**
T_pinch_a = 10 [C]
T_31 = 10 [C] **{temperature of refrigerant out of the evaporator}**
m_dot_d=206.9 **{mass flow rate of brine into the desorber}**
delta_T_cooling = 9**{Change in temperature of cooling water into the condenser at the eveporator}**

"Absorber"
m_dot_21 = m_dot_26 + m_dot_32 **{Mass flow rate of solution out of the absorber}**
m_dot_21 * x_21 = m_dot_26 * x_26
x_21 =X_LIBR('SI',T_21,P_21) **{concetration of solution in the absorber}**
P_21 = P_31
T_21 = T_14 + T_pinch_a **{Temperature of solution out of absorber}**
T_14=T_113 **{Temperature of cooling water into absorber}**
h_21 = H_LIBR('SI', T_21, x_21)
P_14 = P_CT_mid
P_15 = P_14
T_15 = T_14 + 20 [C]
h_14 = enthalpy(water, T=T_14, P=P_14)
h_15 = enthalpy(water, T=T_15, P=P_15)
m_dot_15 = m_dot_14 **{mass flow rate out of the absorber}**

Q_a = m_dot_32 * h_32 + m_dot_26 * h_26 - m_dot_21 * h_21 **{heat transfer at the absorber}**
Q_a = m_dot_14 * (h_15 - h_14) **"Gain m_dot_14"**

LMTD_a =((T_26 - T_15) - (T_21 - T_14)) / (ln((T_26 - T_15) / (T_21 - T_14)))
{logarithmic mean temperature difference at the absorber}

U_a =2.5 [kW/m2-C] **{Coefficient of heat transfer of the absorber}**
Q_a = U_a * A_a * LMTD_a

"solution pump"
eta_pump = 0.95 **{estimated efficiency of the pump}**
m_dot_21=m_dot_22
V_21 = V_LIBR('SI', T_21, x_21) * convert(cm3/g, m3/kg) **{specific Volume of solution}**
W_pump_libr = (m_dot_21 * V_21 * (x_26/(x_26-x_21)) * (P_22 - P_21))
/eta_pump
P_22 = P_28
x_22 = x_21 **{concetration of solution in the shx}**
h_22 =H_LIBR('SI', T_22, x_22)
T_22=T_21

"Solution heat exchanger"

P_23 = P_28
P_25 = P_28
x_25 = x_24
x_23 = x_21
x_26 = x_24
x_24 = x_21 + d_x **{concetration of solution out of desorber}**
P_26 = P_31
h_26 = H_LIBR('SI', T_26, x_26)
P_26 = P_LIBR('SI', T_26, x_26)

eta_shx = 0.6 **{estimated efficiency of solution heat exchanger,SHX}**
T_25 = T_22 * eta_shx + (1 - eta_shx) * T_24
Q_shx = m_dot_22 * (h_23 - h_22) **"Gain h_23"**
Q_shx = m_dot_24 * (h_24 - h_25) **{heat transfer at the solution heat exchanger}**

h_23 = H_LIBR('SI', T_23, x_23)
LMTD_shx = ((T_24 - T_23) - (T_25 - T_22)) / (ln((T_24 - T_23) / (T_25 - T_22)))
U_shx =1.1[kW/m2-C]
Q_shx = U_shx * A_shx * LMTD_shx

"Desorber"
m_dot_23=m_dot_21
P_24 = P_28
P_27 = P_28
T_24 = T_LIBR('SI', P_24, x_24)
m_dot_27 = m_dot_31 **{mass flow rate of refrigerant into condenser}**
m_dot_24 = m_dot_26
h_24 = H_LIBR('SI', T_24, x_24)
T_d = T_LIBR('SI', P_23, x_23) **{Temperature in the desorber}**
T_27 = T_d
h_27 = enthalpy(steam, T=T_27, P=P_27)
P_2 = P_1 **{Pressure into the desorber is same as pressure out of the desorber}**
T_2 =T_1-T_23

m_dot_2d = m_dot_d **{Mass flow rate of brine out of desorber}**

Q_d =m_dot_27 * h_27 + m_dot_24 * h_24 - m_dot_23 * h_23 **{heat transfer rate in the desorber}**
Q_d = m_dot_d * (h_1 - h_2) **"Gain h_2"**

LMTD_d = ((T_1 - T_24) - (T_2 - T_23)) / (ln((T_1 - T_24) / (T_2 - T_23)))
U_d =2.8[kW/m2-C]
Q_d = U_d * A_d * LMTD_d

"Solution expansion valve"
m_dot_26=m_dot_25
h_26=h_25

"Condenser"
m_dot_28=m_dot_32
m_dot_17 = m_dot_16 **{mass flow rate of cooling water from the chiller condenser into CT}**

P_16 = P_CT_mid
P_17 = P_16
T_16 = T_113
T_17 = T_16 + 15 [C]
h_16 = enthalpy(water, T=T_16, P=P_16)
h_17 = enthalpy(water, T=T_17, P=P_17)

Q_c = m_dot_27 * (h_27 - h_28) **{heat transfer rate in the chiller condenser}**
Q_c = m_dot_16 * (h_17 - h_16) **"Gain m_dot_16"**

LMTD_c = ((T_27 - T_17) - (T_28 - T_16)) / (ln((T_27 - T_17) / (T_28 - T_16)))
U_c = 3.5 [kW/m2-C]
Q_c = U_c * A_c * LMTD_c

"Refrigerant Heat Exchanger"
eta_rhx = (T_28 - T_29) / (T_28 - T_31)
P_29 = P_28
P_28 = Pressure(steam, T=T_28, x=x_28)
h_28 = enthalpy(water, P=P_28, x=x_28)
T_28 = T_16 + 20 [C] **{Temperature of refigerant out of the condenser into RHX}**
x_28=0
T_29 = temperature(steam, h=h_29, P=P_29)
x_29 = 0
m_dot_31 * h_31 + m_dot_28 * h_28 = m_dot_29 * h_29 + m_dot_32 * h_32 **"Gain h_29"**
m_dot_32 = m_dot_31**{mass flow rate into the absorber from RHX}**
x_32 = quality(steam, T=T_32, h=h_32)
T_32 = T_28 - 10 [C] **{Temperature of refrigerant into the absorber}**
h_32 = enthalpy(steam, T=T_32, P=P_32)
P_32 = P_31

Q_rhx = m_dot_31 * (h_32 - h_31) **{heat transfer rate in the rhx}**

LMTD_rhx = ((T_28 - T_32) - (T_29 - T_31)) / (ln((T_28 - T_32) / (T_29 - T_31)))
U_rhx =1.1 [kW/m2-C]
Q_rhx = U_rhx * A_rhx * LMTD_rhx

"Refrigerant expansion valve"
h_30 = h_29
m_dot_29 = m_dot_30**{mass flow rate out of the,refrigerant heat exchanger (RHX)}**

"Evaporator"
x_30 = quality(steam, T=T_30, h=h_30)
x_31 = 1**{Quality of dryness fraction of refrigerant vapour out of the eveporator}**
P_31 = pressure(steam, T=T_31, x=x_31)
P_30 = P_31
h_31 = enthalpy(steam, T=T_31, x=x_31)

m_dot_30 = m_dot_31
T_30 = temperature(steam, P=P_30, h=h_30)
Q_e = m_dot_31 * (h_31 - h_30)**"Gain m_dot_31"**
Q_e = m_dot_123 * (h_123 - h_133)

LMTD_e = ((T_123 - T_31) - (T_133 - T_31)) / (ln((T_123 - T_31) / (T_133 - T_31)))
U_e =3.9 [kW/m2-C]
Q_e = U_e * A_e * LMTD_e

"Total area of heat exchangers"

A_HXS=A_a+A_shx+A_d+A_c+A_rhx+A_e

"Performance"

(Q_c+Q_a)-(Q_e+Q_d)=B
COP=Q_e/Q_d

{********OVERALL EXERGY EFFICIENCY OF PLANT********}**

Auxilliary_power=W_pumps+W_fans+W_pump_libr
W_net=W_3actual-Auxilliary_power
eta_overall1=W_net/E_33 **{efficiency as a function of total steam into the transmission}**
eta_overall2=W_net*3/E_n**{efficiency as a function of geo-fluid}**